3rd International Accelerator School for Linear Colliders

Oak Brook, Illinois, USA
October 19-29, 2008

Lecture 7a

Superconducting RF & ILC

Nikolay Solyak
Fermilab

Contents

Part 1

- **Superconductivity basics**
- **Cavity design and constrains**
- **HOM & HOM couplers and dampers**
- **Cavity fabrication and tuning**
- **Surface preparation**
- **Gradient limit and spread**
- **Lorenz force detuning in cavity**
- **Microphonics & Vibration Issues**
- **Slow and Fast Tuners**

Part 2

- Power Couplers
- ILC cryomodules
- Alignment Issues
- Cryogenics
- ILC design and challenges

Acknowledgement

For this presentation I used freely material from presentations and tutorials of colleagues, whom I want to thank:

A.Gurevich, P.Lee, A.Polyanskii - SU

H.Padamsee, Shemelin, M. Liepe - Cornell Uni

P.Kneisel, G.Giovati - JLAB

J. Sekutowicz, L.Lilje, W. Singer, D. Reschke, A. Matheisen, G.Kreps, W.-D. Moeller, D.Kostin, B. Petersen - DESY

S. Noguchi, K. Saito, T. Saeki, S.Kazakov - KEK

C.Pagani, V. Palmieri - INFN

T. Garvey, H.Jenhani – LAL

C. Adolphsen - SLAC

T.Arkan, Y.Orlov, I.Gonin,Y.Pischalnikov, V.Yakovlev, T.Peterson, G.Wu et.al - FNAL

Recommended Literature:

- H.Padamsee J. Knobloch, T. Hays, RF superconductivity for accelerators, John Wiley&Sons, Inc; ISBN 0-471-15432-6
- V.Shmidt, "Introduction in physics of superconductivity" , lectures, Moscow 2000
- Holger J. Podlech, Introduction to Superconducting RF,2007,Mol, Belgium
- S.Noguchi, SRF Basics, ILC school, Hayama Japan,2006
- P.Kneisel, SRF Cavity Technology, ILC school, Hayama Japan,2006
- C.Pagani, ILC Cryomodule and Cryogenics, ILC school, Hayama Japan,2006
  A. Gurevich "General aspects of superconductivity", tutorial SRF 2007, Bejing

Proceedings of the Workshops on RF Superconductivity 1981 – 2007 and

- TTC Workshop at Frascati, Dec.2005 - http://www.lnf.infn.it/conference/ilc05/
- TTC Workshop at KEK, Sept.2006 - http://lcdev.kek.jp/TTC/
- SRF 2003, Travemuende, Germany - http://srf2003.desy.de/
- SRF 2005, Ithaca,NY- http://www.lns.cornell.edu/public/SRF2005/
- SRF 2007, Bejing - http://www.pku.edu.cn/academic/srf2007/home.html

Superconductivity basics

Basic phenomena:

- History of discovery
- Phase transition, Specific heat and Meissner effect
- London equations, magnetic penetration depth
- Type II superconductors, vortices
- GL and BCS theories, energy gap
- RF losses

History of Discovery

Superconductivity was discovered in 1911 by Heinke Kamerling Onnes and Giles Holst after Onnes was able to liquify helium in 1908. Nobel Prize in 1913

"for his investigations on the properties of matter at low temp which led, inter alia, to the production of liquid helium" .

H. K. Onnes, Commun. Phys. Lab.12,120, (1911); Nobel lecture, 1913..

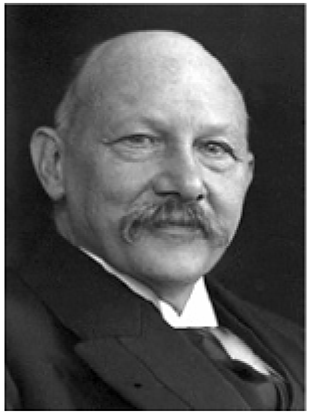

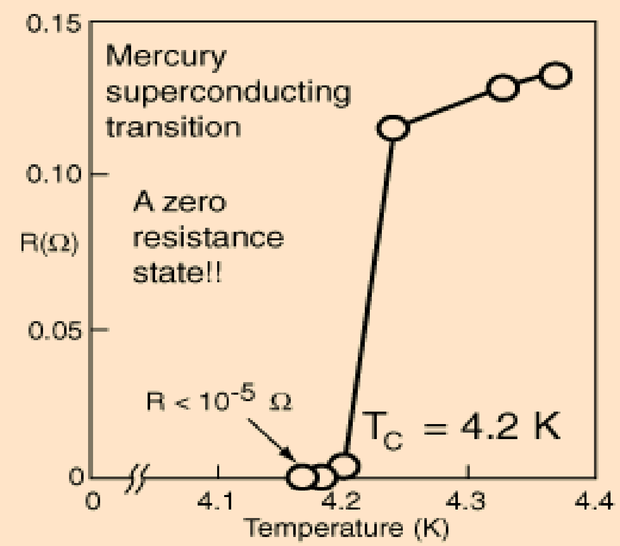

H. K. Onnes, Commun. Phys. Lab.12,120, (1911)

- The mercury was purified by distillation (very important → ***resistance*** at low ***T*** is dominated by impurity effects). They found that the resistivity suddenly dropped to zero @ 4.2K.
- This phenomenon was called superconductivity and the temperature at which it occurred is called its critical temperature.
- 1986: High-Temperature Superconductivity: T_c increased from *30°K → 130°K*

Superconducting materials

conventional (type I, soft) superconductors

(**except** Niobium, Technetium and Vanadium)

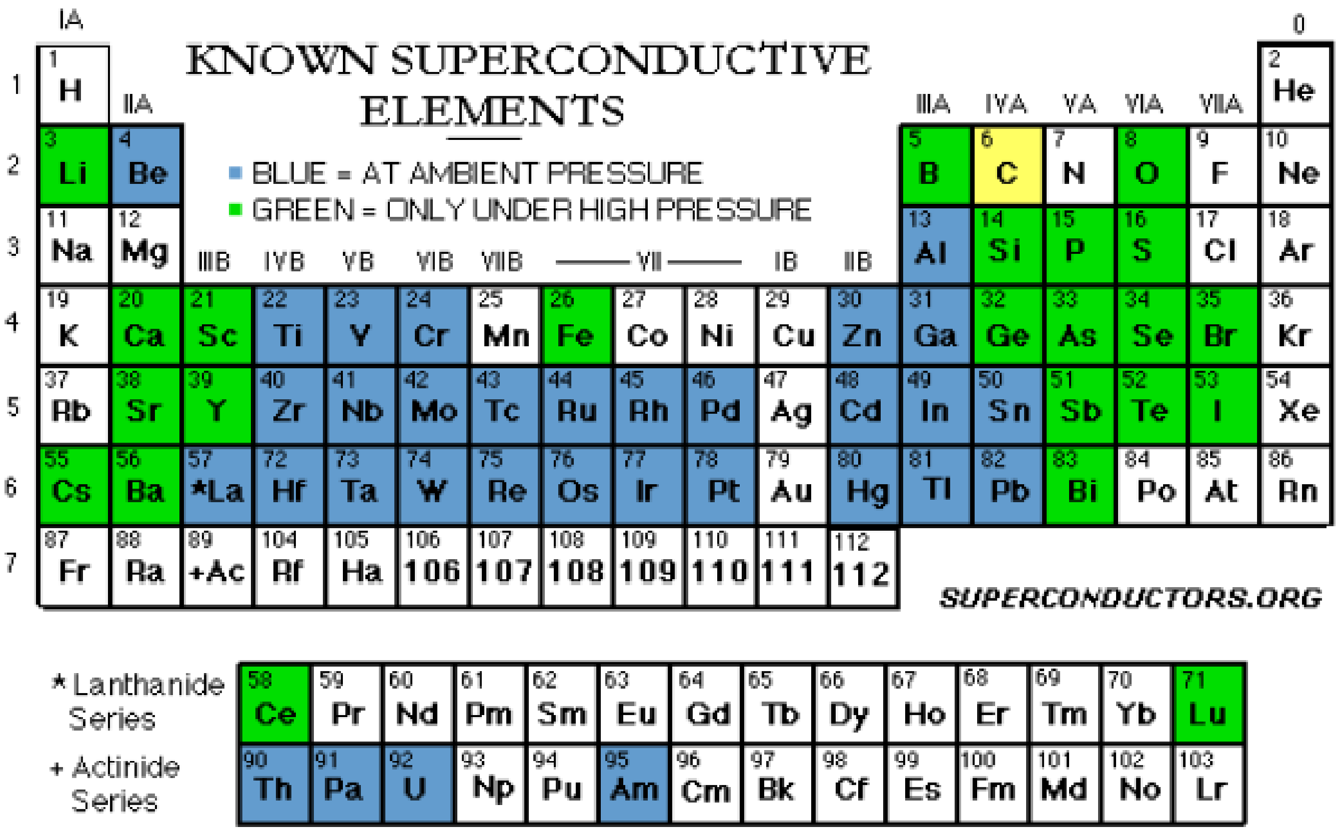

Remarkably, the best conductors at room temperature (gold, silver, and copper) do not become superconducting at all. They have the smallest lattice vibrations, so their behavior correlates well with the BCS theory

Critical Temperature of SC materials

Mat.	Tc
Be	0
Rh	0
W	0.015
Ir	0.1
Lu	0.1
Hf	0.1
Ru	0.5
Os	0.7
Mo	0.92
Zr	0.546
Cd	0.56
U	0.2
Ti	0.39
Zn	0.85
Ga	1.083

Mat.	Tc
Al	1.2
Pa	1.4
Th	1.4
Re	1.4
Tl	2.39
In	3.408
Sn	3.722
Hg	4.153
Ta	4.47
V	5.38
La	6.00
Pb	7.193
Tc	7.77
Nb	9.46

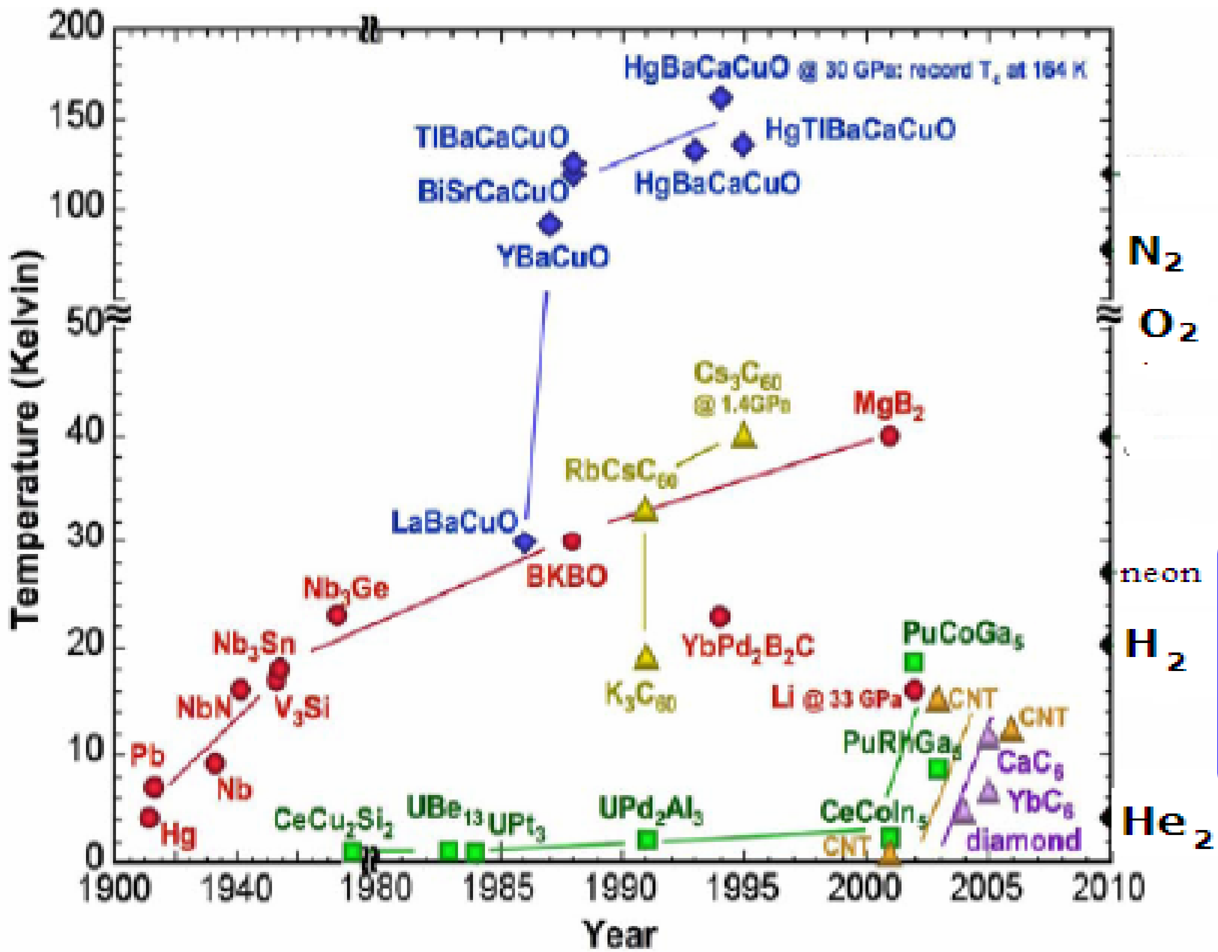

Material	T-Critical
Gallium	1.1 K
Aluminum	1.2 K
Indium	3.4 K
Tin	3.7 K
Mercury	4.2 K
Lead	7.2 K
Niobium	9.3 K
Niobium-Tin	17.9 K
La-Ba-Cu-oxide	30 K
Y-Ba-Cu-oxide	92 K
Tl-Ba-Cu-oxide	125 K

Type-II

1986 – High-temperature superconductivity
2001 – Magnesium diboride (Mg_2B) - Type II, T_c~ 40K

HT superconducting materials

Unconventional Type-II superconductors:

- metal alloys or complex oxide ceramics
- high temperature superconductors (complex copper oxide ceramics)
- pure metals: Nb, Tc, V

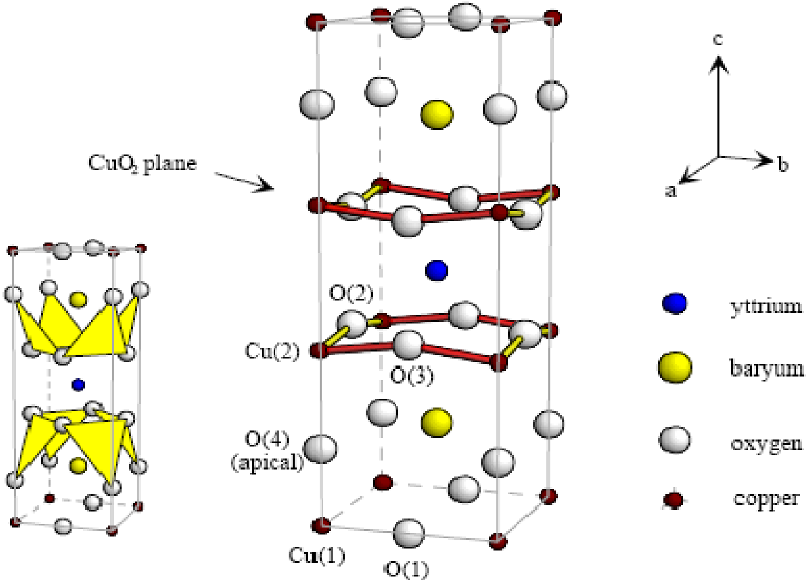

1986: Bednorz, Müller
(Nobel 1987)

Z. Phys. B, 64, 189 (1986)

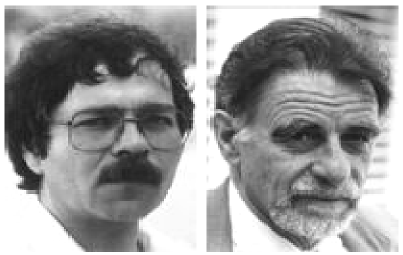

Alloys

Material	Transition Temp (K)	Critical Field (T)
NbTi	10	15
PbMoS	14.4	6.0
V_3Ga	14.8	2.1
NbN	15.7	1.5
V_3Si	16.9	2.35
Nb_3Sn	18.0	24.5
Nb_3Al	18.7	32.4
$Nb_3(AlGe)$	20.7	44
Nb_3Ge	23.2	38

From Blatt, Modern Physics

metal-oxide compounds
(perovskites)

Metal-oxide	Tc [K]
(La1.85Ba.15)CuO4	30K
YBa2Cu3O7	92K
HgBa2Ca2Cu3O8	133-135K

Courtesy of M.Calame, University of Basel

Phase Transition (1)

In normal conductor electron gas theory predicts relation between thermal conductivity ***k*** and electron conductivity **σ** of metal

$$\frac{k}{\sigma} = \frac{3}{2}\left(\frac{k_B}{e}\right)^2_{T_c} T$$ Wiedemann-Franz

$$k = \frac{1}{2} v^2 \tau \cdot C_v$$

$$C_v = \gamma T + A T^3$$

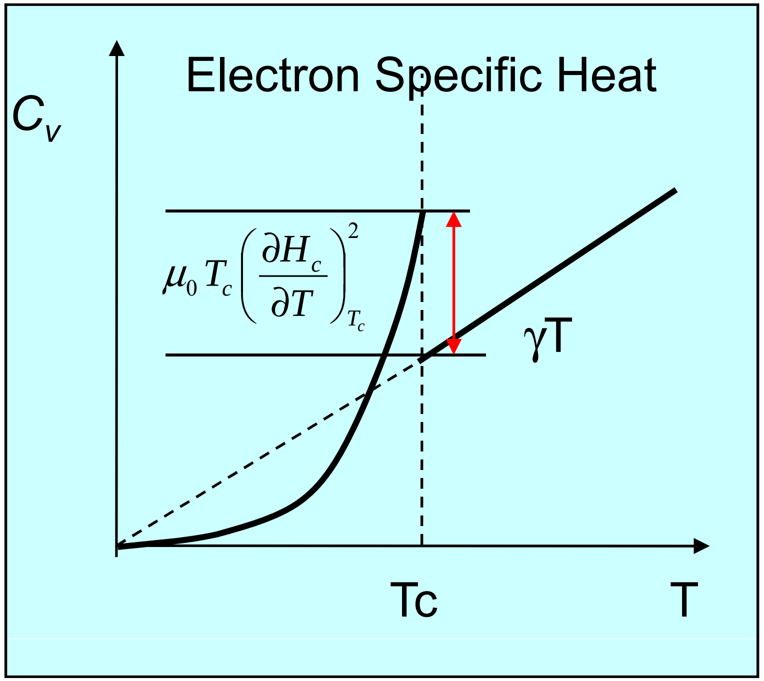

Cv -specific heat with electron and photon contribution added

In superconductor experimentally observed different T dependence

$$C_v \propto \exp\left(-\frac{\Delta}{k_B T}\right)$$

Evidence for energy gap

Meissner effects and critical field

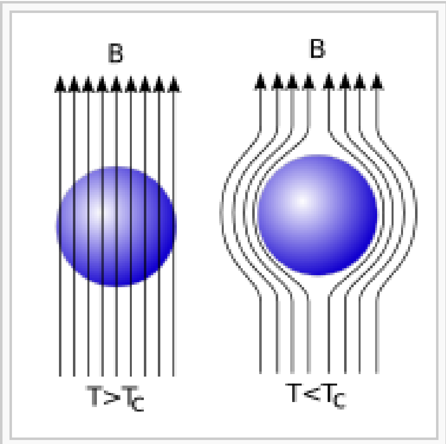

Walther **Meissner** and Robert **Ochsenfeld,** 1933 - exclusion magnetic flux inside superconductor – perfect diamagnetism (different from ideal conductor)

A magnet levitating above a superconductor

Key experimental facts

- Magnetic field is expelled from superconductor (at DC)
- Superconductivity destroys by magnetic field $H > H_c(T)$
- Thermodynamic critical magnetic field $H_c(T)$

$$H_c(T) = H_c(0)\,[1-(T/T_c)^2]$$

- Behavior of good normal material and superconductors is similar in AC magnetic field

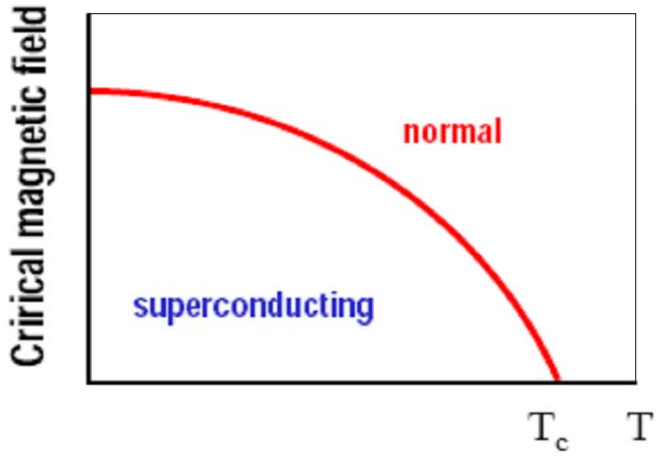

Type-I and Type II superconductors

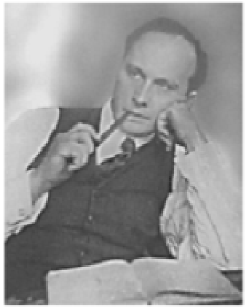

Measurements of magnetization *M(H)* have shown partial Meissner effect in many superconducting materials (mostly alloys) - *Shubnikov 1935*

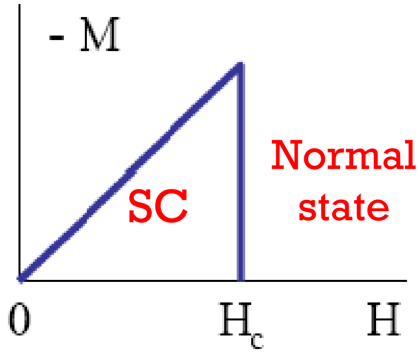

Complete Meissner effect in type-I superconductors

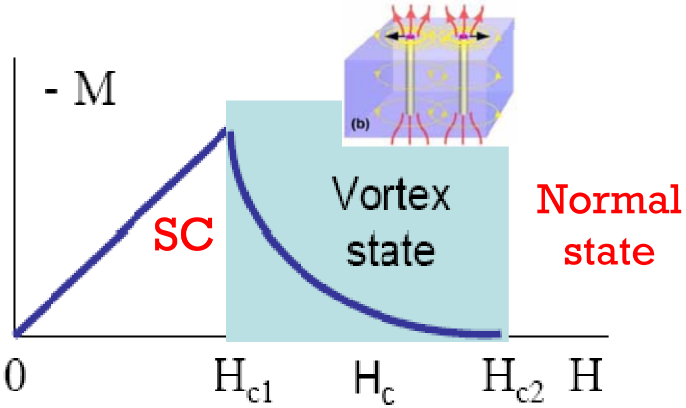

High-field partial Meissner effect in type-II superconductors

Pure Nb is weakly type II ($H_{c1} \approx 16$ mT, $H_c \approx 19$ mT, $H_{c2} \approx 30$ mT);
Impurities decrease H_{c1} and increase H_{c2}, but do not affect H_c

London equations (1935)

- Two-fluid model: coexisting SC and N "liquids" with the densities $n_s(T) + n_n(T) = n$.

- Electric field E accelerates only the SC component, the N component is short circuited.

- Second Newton law for the SC component: $m dv_s/dt = eE$ yields the first London equation:

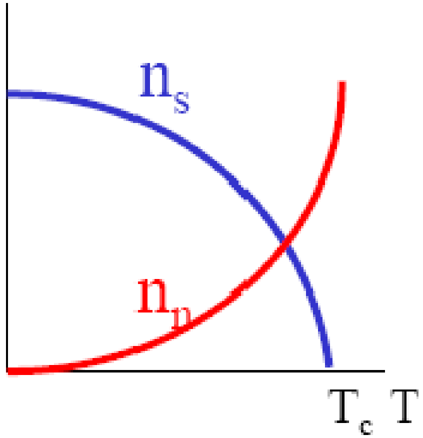

$$dJ_s/dt = (e^2 n_s/m)E \quad \Longleftrightarrow \quad J = \sigma E$$

(ballistic electron flow in SC) (viscous electron flow in metals)

- Using the Maxwell equations, $\nabla\times E = -\mu_0 \partial_t H$ and $\nabla\times H = J_s$ we obtain the second London equation:

$$\lambda^2 \nabla H - H = 0$$

- London penetration depth: $\lambda = \left(\frac{m}{e^2 n_s(T) \mu_0} \right)^{1/2}$

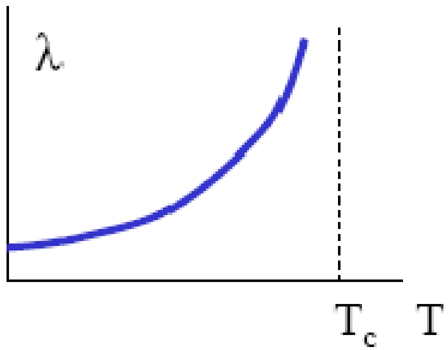

Dc screening of the magnetic field

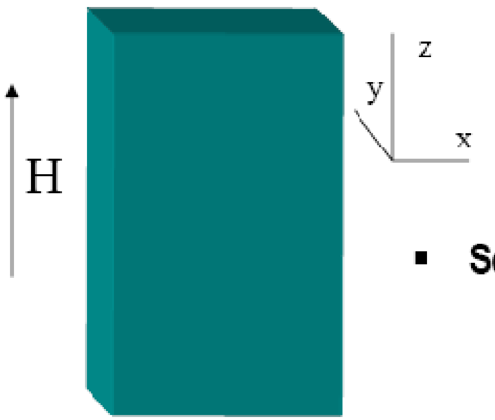

- London equation

$$\lambda^2 \frac{\partial^2 H_z}{\partial y^2} - H_z = 0$$

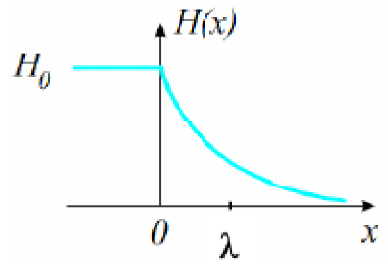

- Screening surface current density $J_s(y)$:

$$H(y) = H_0 e^{-y/\lambda}, \qquad J_s(y) = \frac{H_0}{\lambda} e^{-y/\lambda}$$

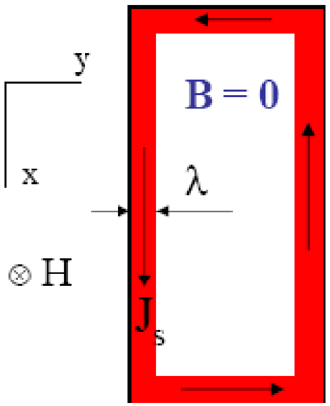

- Meissner effect: no magnetic induction B in the bulk.
- J(0) at the surface cannot exceed the depairing current density J_d :

$$J_d = \frac{H_c(T)}{\lambda(T)} \cong J_0 \left(1 - \frac{T^2}{T_c^2}\right)^{3/2}$$

$J_d(0) \approx 2.8$ MA/mm^2 for pure Nb

Modification of London equations

- If size of sc pair $\xi_0 > \lambda_L$ ➔ non-local electrodynamics. London equation will modified with new a scale λ_p (Pippard)

$$\lambda_p = \left(\frac{\sqrt{3}}{2\pi} \xi_0 \lambda_L^2 \right)^{1/3}, \qquad \lambda << \xi \ (\text{Pippard Limit})$$

Quantum modification ➔ magnetic flux quantization

Wave function: $\psi(r) = (n_s/2)^{1/2} e^{i\theta(r)}$

Momentum: $\hbar \nabla \theta = 2m\vec{v}_s + \frac{2e}{c}\vec{A}$

Current: $\vec{j}_s = n_s e \vec{v}_s = \frac{n_s e}{m} \vec{p}_s$

or

$$\vec{j}_s = \frac{1}{c\Lambda}\left(\frac{\Phi_0}{2\pi} \nabla \theta - \vec{A} \right)$$

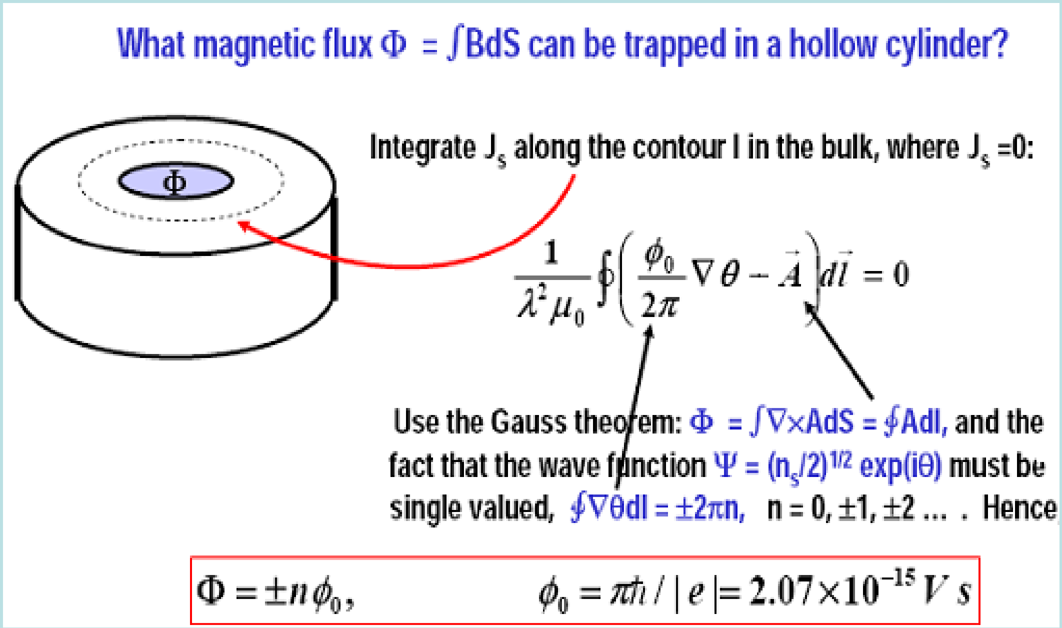

Surface resistance

London equations

$$\frac{\partial \vec{J}_s}{\partial t} = -\frac{\vec{E}}{\lambda^2 \mu_0}, \qquad \lambda^2 \nabla^2 \vec{H} - \vec{H} = 0$$

$$j_s = j_{s0} e^{i\omega t}; \qquad j_s = \frac{-i}{\omega \mu_0 \lambda_L^2} E = -i\sigma_s E$$

$$\sigma_s = \frac{n_s e^2}{m\omega}; \qquad \sigma_n = \frac{n_n e^2 \tau}{m}; \qquad \sigma = \sigma_n - i\sigma_s$$

$$\nabla^2 E = \tau_{tot}^2 E; \qquad \tau_{tot}^2 = \sqrt{i\omega\mu_0(\sigma_n - i\sigma_s)}$$

$$Z_s = \sqrt{\frac{i\omega\mu_0}{(\sigma_n - i\sigma_s)}} = R_s + iX_s \qquad R_s = \frac{1}{2}\sigma_n \omega^2 \mu_0^2 \lambda_L^3; \qquad X_s = \omega\mu_0\lambda$$

$$R_s \propto \omega^2 \quad \textit{and} \quad R_s \propto \sigma_n \propto n_n \propto \exp(-\frac{\Delta}{k_B T})$$

also $R_s \propto \lambda_L^2 = \dfrac{m}{n_s e^2 \mu_0}$

BCS theory gives more accurate result

Success of Two Fluid Model

- Specific Heat
- Meissner Effect
- T Dependence of Hc
- T Dependence of λ
- Impurity Effect
- RF surface resistance

Difficulties:

- Predicted negative boundary energy between **sc** and **nc** phases ➔ in magnetic field is favorable for SC to brake in multilayer **sc-ns-sc-ns** structure.

(not true for Type-I superconductor)

GL free energy

- Complex superconducting order parameter $\Psi = (n_s/2)^{1/2}\exp(i\theta)$
- For $T \approx T_c$, Ψ is small so the free energy can be expanded in the Taylor series in Ψ:

$$F = F_n + \int dV \left[\alpha(T)|\Psi|^2 + \frac{\beta}{2}|\Psi|^4 + \frac{\hbar^2}{2m^*}\left|\left(\nabla + \frac{2\pi i\vec{A}}{\phi_0}\right)\Psi\right|^2 + \frac{\mu_0 H^2}{2} \right]$$

nonlinear inhomogeneity magnetic

- The coefficient $\alpha(T) = \alpha_0(T - T_c)/T_c$ changes sign at T_c

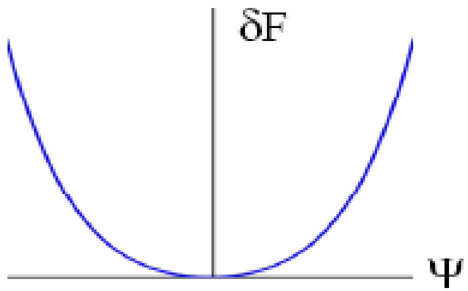

Normal state

$T > T_c$, $\Psi = 0$

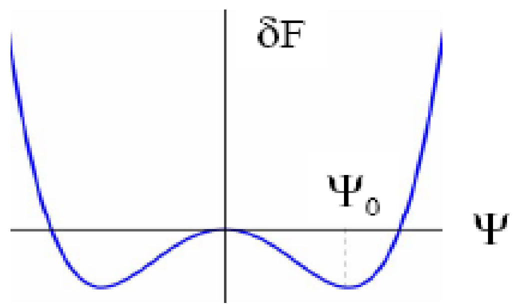

Superconducting state

$T < T_c$, $\Psi_0 = (|\alpha|/\beta)^{1/2}$

Energy gain define critical magnetic field :

$$\frac{F_n - F_s}{V} = \frac{\alpha^2(T)}{2\beta} = \frac{\mu_0 H_c^2(T)}{2}$$

Ginzburg-Landau equations

Energy minimization conditions $\delta F/\delta\Psi^* = 0$ and $\delta F/\delta A = 0$ yield the GL equations for the dimensionless order parameter $\psi = \Psi/\Psi_0$

$$\xi^2\left(\nabla + \frac{2\pi i}{\phi_0}\vec{A}\right)^2\psi + \psi - \psi|\psi|^2 = 0,$$

$$\nabla\times\nabla\times\vec{A} = \vec{J}_s = -\frac{|\psi|^2}{\lambda^2}\left(\frac{\phi_0}{2\pi}\nabla\theta + \vec{A}\right)$$

- Two coupled complex nonlinear PDE for the pair wave function $\psi(r)$ and the magnetic vector-potential $A(r)$, $(B=\nabla\times A)$.
- Two fundamental lengths ξ and λ
- Boundary condition between a superconductor and vacuum $J_s = 0$:

$$\left(\nabla + \frac{2\pi i}{\phi_0}\vec{A}\right)\psi\vec{n} = 0$$

Fundamental lengths λ and ξ and the GL parameter κ = λ/ξ

- Magnetic London penetration depth:

$$\lambda(T) = \left(\frac{m\beta}{2e^2\mu_0\alpha_0}\right)^{1/2}\sqrt{\frac{T_c}{T_c - T}}$$

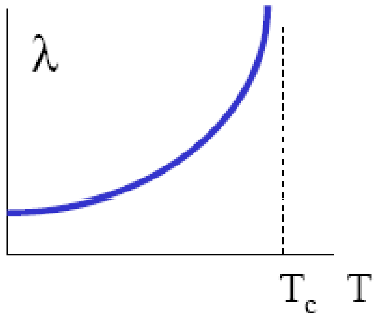

- Coherence length – a new scale of spatial variation of the superfluid density n_s(r) or superconducting gap Δ(r):

$$\xi(T) = \left(\frac{\hbar^2}{4m\alpha_0}\right)^{1/2}\sqrt{\frac{T_c}{T_c - T}}$$

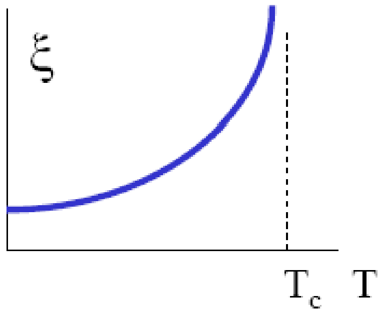

- The GL parameter κ = λ/ξ is independent of T.
- Critical field H_c(T) in terms of λ and ξ:

$$B_c(T) = \frac{\phi_0}{2\sqrt{2}\pi\xi(T)\lambda(T)}$$

Parameter of order κ_{GL}

$\kappa_{GL} < \frac{1}{\sqrt{2}}$ $\qquad \kappa_{GL} = \frac{\lambda_L}{\xi_0}$ $\qquad \kappa_{GL} > \frac{1}{\sqrt{2}}$

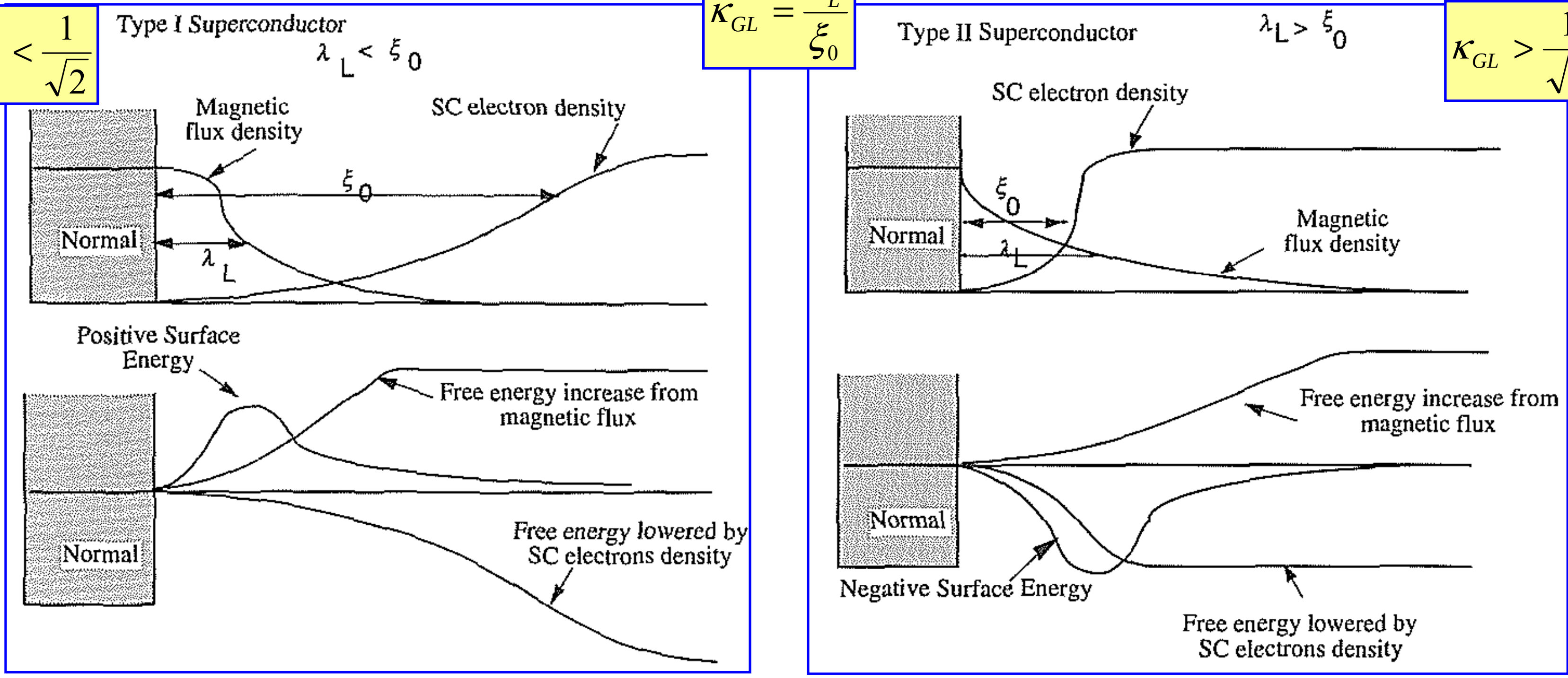

+Density of sc electrons suppressed over the distance ξ_0

- Admitting the applied field He over λ_L

Net boundary energy per unit area:

$$\Delta E = \frac{\mu_0}{2}\left(\xi_0 H_c^2 - \lambda_L H_e^2\right)$$

He – external field

Vortex in superconductor

Single vortex line

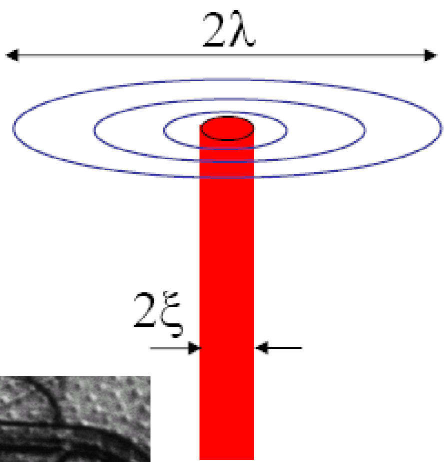

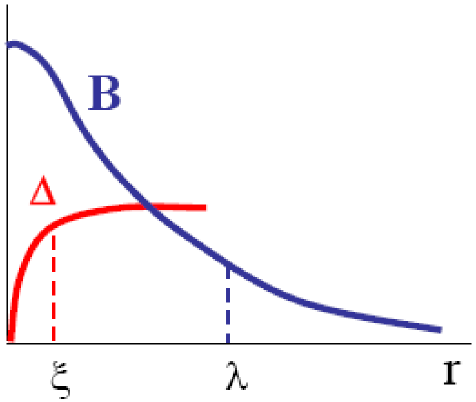

- Small core region $r < \xi$ where $\Delta(r)$ is suppressed
- Region of circulating supercurrents, $r < \lambda$.
- Each vortex carries the flux quantum ϕ_0

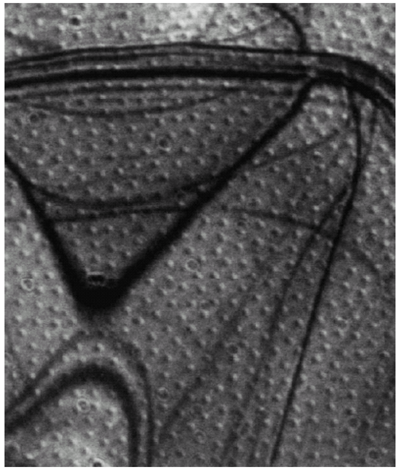

Picture of vortexes

Important lengths and fields

- Coherence length ξ and magnetic (London) penetration depth λ

$$B_{c1} = \frac{\phi_0}{2\pi\lambda^2}\left(\ln\frac{\lambda}{\xi} + 0.5\right), \qquad B_c = \frac{\phi_0}{2\sqrt{2}\pi\lambda\xi}, \qquad B_{c2} = \frac{\phi_0}{2\pi\xi^2}$$

A.Gurevich

Type-II superconductors: $\lambda/\xi > 1/\sqrt{2}$: For clean Nb, $\lambda \approx 40$ nm, $\xi \approx 38$ nm

BCS Theory of Superconductivity

- SC was explained in 1957 by John Bardeen, Leon Cooper, and Robert Schrieffer (BCS theory). Nobel Prize,1972.
- It was simultaneously explained by Nikolay Bogoliubov (Bogoliubov transformations).

Key mechanism - electrons near Fermi level are pairing into Cooper pairs through interaction with the crystal lattice; the coupling to the lattice is called a phonon interaction.

ξ - Coherence length

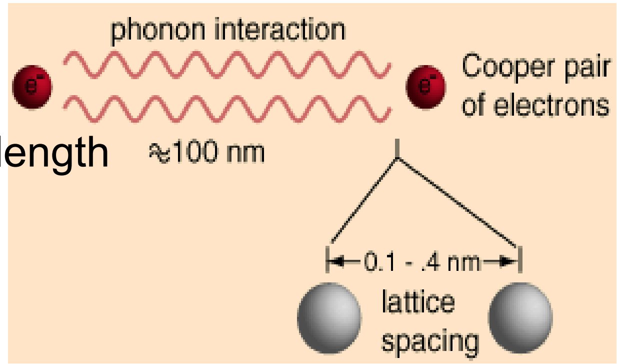

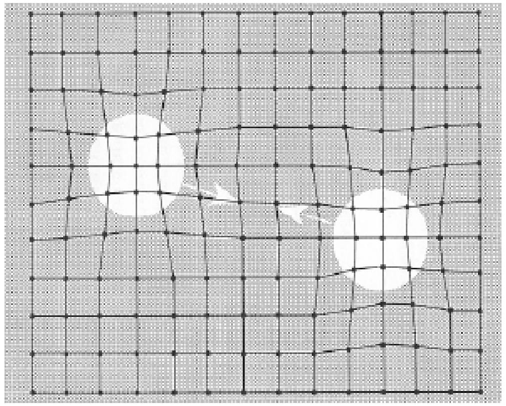

Polarization of atomic lattice by electrons → Second electron “feels” attraction→ Pairing decrease energy → bozons $\{\vec{p}\downarrow, -\vec{p}\uparrow\}$

Fermi distribution

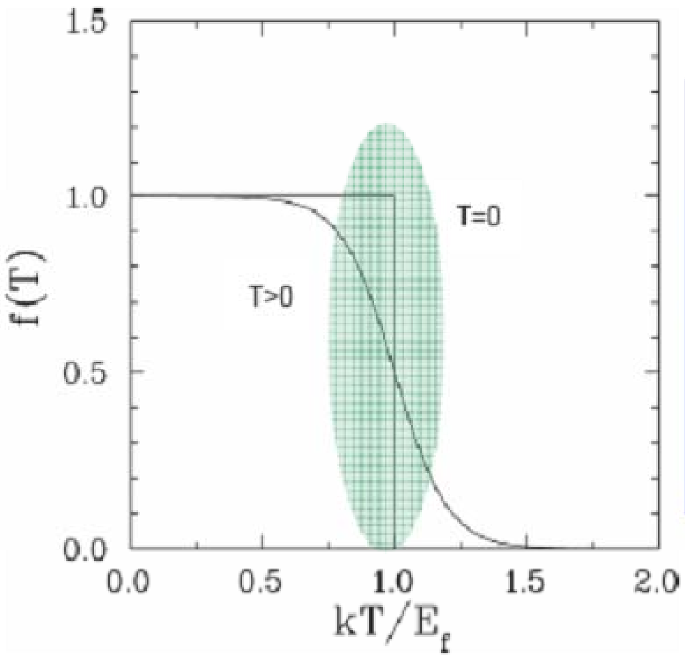

Electrons are fermions → Pauli

Fermi-liquid (electron gas)
→ All states are filled up to the Fermi-energy (T=0)
→ For T>0: broadening around E_F
→ Only e^- close to E_F contribute to scattering
→ Only these electrons can form Cooper pairs

Energy gap is a function of energy:

$$\Delta(T) = \Delta(T)\left[\cos(\pi \frac{T^2}{T_c^2})\right]^{1/2}$$

Pairs are bosons which can condense into the same energy level. The electron pairs have a slightly lower energy and leave an energy gap above them on the order of .001 eV

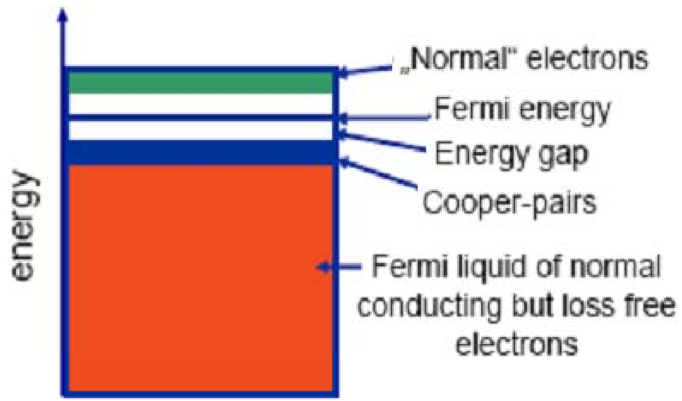

RF dissipation

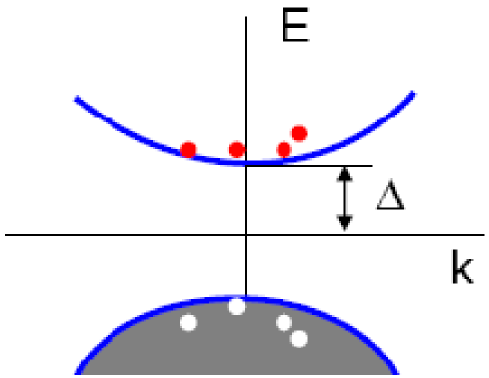

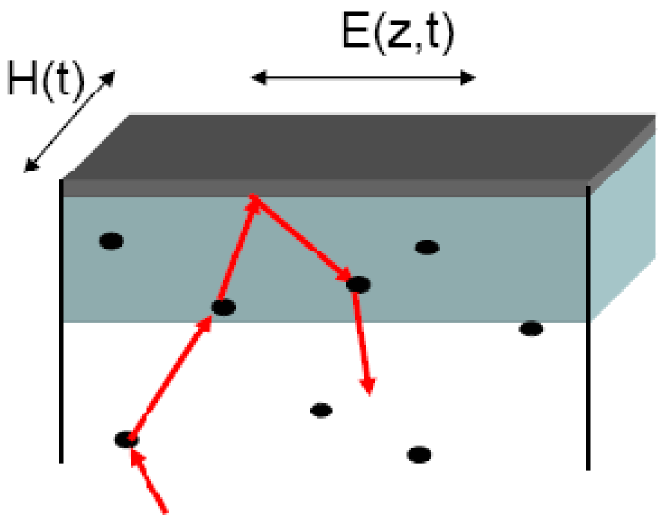

- Thermal activation of normal electrons

  $n_a = n_0(\pi T/2\Delta)^{1/2}\exp(-\Delta/T)$

- Accelerating electric field

  $E(z,t) = \mu_0\omega\lambda H_\omega e^{-\lambda|z|}\sin\omega t$

- Scattering mechanisms and normal state conductivity: $\sigma_n = e^2 n_0 l/p_F$, $p_F = \hbar(3\pi^2 n_0)^{1/3}$

- Surface: from specular to diffusive

- Normal skin effect ($l \ll \lambda$): multiple impurity scattering in the λ - belt:

  $R_s \sim (\mu_0^2\omega^2\lambda^3\sigma_n\Delta/T)\exp(-\Delta/T)$

- Anomalous skin effect ($l \gg \lambda$): scattering by the gradient of the ac field E(z):

  Effective $\sigma_{eff} \sim e^2 n_0\lambda/p_F$; $l \rightarrow \lambda$

Surface Resistance

$$R_S = R_{BCS} + R_{residual}$$

Residual from trapped flux:

$$R_{mag} = \frac{H_{ext}}{2H_{c2}} R_n = 0.3(n\Omega) \cdot H_{ext}(mOe)\sqrt{f(GHz)}$$

Hc2=2400 Oe, RRR=300;

Rn=1.2mΩ at 1GHz

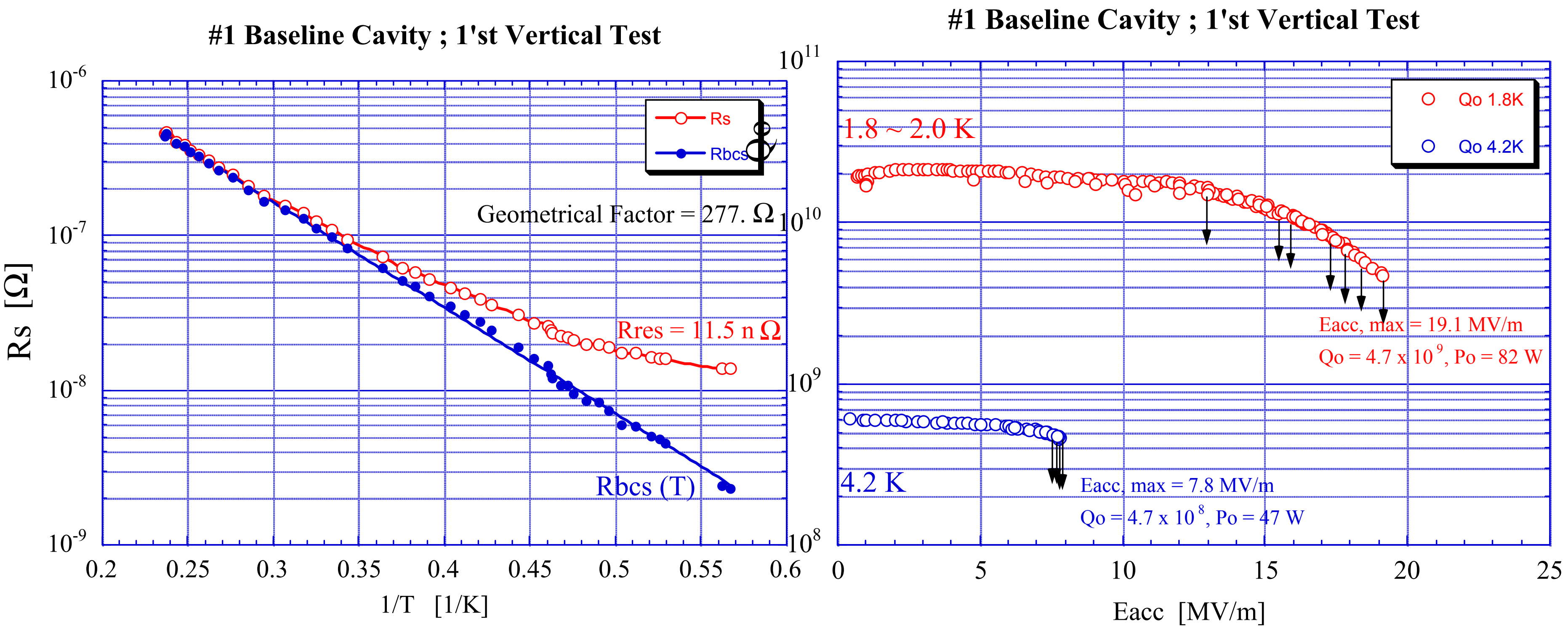

SC materials

Material	T_c (K)	$H_c(0)$ [T]	$H_{c1}(0)$ [T]	$H_{c2}(0)$ [T]	$\lambda(0)$ [nm]
Pb	7.2	0.08	na	na	48
Nb	9.2	0.2	0.17	0.4	40
Nb_3Sn	18	0.54	0.05	30	85
NbN	16.2	0.23	0.02	15	200
MgB_2	40	0.43	0.03	3.5	140
YBCO	93	1.4	0.01	100	150

Fluxoid	Φ_0	2.068×10^{-15} Wb
Boltzman Constant	k_B	1.38×10^{-23} JK^{-1}

Niobium has the highest Hc1 – good for SRF applications

Nb Surface – Theory and Reality

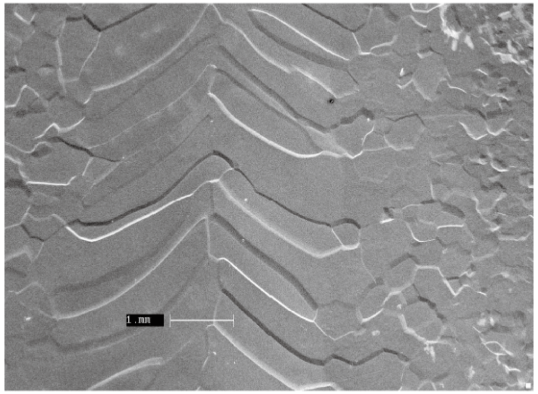

(a) 117μm BCP

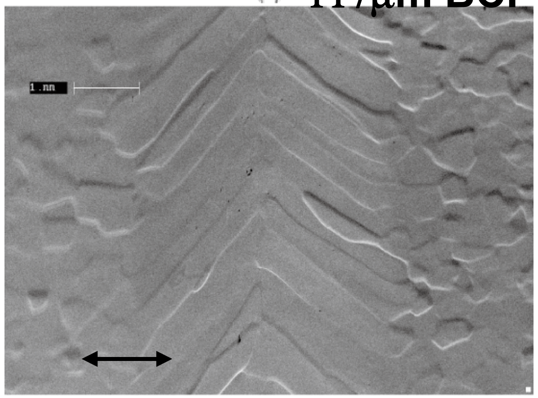

1 mm (b) +90μm EP

EBW Seam

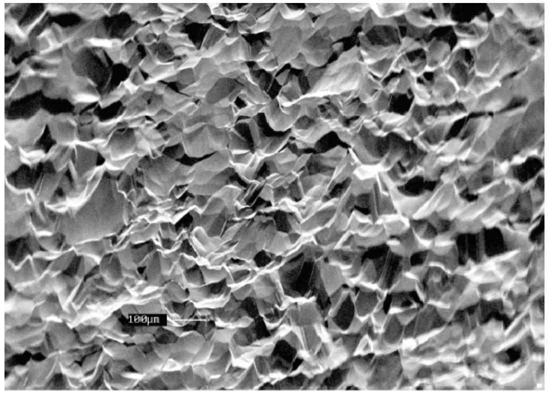

(a) 117μm BCP

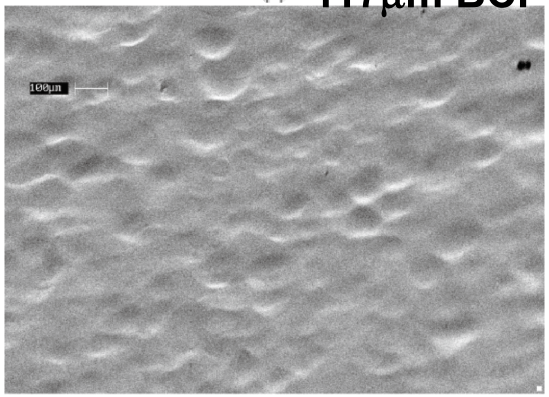

100 μm (b) +90μm EP

- Material is not uniform.
- Surface Condition is essential, but is usually irregular and contaminated.
- Oxide layers, grain boundaries.
- No Theory except BCS Surface Resistance.
- Many Steps in Production & Clean Works to improve resistance

H-field enhancement

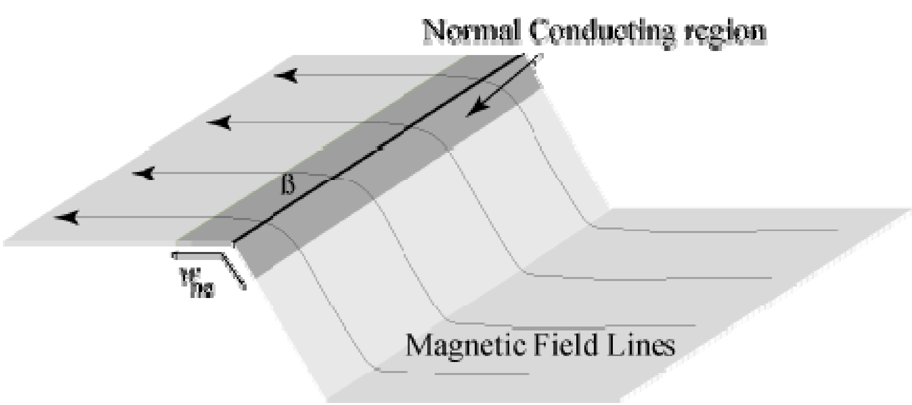

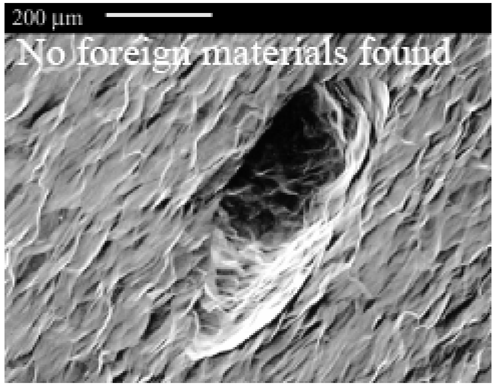

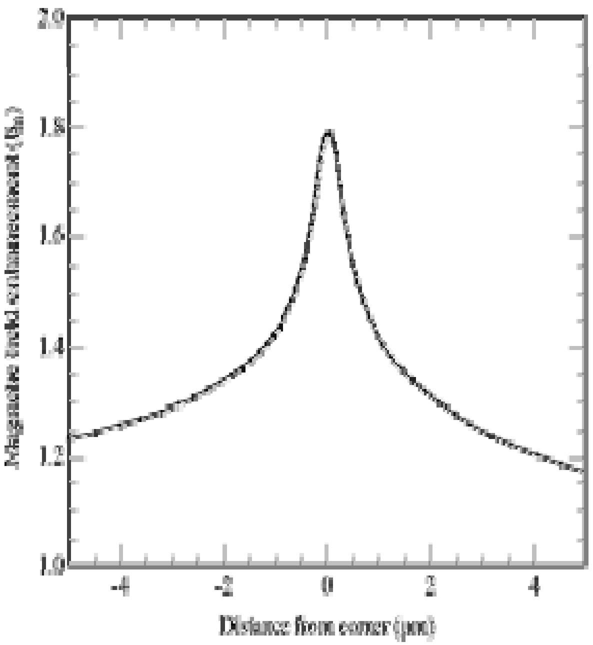

(a)

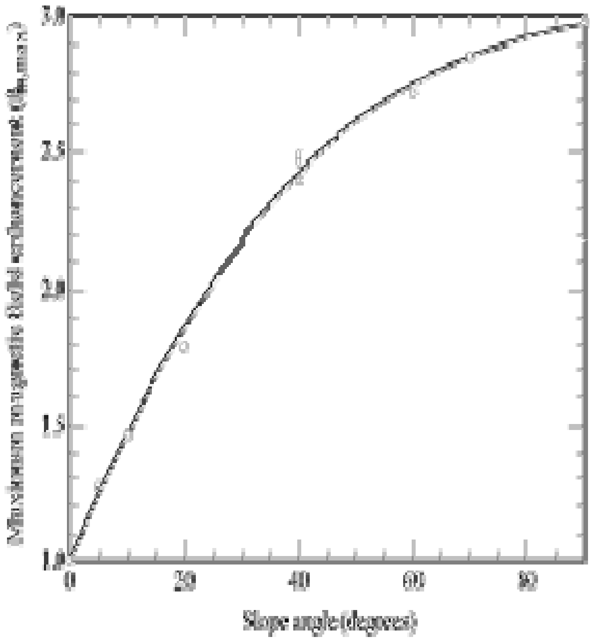

(b)

H-field enhancement is calculated at the edge of the µm size holes/pits .

V.Shemelin, Cornel Uni

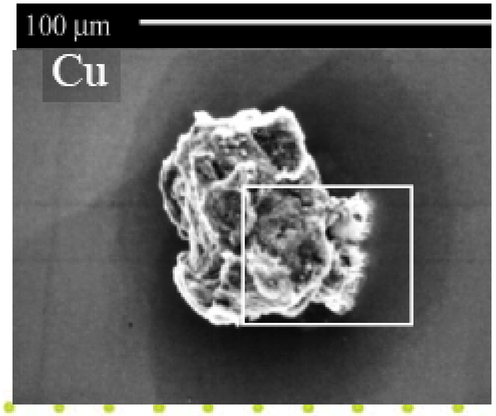

Vortex penetration: Magneto-Optical Imaging

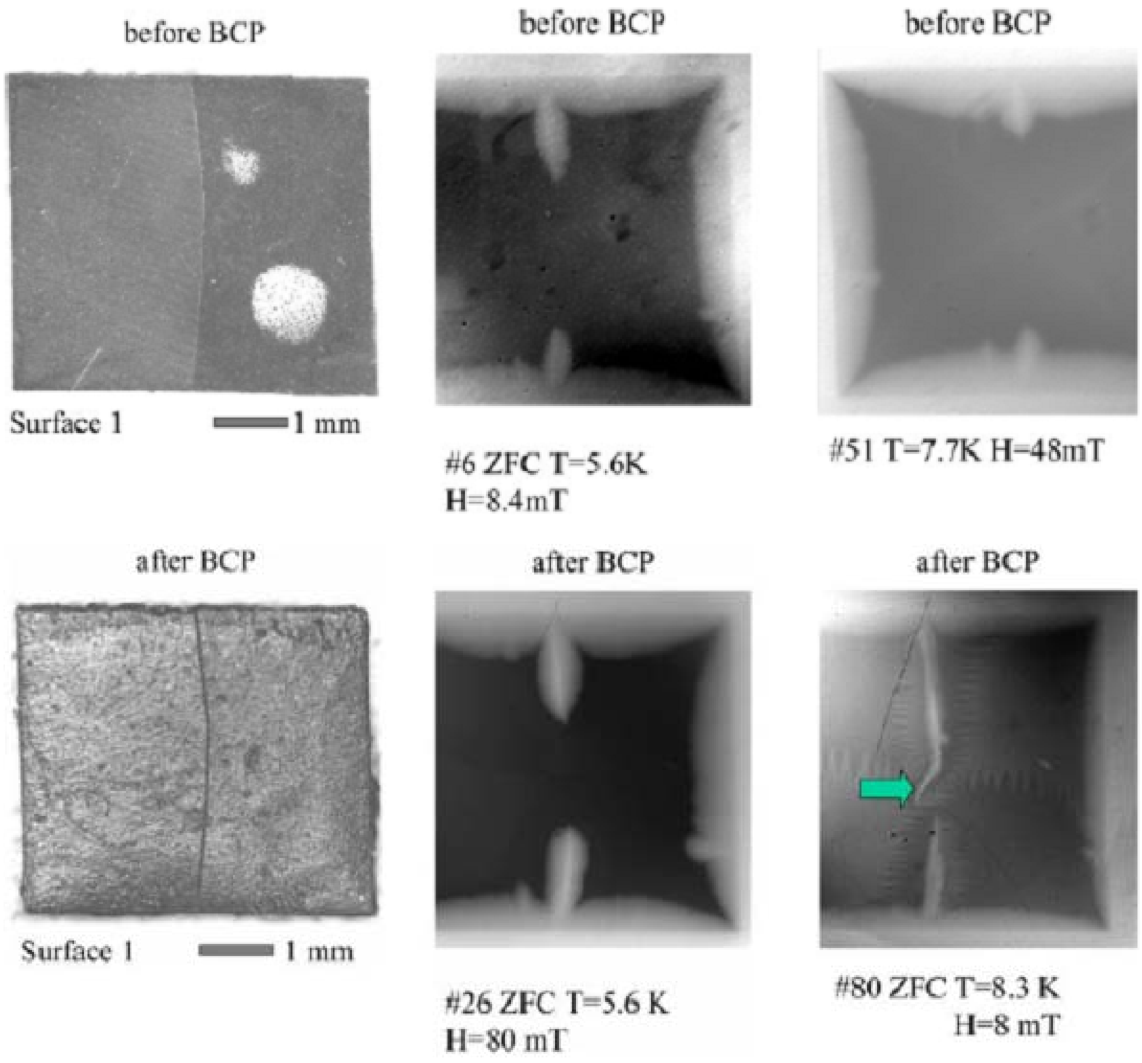

vortex penetration study in bi-crystal samples using magneto-optical measurements:

→Weaker super-conductivity in grain boundary ?

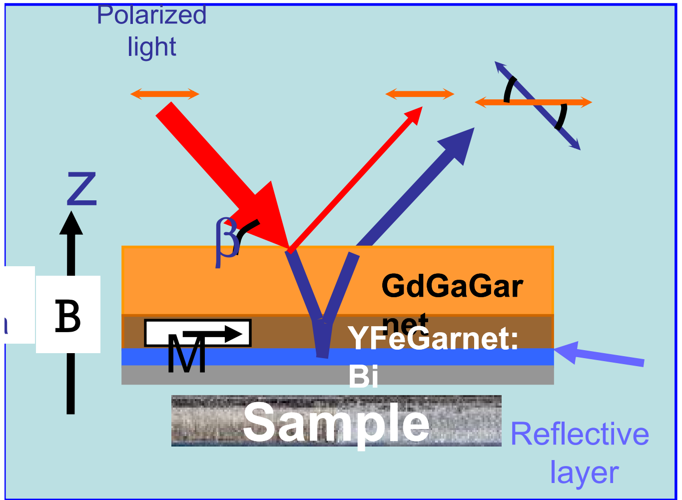

A.Polyanskii, P. Lee

SRF Cavity design and Constrains

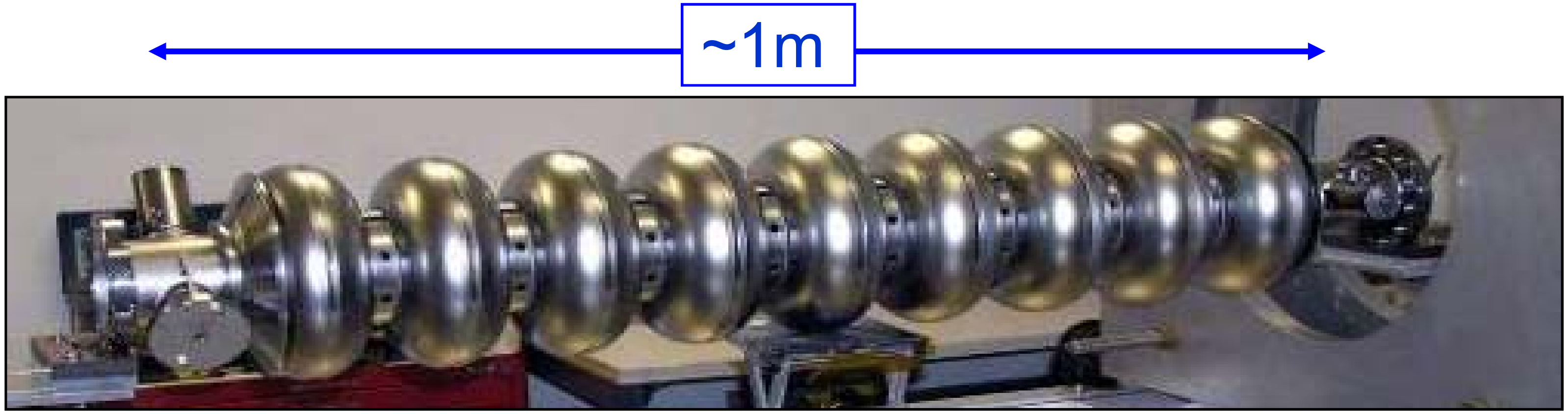

9-cell 1.3GHz Niobium Cavity

Max Achieved gradient = 42 MV/m

ILC acceptance = 35 MV/m

Baseline gradient = 31.5 MV/m (-10%)

Geometry of SC accelerating cavities

Most of projects are using multi-cell standing wave cavities

What is the cavity design constrains?

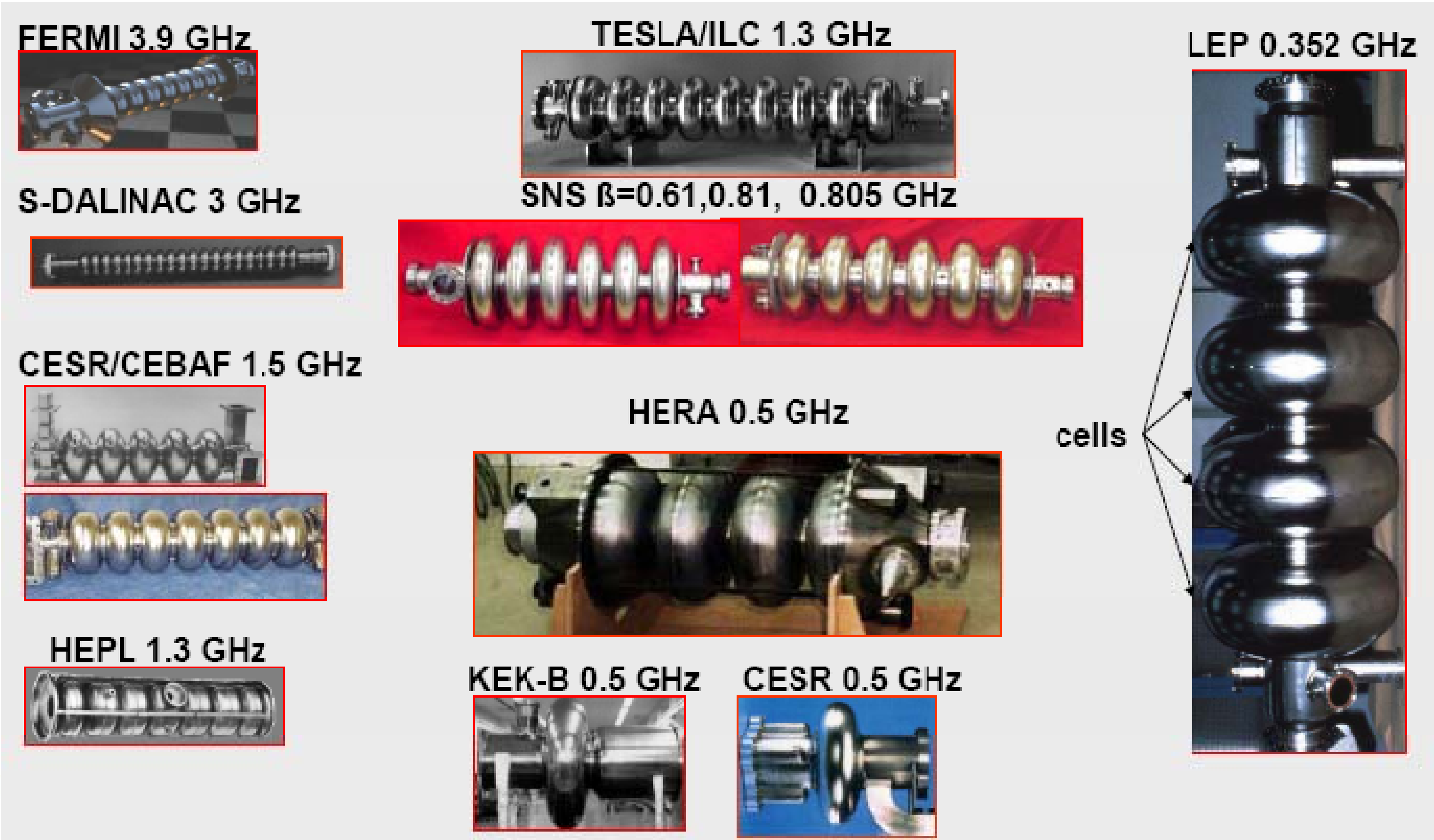

Cavity Design constrains

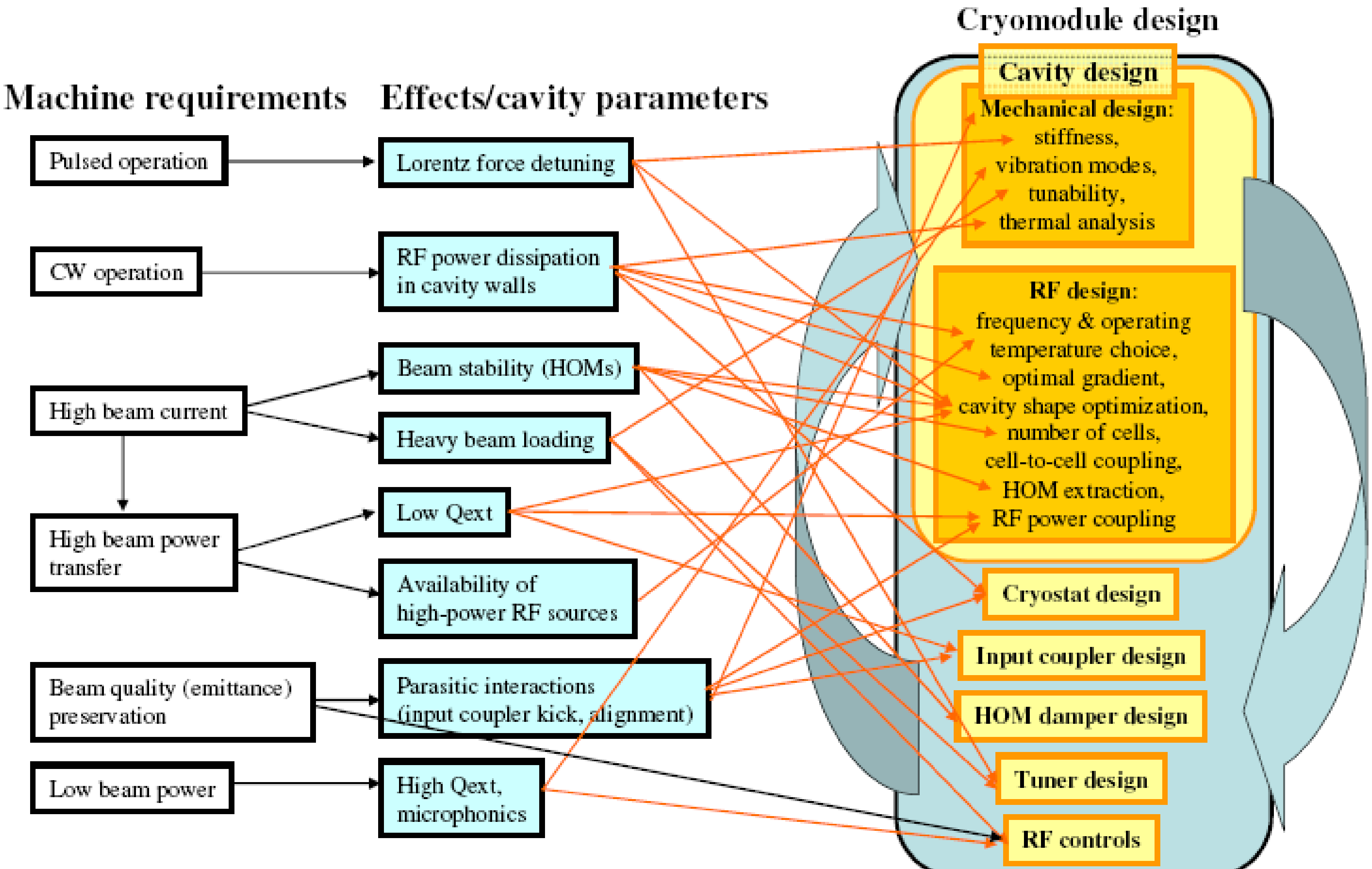

Cavity basic parameters

Main characteristics of SC acceleration structure:

- Resonance frequency of the operating mode f_0;
- Acceleration gradient E;
- Shunt impedance r per unit length; Shunt impedance is relationship between the acceleration gradient and dissipated power P per unit length of the structure. P is the sum of Ohmic losses in the structure P_{Ohm} and the power radiated through the coupling ports P_{rad}.

$$r = E^2 / P$$

- Unloaded quality factor Q_0 and geometry factor G:

$$Q_0 = \frac{\omega W}{P_{Ohm}} = \frac{\omega\mu_0 \int_V |H|^2 \, dV}{R_s \int_S |H|^2 \, dS} \equiv \frac{G}{R_s}, \qquad G = \frac{\omega\mu_0 \int_V |H|^2 \, dV}{\int_S |H|^2 \, dS}$$

(R_s - surface resistance, W - energy stored in the structure per unit length).

Cavity basic parameters (2)

- *(r/Q)* determines the relation ship between the acceleration gradient and energy stored in the acceleration structure *W* per unit length:

$$\left(\frac{r}{Q}\right) = \frac{E^2}{\omega W}$$

- Coupling to the feeding line:

$$\beta = \frac{P_{rad}}{P_{Ohm}}$$

- Loaded Q:

$$Q = \frac{\omega W}{P} = \frac{Q_0}{1+\beta}$$

- Field enhancement factors:

a) Electric: $$k_e = \frac{E_{surf\ pk}}{E};$$

b) Magnetic: $$k_m = \frac{B_{surf\ pk}}{E};$$

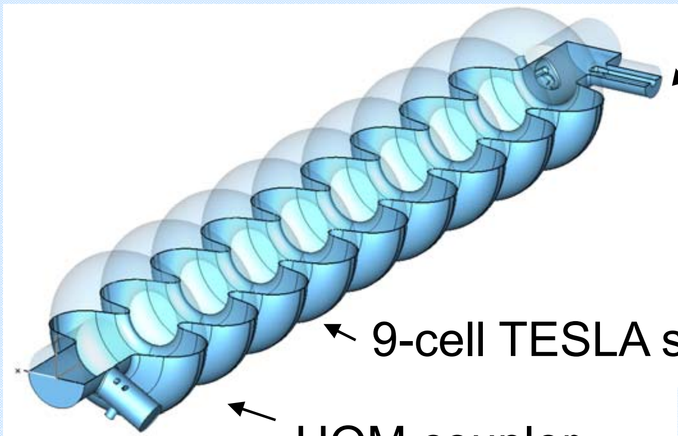

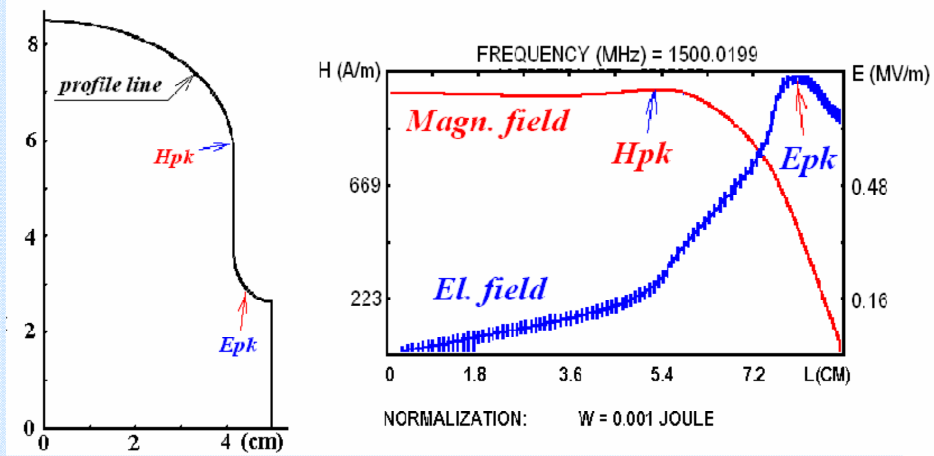

Geometry of an inner half-cell of a multicell cavity and field distribution along the profile line.

Cavity basic parameters (3)

- Coupling coefficient: $k_c = 2\frac{f_\pi - f_0}{f_\pi + f_0};$
- High Order Modes (HOM):

a) Monopole HOM spectrum – losses, bunch-to-bunch energy spread;

b) Dipole HOM spectrum – transverse kick, beam emittance dilution.

HOM frequencies, (r/Q)s and loaded Q-factors are critical, and are the subject of the structure optimization.

- **The structure cell geometry:**

Constrains:

-low field enhancement factors;

-no multipactoring.

Elliptical shape for the cell and the iris.

Examples:

- TESLA structure;
- Low Loss structure;
- Re-Entrant structure.

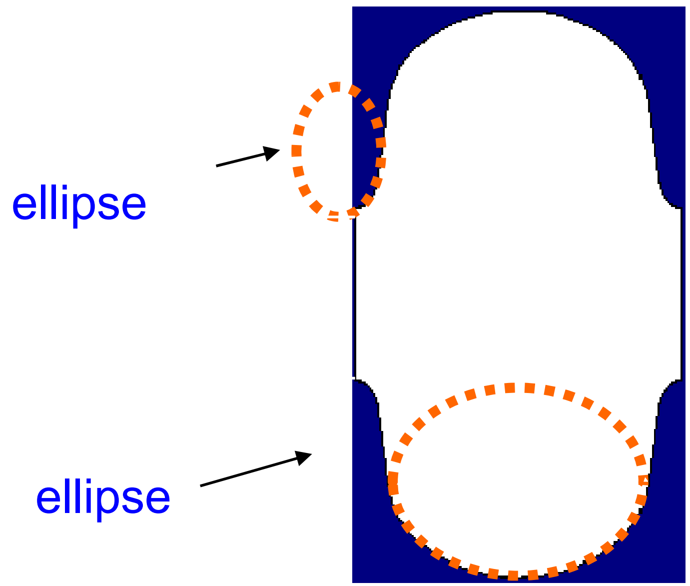

Aperture limitations

Large aperture is preferable!

- **Transverse wake:** $W_{\perp} \sim a^{-3}$

Transverse wake causes transverse beam instability and emittance dilution.

- **Coupling:** $k_c \sim a^{3\div 4}$

Small coupling causes severe tuning tolerances in order to achieve the filed longitudinal distribution flatness: $(\delta f / f) \sim k_c / N^{3/2}$

Small aperture is preferable!

- **(r/Q):** $(r/Q) \sim (r/Q)_0 - (r/Q)' \times a^{1\div 2}$

Small (r/Q) requires higher stored energy, longer filling time.

- **Electric field enhancement:** $k_e \sim k_0 + k' \times a^{1\div 2}$

Optimization: trade-off between these limitations.

Cavity Shape Optimization

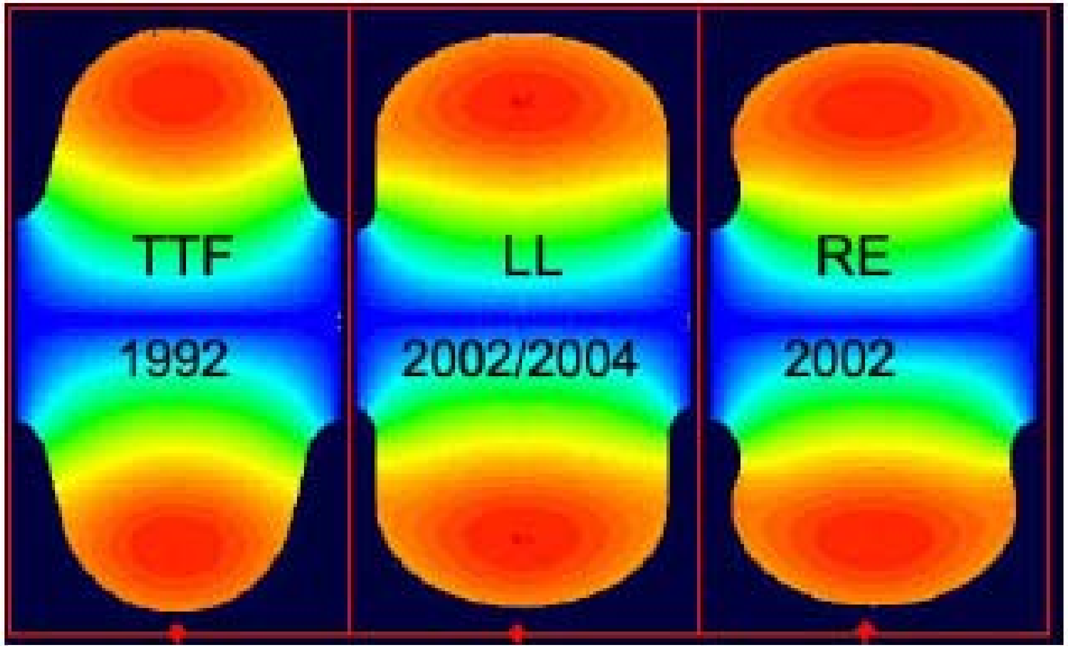

	TESLA	LL	RE
Aperture, mm	70	60	70
k_c,%	1.9	1.52	2.38
K_e = E/Eacc	1.98	2.36	2.39
k_m, mT/(MeV/m)	4.15	3.61	3.78
(r/Q), Ω	113.8	133.7	120.6
G, Ohm	271	284	280

HOM extraction/damping.

Criteria:

•Transverse modes: beam emittance dilution;

•Longitudinal modes: power losses, field enhancement, bunch-to-bunch energy spread.

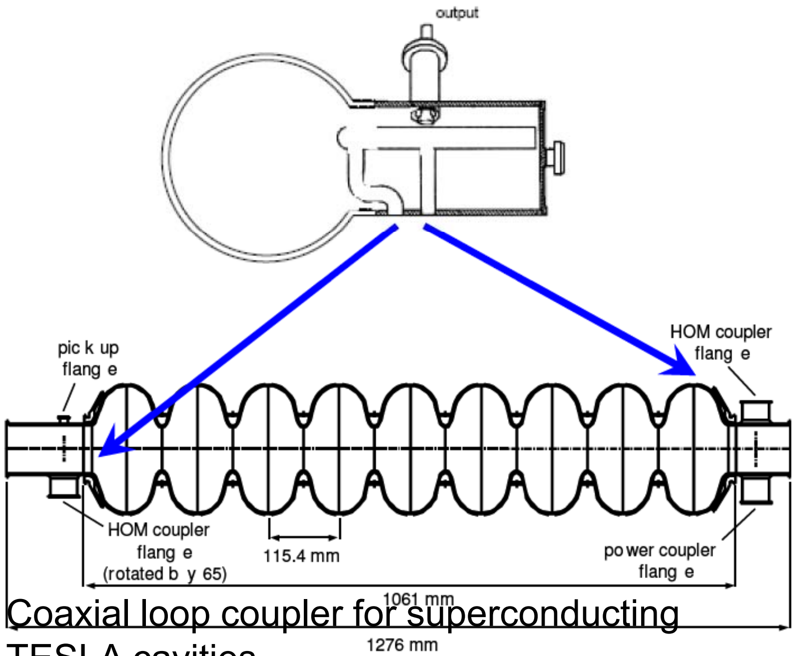

Coaxial loop coupler for superconducting TESLA cavities

Trapped modes.

The end cells are to be optimized in order to prevent the field distribution for HOMs having small field in the end cavities, so-called trapped modes. For the trapped modes it is a problem to reduce the loaded Q-factor to acceptable level.

RF kick caused by the input and HOM couplers.

Simple estimations of the transverse fields caused by the main coupler:

RF voltage*: U=(2PZ)1/2*, *Z*–coax impedance;

for *P*=300 kW and *Z*≈70 Ohms → *U* ≈ 6 kV

Transverse kick:

$$v = \frac{\Delta p_y c}{\Delta U_{acc}} \approx \frac{U}{2U_{acc}} = \frac{6kV}{2\times 30MV} = 10^{-4}$$

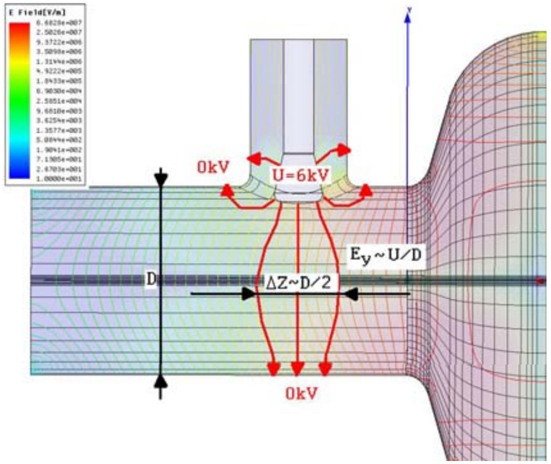

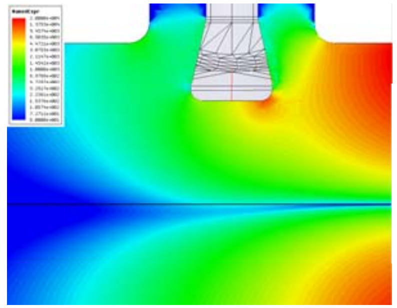

Transverse kick caused by the couplers acts on a bunch the same direction for all the RF cavities of the linac.

Real part may be compensated by the linac feedback system; **Imaginary** part dives the beam emittance dilution (here β is beta-function, σ is the bunch length, and U_0 is the initial beam energy):

$$\gamma\varepsilon \approx \gamma(z_{\max})y_{\max}y'_{\max} = \frac{\pi^2 v^2 E^2 \sigma^2 \beta^3 \gamma_0}{\lambda_{RF}^2 U_0^2}$$

Wakefield caused by the input and HOM couplers

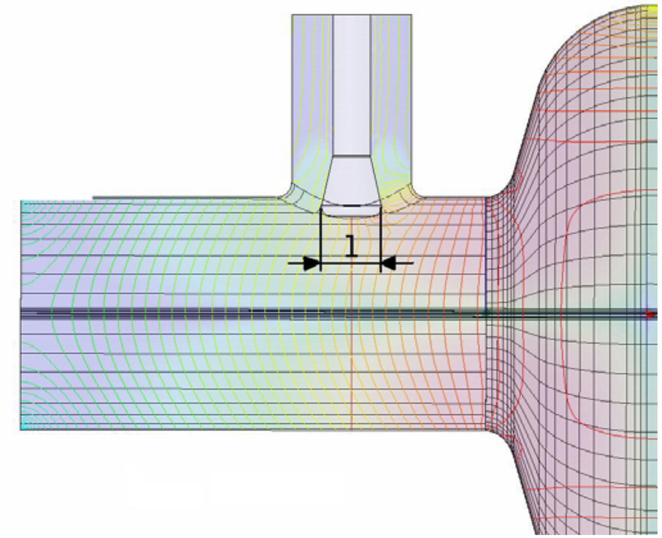

The couplers disturb the axial symmetry of the acceleration structure and cause the transverse kick, that depends on the particle longitudinal position inside a bunch, that, in turn, leads to the beam emittance dilution.

The catch-up length:

$L \sim a^2/2\sigma$; For ILC L~2.5 m, or about two periods (a=39 mm,σ=0.3 mm)

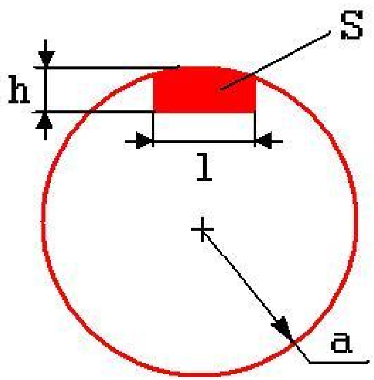

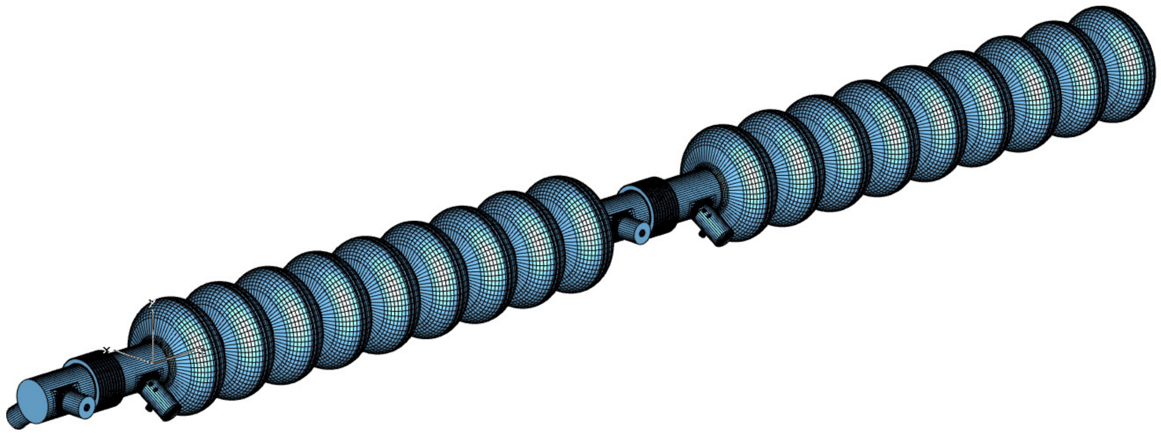

GdfidL simulations of Wakefielsds

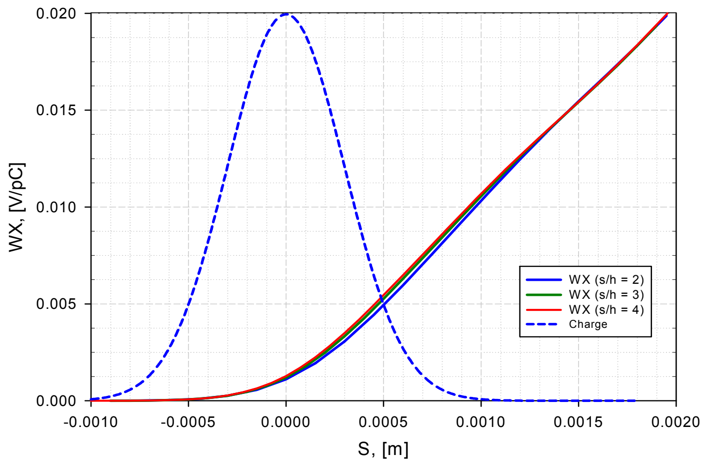

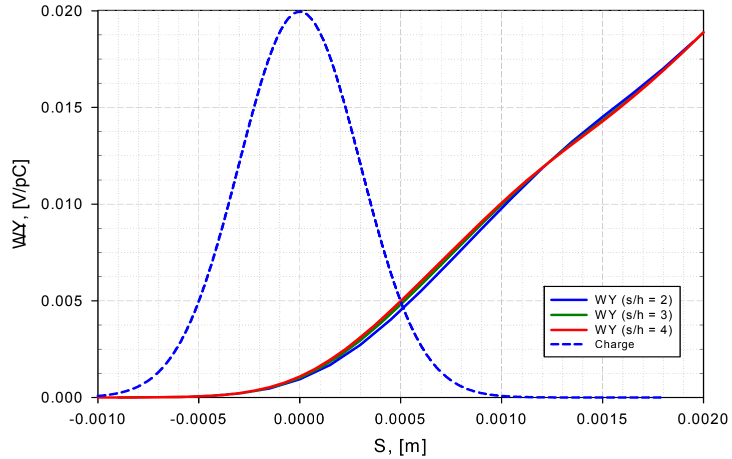

The wake field wake dependence on the longitudinal coordinate s for different mesh size for σ =0.3 mm for different numerical mesh parameters.

In ILC bunch compressor the wake leads to the unacceptable vertical emittance dilution. Cure is the new coupler design that preserve the structure axial symmetry.

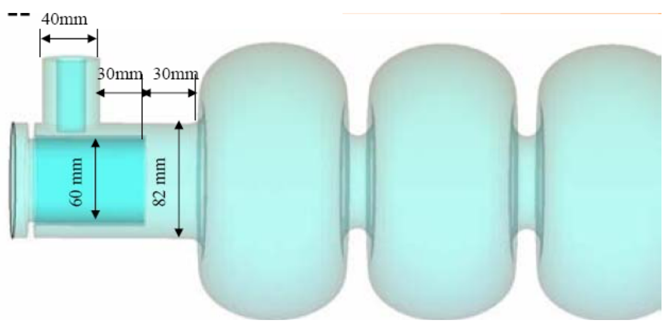

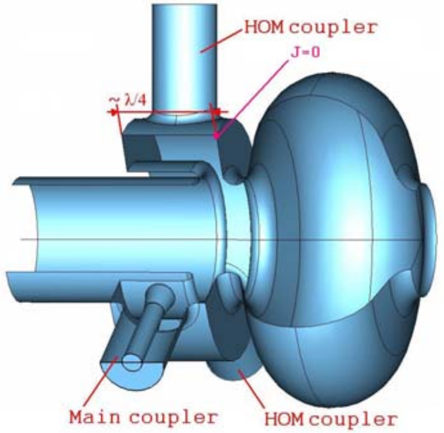

Tools for SC structure simulations:

I. **Field calculations:**
   -Spectrum, (r/Q), G, β
   -Field enhancement factors
   - HFSS (3D);
   - Microwave Studio (3D);
   - Omega-3P (3D); Analyst (3D);
   - SLANS (2D, high precision of the field calculation).

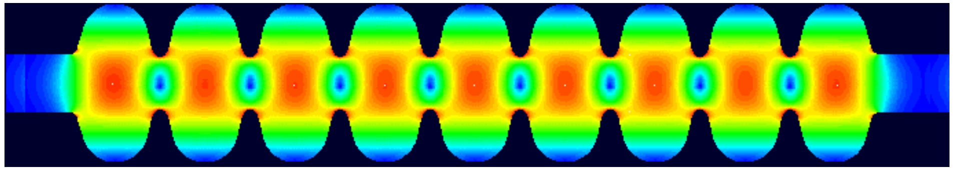

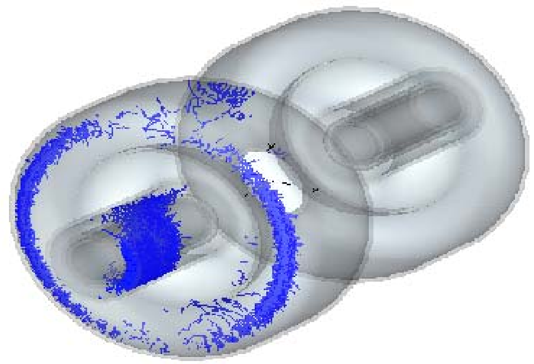

II. **Multipactoring (2D, 3D)**
   - Analyst; Omega-3P
   - Microwave Studio (3D); etc.

III. **Wakefield simulations (2D, 3D):**
   - GdfidL; PBCI; ECHO
   - MWS

IV. **Mechanical simulations:**
   Lorenz force and Lorenz factor,
   Vibrations,
   Thermal deformations.

a. ANSYS

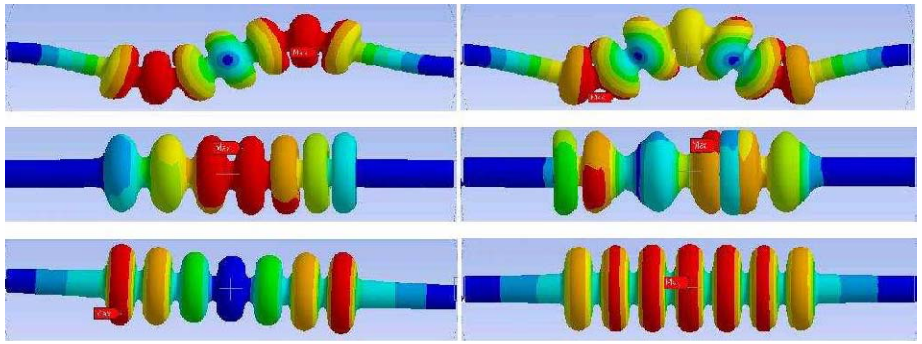

Frequencies ~ 50… 400 Hz

HOM and
HOM couplers and
Dampers

Effects of HOM

beam looses energy into HOMs, mostly on monopole

- extra cryogenic power
- energy spread - much smaller than σ_E due to RF stabilisation

off-axis particles receive kicks from dipole HOMs

- Beam Break-Up - depends on frequency distribution among cavities
- emittance growth

Tilt of cavities

- monopole modes transverse component when projected on beam trajectory
- beam receives an extra kick

interaction with beam depends on (r/Q)

➢ HOMs close to light cone are likely to interact strongly with beam

interaction with beam depends on stored energy

➢ high Q HOM are more dangerous

Damping of high (r/Q) HOM is mandatory

Dipole Wakefields

- Dipole delta-wake
  - Using the Panofski-Wenzel theorem

$$W_{\perp}^{\delta}(\zeta, a) = \sum_n 2k_{\|_n}(a)\frac{c}{\omega_n}\sin\left(\omega_n \frac{\zeta}{c}\right)$$

  - For dipole modes: $E_z \propto a \Rightarrow k_{\|n} \propto a^2$
    - (a = offset of integr. path)

- Kick factor

$$k_{\perp n} = \frac{|V_n(a)|^2}{4 U_n a^2}\frac{c}{\omega_n}$$

➢ Often also normalized to the length of the cavity

- Normalized dipole delta-wake

$$W_{\perp}^{\delta\prime}(\zeta) = \sum_n 2k_{\perp n}\sin\left(\omega_n \frac{\zeta}{c}\right)$$

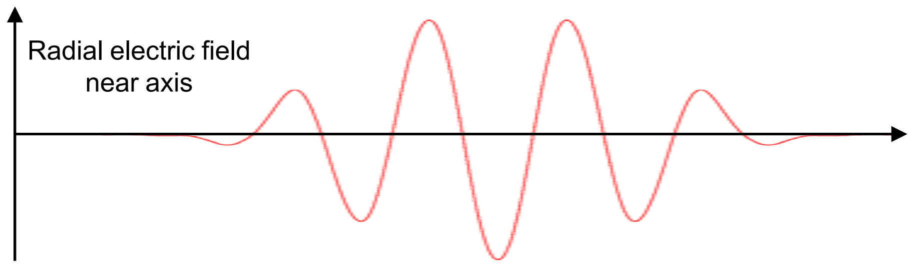

HOM damping

HOM Couplers

- extract HOM power out of cryomodule = reduce stored energy
- design HOM couplers in order to get Q_{ext} as low as possible
  for SC cavities, Q_0 >> Q_{ext} so Q_L = Q_{ext}
- SC couplers to reduce RF losses
- 2 couplers per cavity

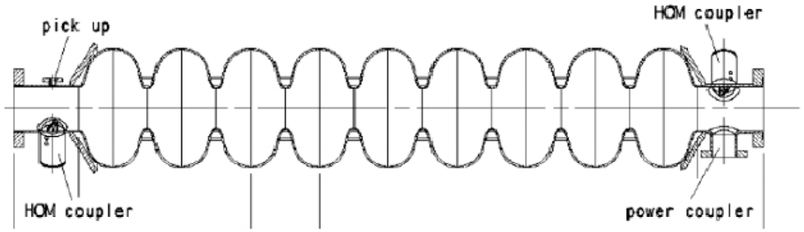

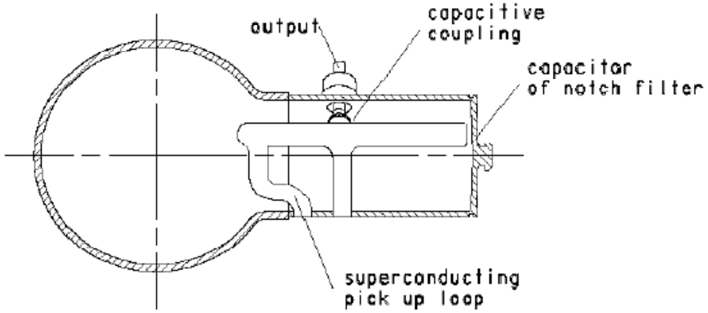

DESY

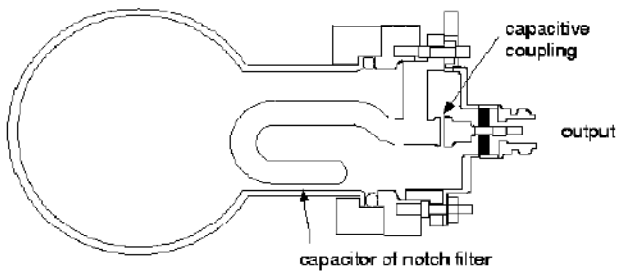

SACLAY

HOM couplers installed at each side of the TESLA cavity. Two types are used at the TTF cavities: a welded type (left) and a demountable type (right)

Dispersion Diagram for the TESLA Cavity

Dipole passbands

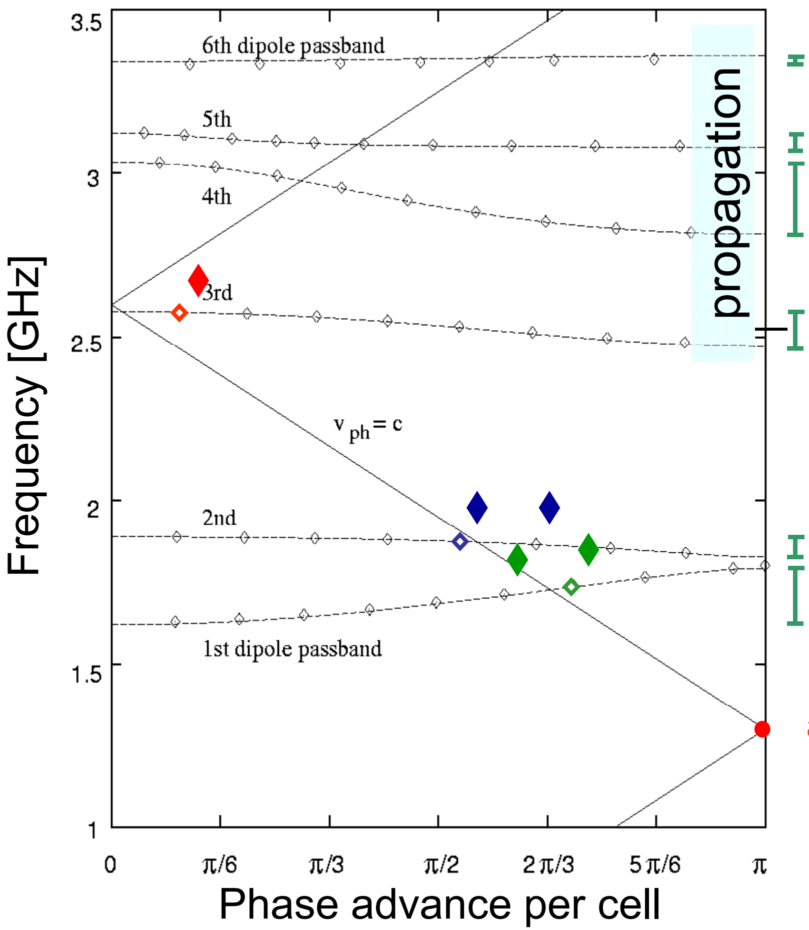

dipole "passbands"

accelerating mode

Beyond cutoff = no propagation

- mode properties easy to compute for one cavity.

ex: M1,M2 bands; D1,D2 bands

Above cutoff = propagation

BUT trapped mode may exist (high Q)

- difficult to predict field distribution for whole module since mode properties depend both on individual cavity characteristics on beam tube, couplers
- ex: D3, D5, D6 bands

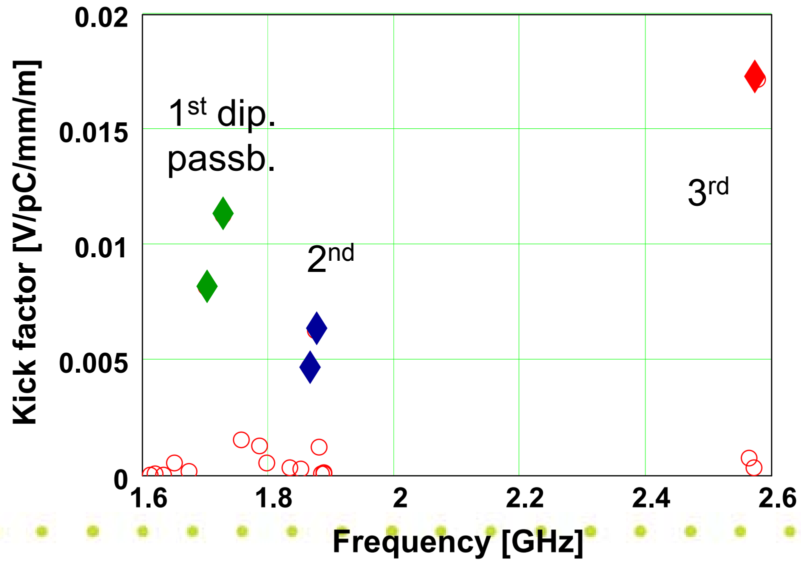

“Trapped” modes in 5th passband

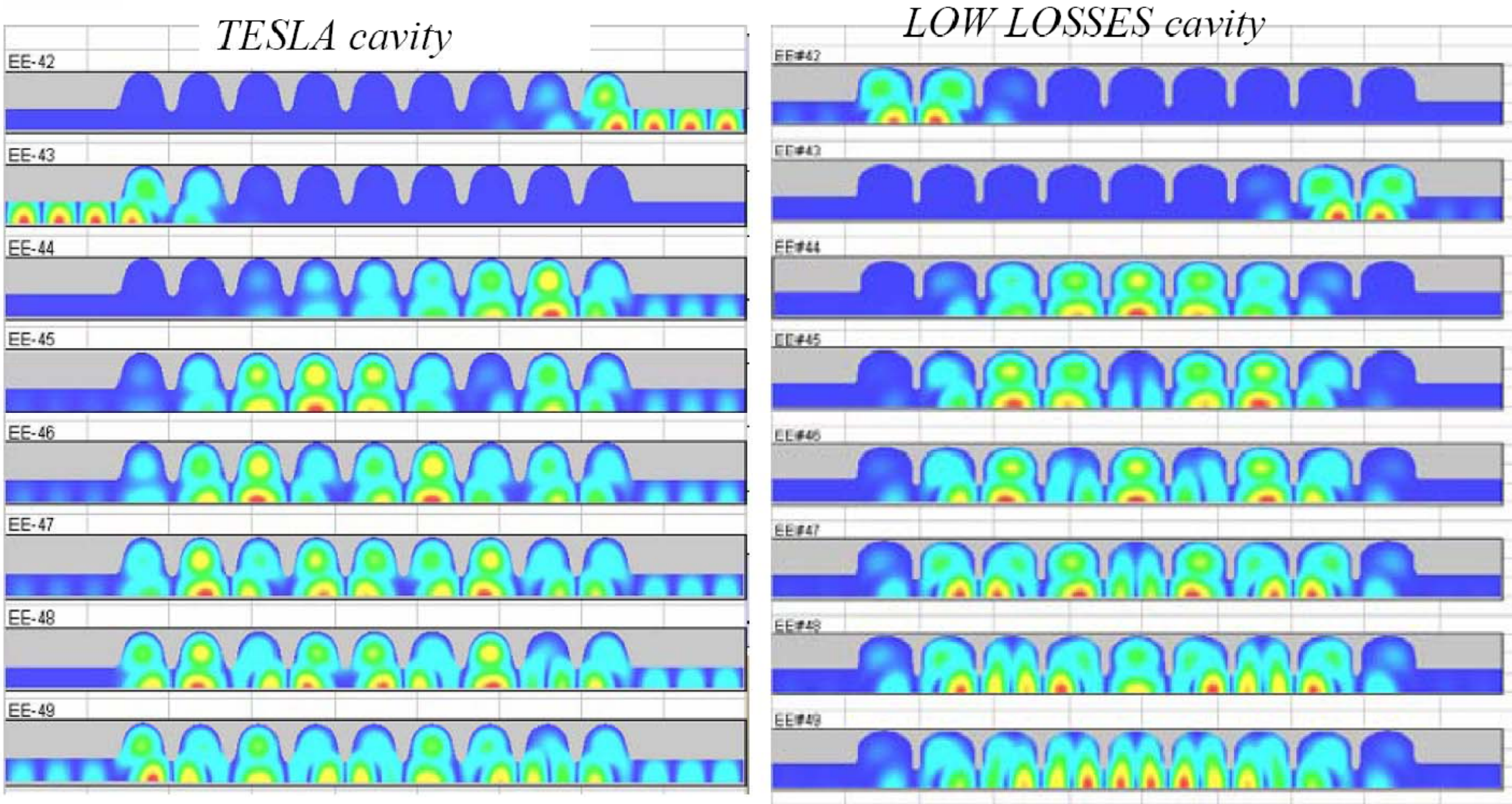

Asymmetric ends can help to improve dump HOM’s in LL cavity (as TESLA)

Dipole HOM excitation

Wake Potentials :

$W_{\parallel} \propto (r/Q) \times r_0^{\,m} r_1^{\,m} \times \cos m(\theta_0 - \theta_{HOM})$ $\rightarrow$ HOM couplers

$W_{\perp} \propto (r/Q) \times r_0^{\,m} r_1^{\,m-1} \times m \cos m(\theta_0 - \theta_{HOM})$ $\rightarrow$ BPM

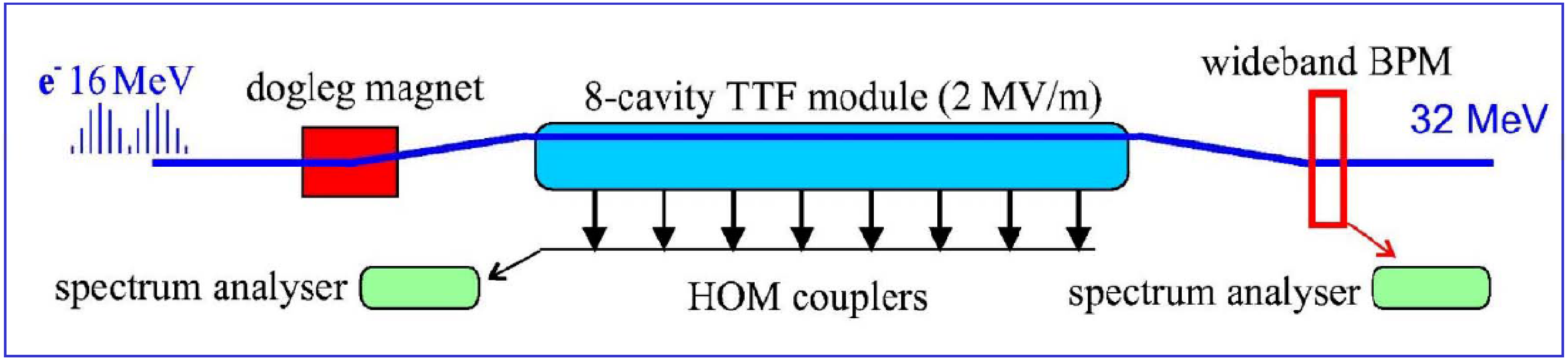

TTF dogleg magnet operates only in *x*-plane : $\delta x = \pm$ 2cm

monopole	m = 0 : $P_{HOM} \propto \delta x^0$, $\delta x_{BPM} = 0$
dipole	m = 1 : $P_{HOM} \propto \delta x^2$, $\delta x_{BPM} \propto \delta x$
quadrupole	m = 2 : $P_{HOM} \propto \delta x^4$, $\delta x_{BPM} \propto \delta x^3$

3rd dipole passband high Q HOMs

HOM : f = 2.585 GHz , $Q = 10^6$
measured with 216 MHz Injector #1 in Module 1, in 1998.

f_{mod} =15 MHz

BPM signal

125 µs beating due to 8 kHz off resonance

HOM coupler signal

decay time
$\Rightarrow Q = 10^6$

HOM
f =2.575794
Q=2 10^6

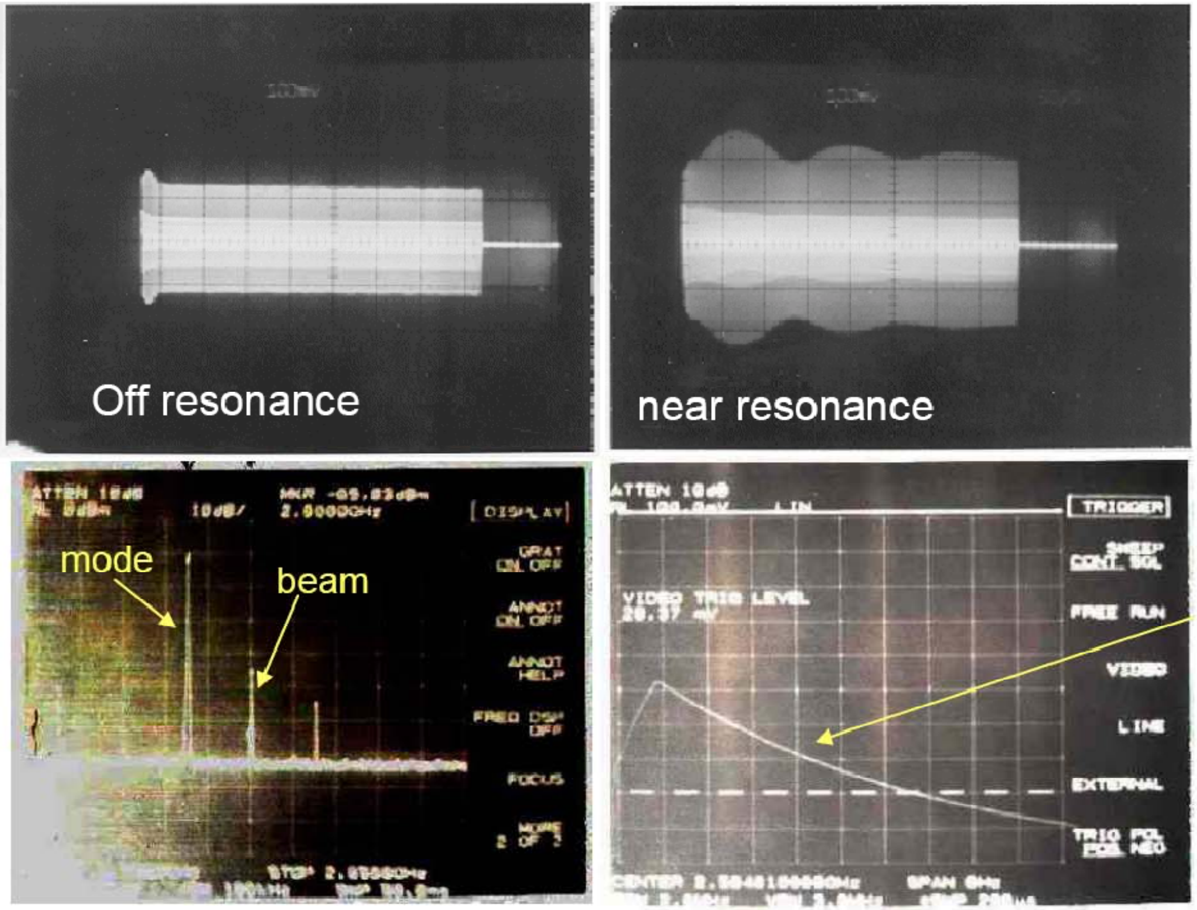

frequency domain

time domain

D5 Passband

High Q modes

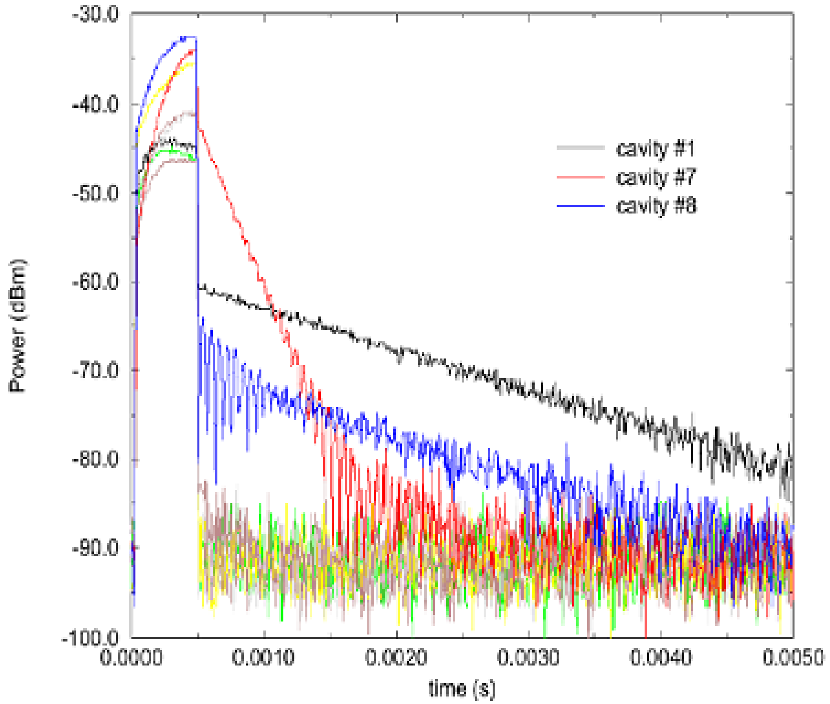

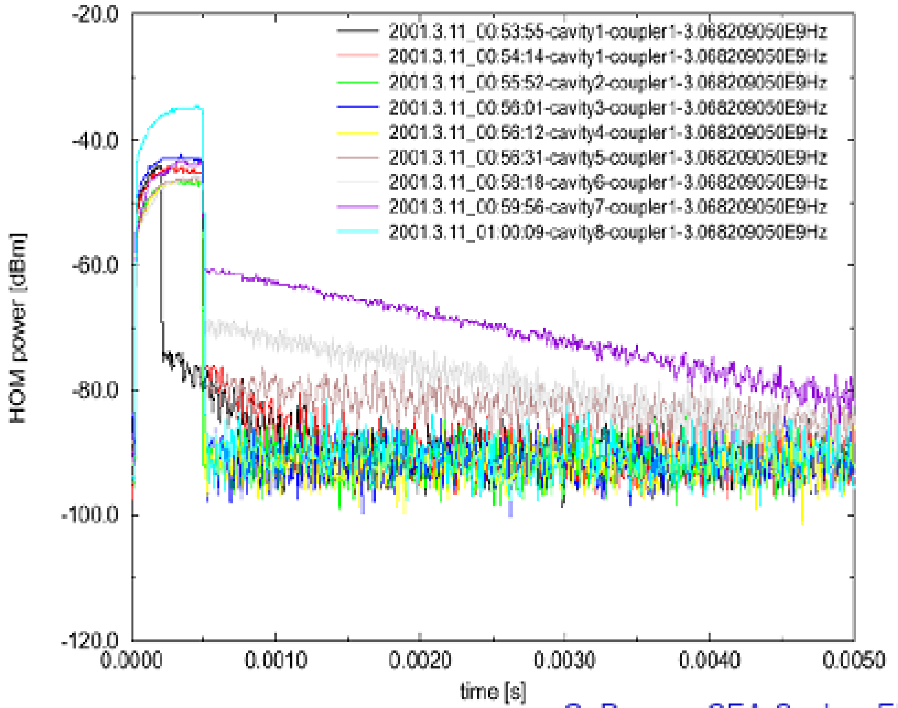

G. Devanz CEA-Saclay EPAC02

f = 3.063724 GHz

Q = 1.7 10^7

f = 3.068209 GHz

Q = 3.4 10^7

An example of time domain signal from HOM coupler measured with a spectrum analyzer.

Re-designing of HOM coupler to improve damping

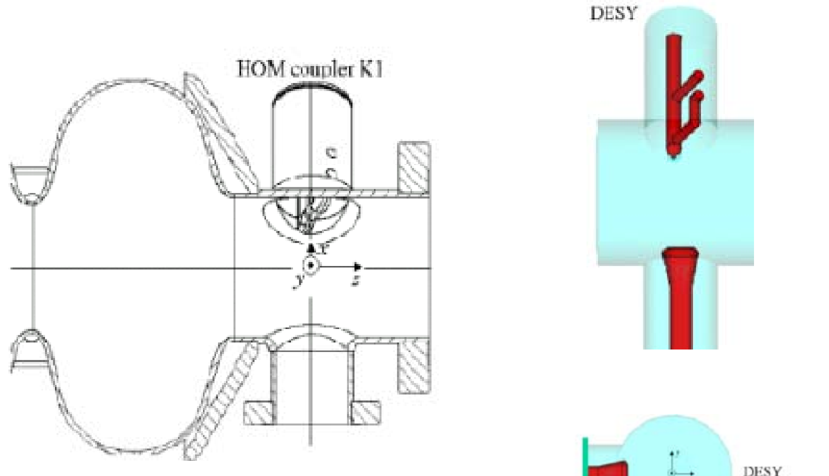

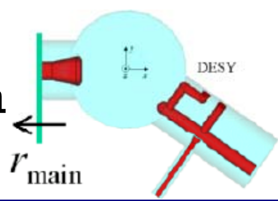

Orientation of downstream HOM and main couplers.

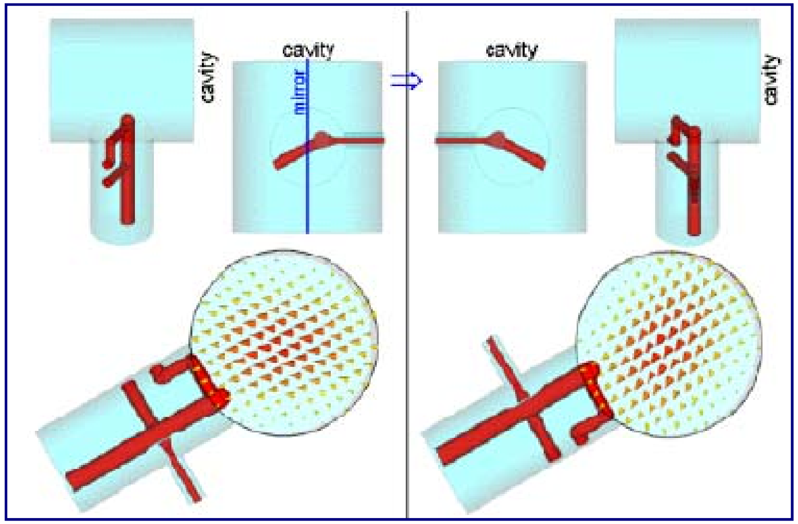

Original (left) and redesigned mirroring modification of upstream coupler (right) – *M.Dohlus*

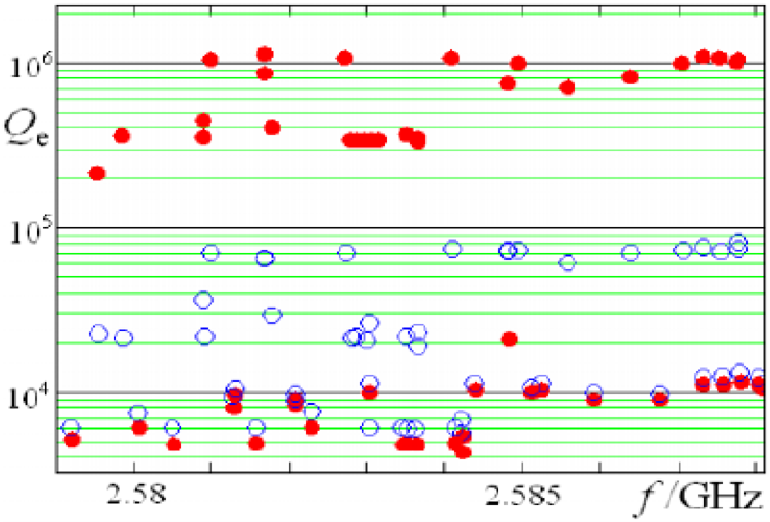

Q-values of different modules with randomly detuned cavities at the upper end of the third dipole band. Original couplers (red circles) and the modified upstream couplers (blue one)

M. Dohlus et al., HIGHER ORDER MODE ABSORPTION IN TTF MODULES IN THE FREQUENCY RANGE OF THE THIRD DIPOLE BAND, EPAC 2002

Cavity HOMs can be used as a BPM

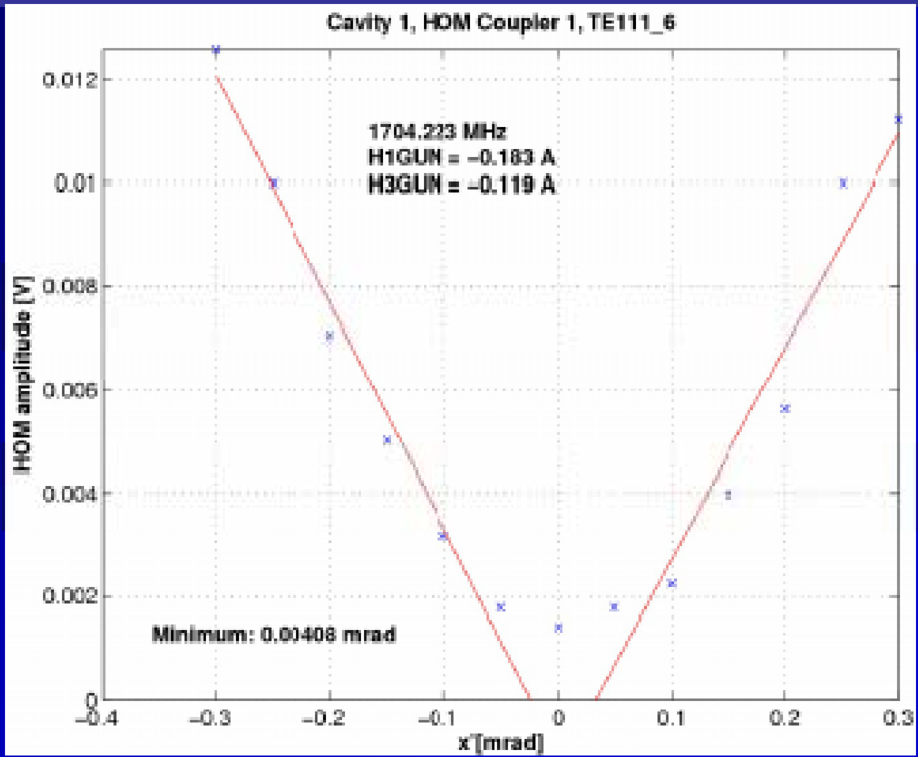

Angular scan resolution and accuracy < 50 μrad

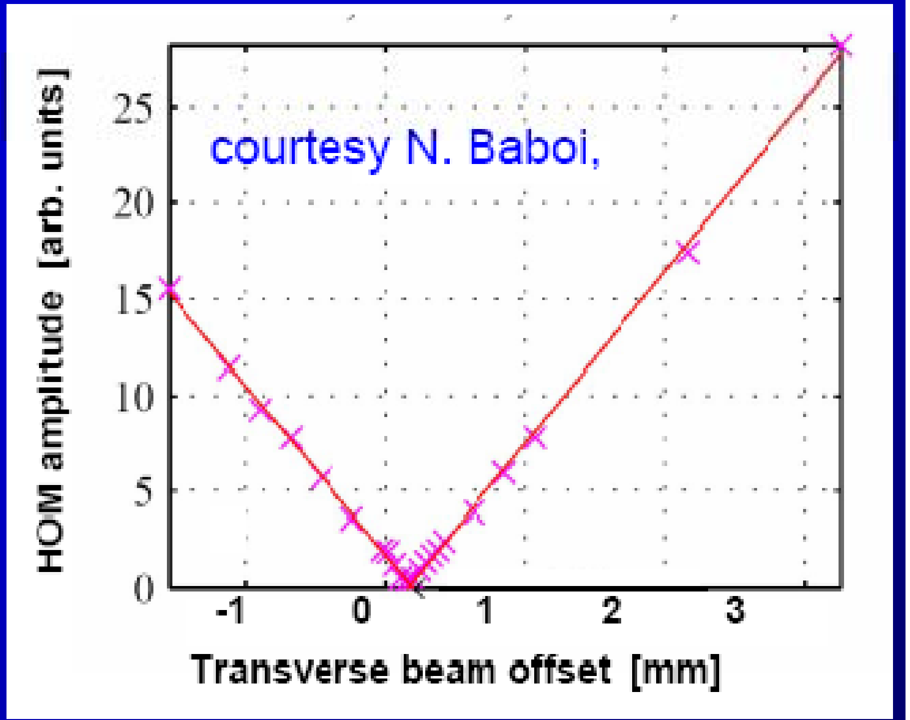

Relative position resolution ~ 4 μm

(cf. M. Ross and J. Frisch).

What is HOM absorber ?

monopole losses TESLA-TDR

Collider (500GeV) losses per module

$f_{rep} = 5$ Hz	$P = 23.3$ W
$T_{HF} = 0.95$ ms	$P(f > 5\text{ GHz}) = 17.4$ W
$\sigma_{bunch} = 400\ \mu$m	$P'(f > 10\text{ GHz}) = 12.7$ W
$N_{bunch} = 2820$	$P'(f > 20\text{ GHz}) = 8.1$ W
$q_{bunch} = 3.2$ nC (9.5 mA)	$P'(f > 50\text{ GHz}) = 3.0$ W
	$P'(f > 100\text{ GHz}) = 0.7$ W

trapped &
quasi trapped modes:
resonant
effects

propagating modes

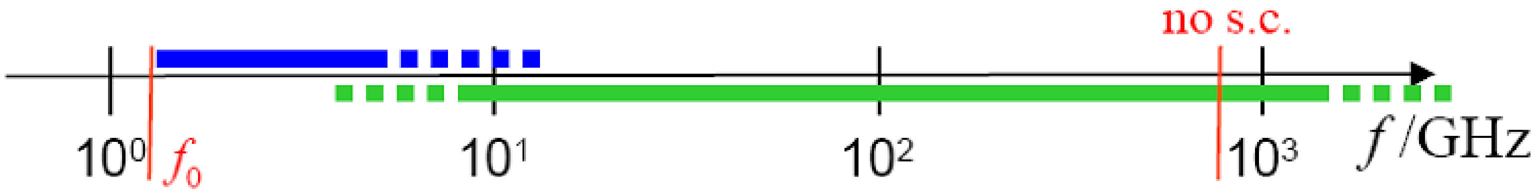

HOM couplers

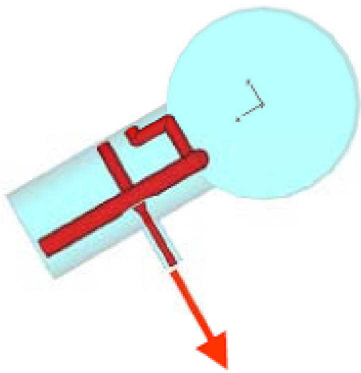

coax to warm load

HOM absorbers

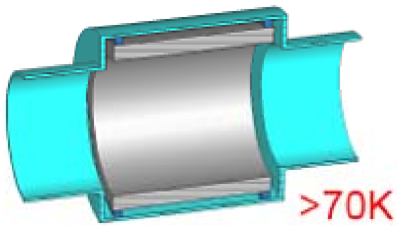

no transmission lines or waveguides
⇒ absorber at temperature level with
good cryo efficiency

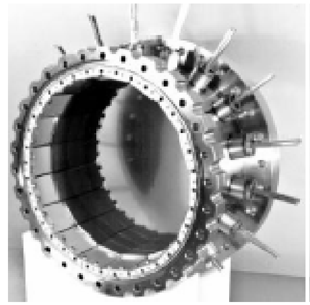

Cornell design

absorbers in interconnections between modules
T > 70K

Absorbing High Frequency HOM Power

Calculations
M. Dohlus

HOM absorption: all = 1000

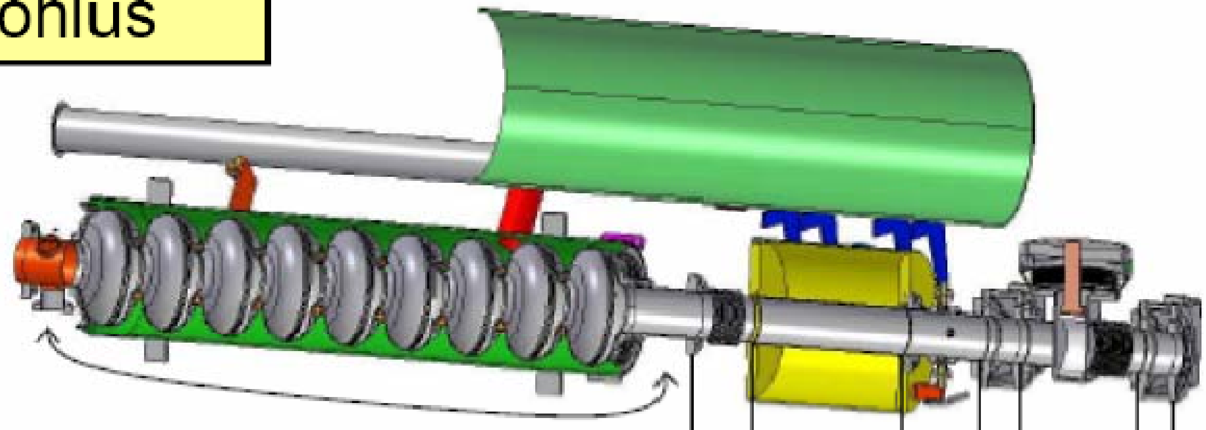

<table>
<tr><td>72.2</td><td>cu
2.4</td><td>3.0</td><td>1.5</td><td>10.4</td><td>0.7|
1.5|894.4|1.5|
|2.0</td><td>10.4</td><td>$\eta = 79.4\%$</td></tr>
<tr><td>rest</td><td>bellows
24</td><td>quadrupole
30</td><td>bpm
15</td><td>shutter
8</td><td>absorber
7|15|..|15|20</td><td>shutter
8</td><td>(effective length / cm)</td></tr>
<tr><td>68.1</td><td>st
26.4</td><td>32.8</td><td>16.2</td><td>8.6</td><td>7.6|
16|777.9|16.3|
|21.4</td><td>8.7</td><td>$\eta = 67.8\%$</td></tr>
</table>

absorption efficiency (including 10% safty margin)

Cavity Fabrication and Tuning

Material

- Niobium (Nb) (A=91, Tc=9.2 K; superheating field of approx. 240 mT) is the favorite material for the fabrication of SC RF cavities.
  - chemically inert (pentoxide layer)
  - easily machined and deep drawn (like OFHC cooper)
  - available as bulk and sheet material in different grades of purity (RRR > 250)
  - Can be further purified by UHV heat treatment or solid state gettering
  - majority of SC RF cavities worldwide are formed from Nb sheet material

High affinity to interstitial impurities like H, C,N,O (in air T < 150 C)
Joining by electron beam welding
Metallurgy not so easy
Hydrogen can readily be absorbed and can lead to Q-degradation in cavities

Niobium production

- The primary mineral is known as pyrochlore.
- Columbite, a mineral with a ratio of Nb_2O_5:Ta_2O_5 ranging from 10:1 to 13:1, occurs in Brazil, Nigeria, and Australia, also other countries in central Africa. Niobium is recovered when the ores are processed for tantalum.

Largest mines are:

- #1: Araxá, Brazil and is owned by Companhia Brasileira de Metalurgia e Mineração (CBMM). The reserves are ~ 460 million tons.
- #2: Brazil is owned and operated by Anglo American Brasil Mineração Catalão and contains 18 M tones (Nb_2O_3=1.34%)
- #3 Niobec Mine in Quebec, Canada, owned by Cambior, with reserves of 18 k tons.

In all three facilities, the pyrochlore mineral is processed by primarily processing technology to give a concentrate ranging from - 60% niobium oxide.

Mass production of high purity Nb for RF cavities

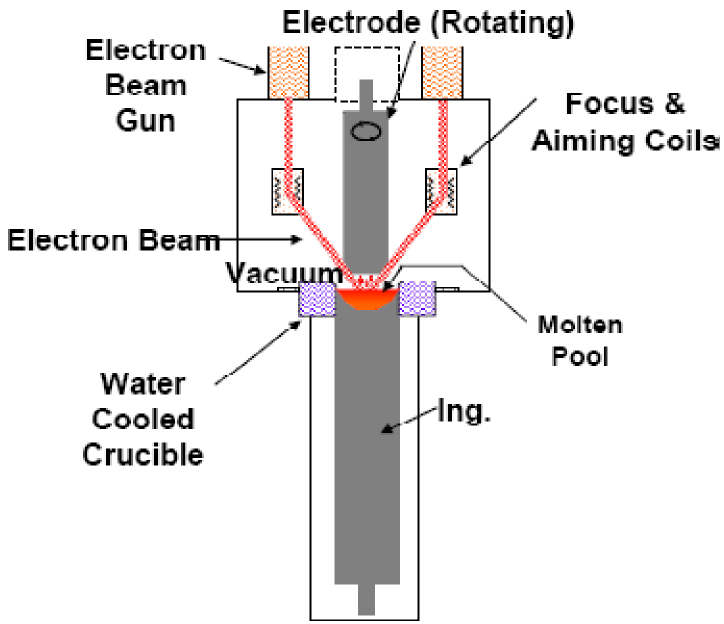

Electron Beam melting of Nb

High Purity Niobium(RRR>250) is made by multiple electron beam melting steps under good vacuum, resulting in elimination of volatile impurities

There are several companies, which can produce RRR niobium in larger quantities:

- Wah Chang (USA),
- Cabot (USA),
- W.C.Heraeus (Germany),
- Tokyo Denkai(Japan),
- Ningxia (China),
- CBMM (Brasil)

The melting temperature is a compromise between the maximization of purification and minimization of the material losses by evaporation.

Fabrication of Nb sheets at Tokyo Denkai

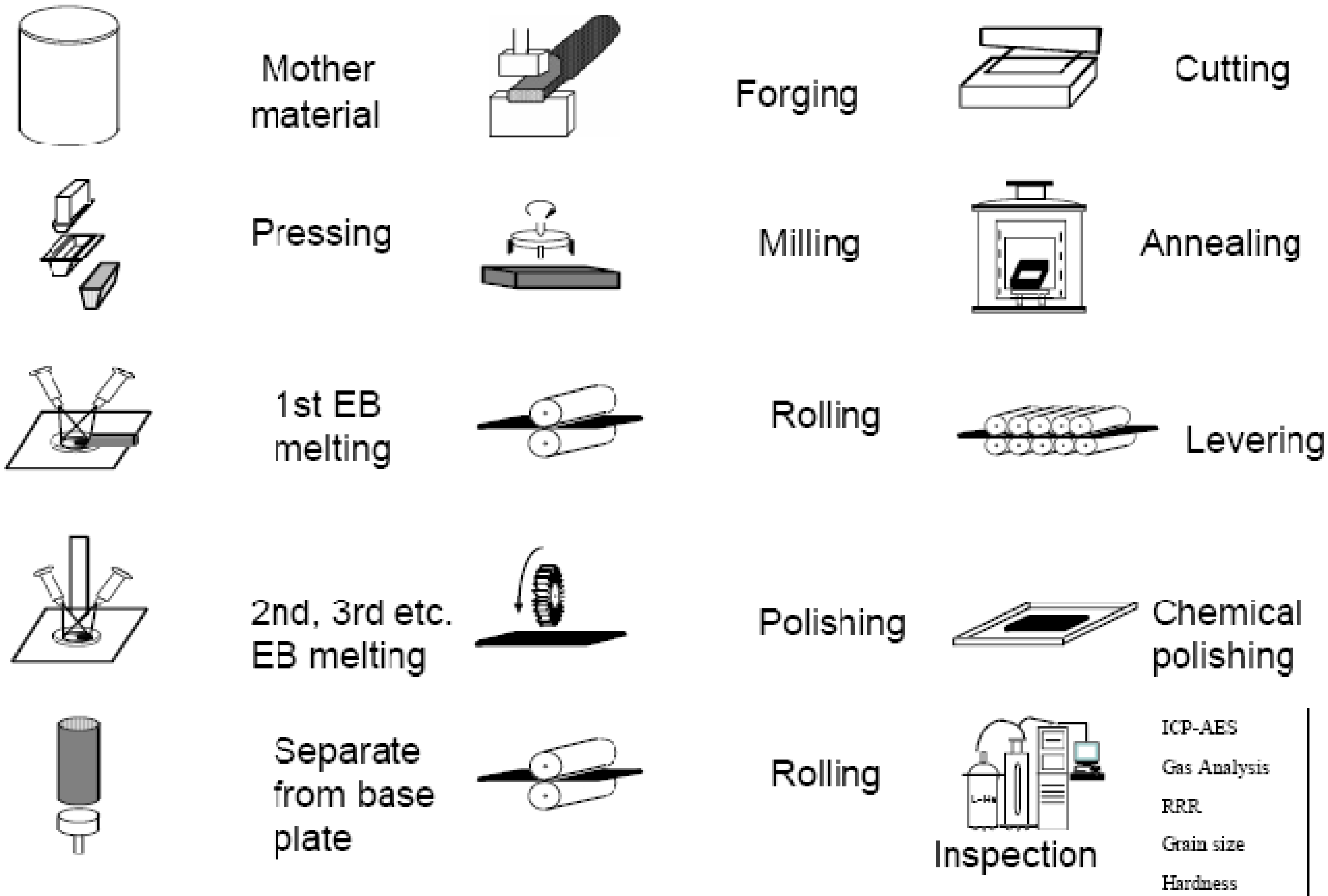

In the final sheet the purity of niobium should be not inferior as in the ingot

Specifications

Technical Specification to Niobium Sheets for XFEL Cavities.

Concentration of impurities in ppm (weight)				Mechanical properties	
Ta	≤ 500	H	≤ 2	RRR	≥ 300
W	≤ 70	N	≤ 10	Grain size	≈ 50 μm
Ti	≤ 50	O	≤ 10	Yield strength, $\sigma_{0,2}$	$50<\sigma_{0,2}<100$ N/mm² (Mpa)
Fe	≤ 30	C	≤ 10	Tensile strength	> 100 N/mm² (Mpa)
Mo	≤ 50			Elongation at break	30 %
Ni	≤ 30			Vickers hardness HV 10	≤ 60

No texture: The difference in mechanical properties (Rm, Rp0,2, AL30) orthogonal and parallel to main rolling direction < 20% (cross rolling).

Niobium structure after BCP etching

Material input control

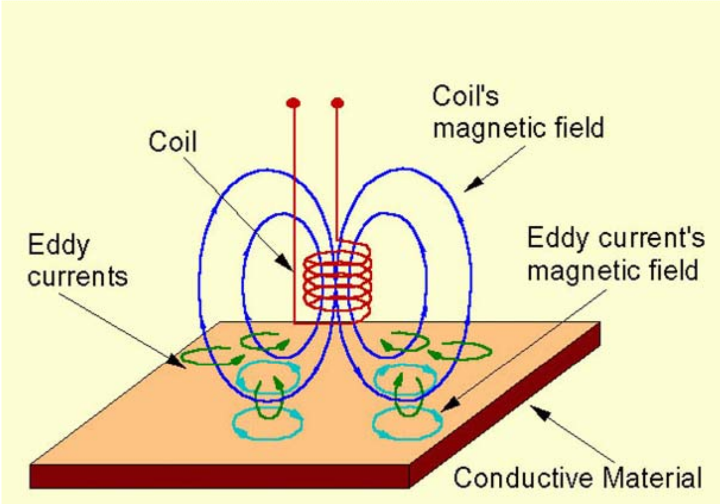

Eddy current scanning

Disks are cut from high purity niobium sheet and eddy current scanned for pits, scratches or inclusions of foreign materials

Discs with inclusions of foreign materials or damage are rejected

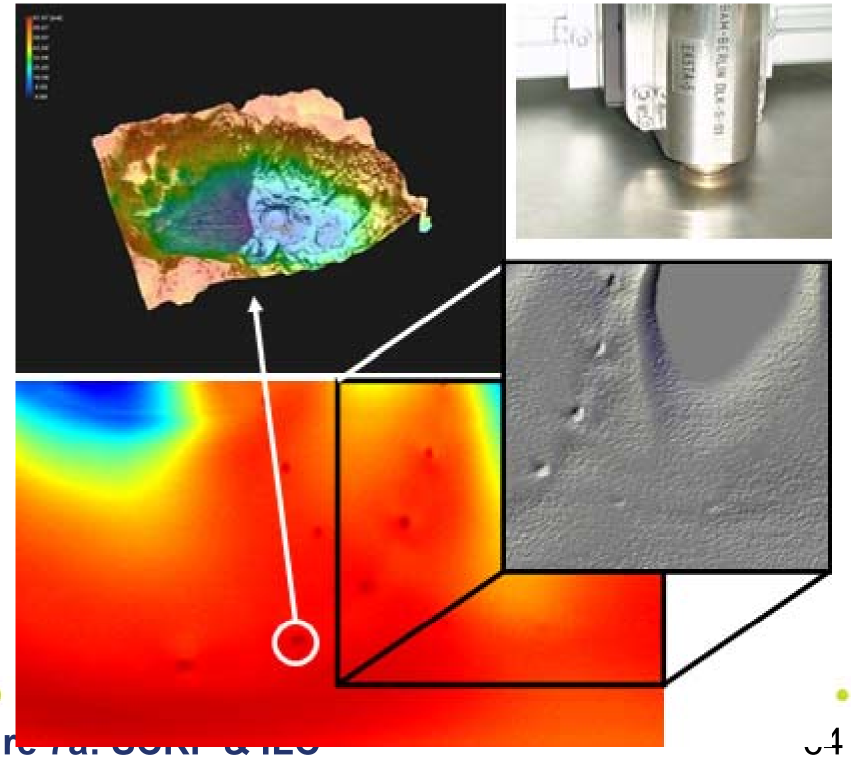

Overview over cavity fabrication

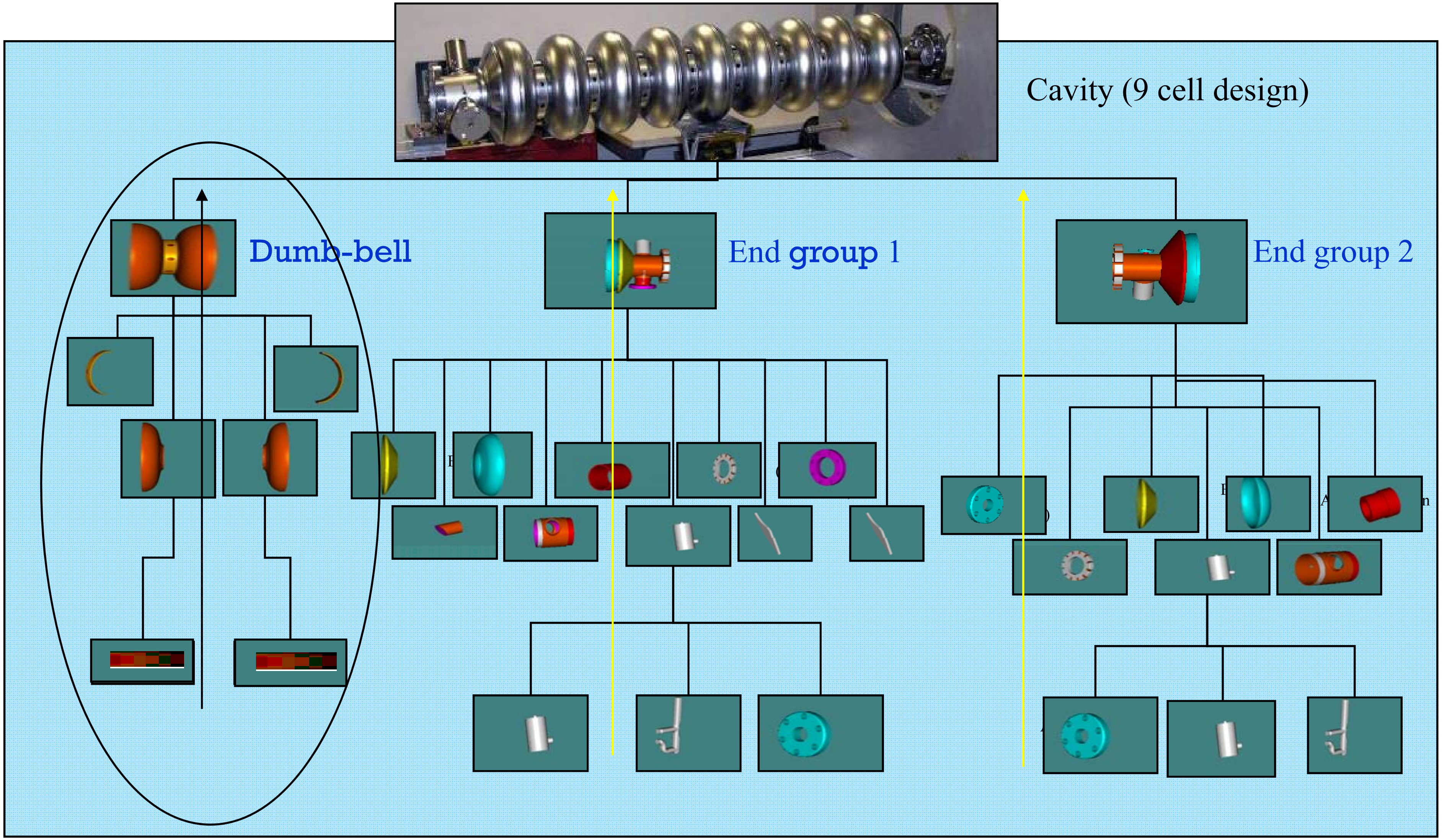

Cavity production steps: half cells

- Eddy current scanning of Niobium sheets.
- Cut disk blanks with hole in the center
- Flow forming of half cell and trimming iris and equator area with extra length for tuning and welding shrinkage compensation. No extra length for a tuning in mid- cells. If pass visual inspection :
- Frequency and length measurements. Sensitivity of the frequency to extra length is 14 MHz/mm at iris and -55 MHz/mm at equator.
- EB welding of two half cell at iris to form dumbbell. Partial penetration welding from both sides.

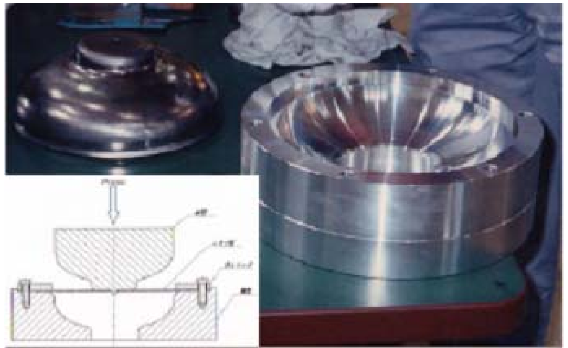

Deep drawing

Disks are then deep drawn in a hydraulic press

Control of half-cell geometry

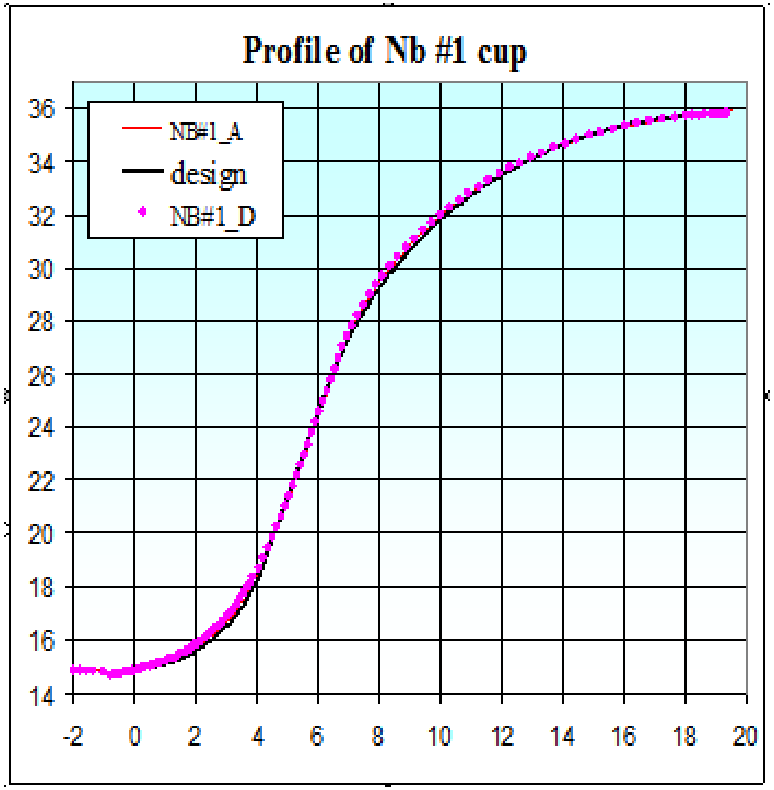

CMM cell profile measurement compared to design shape

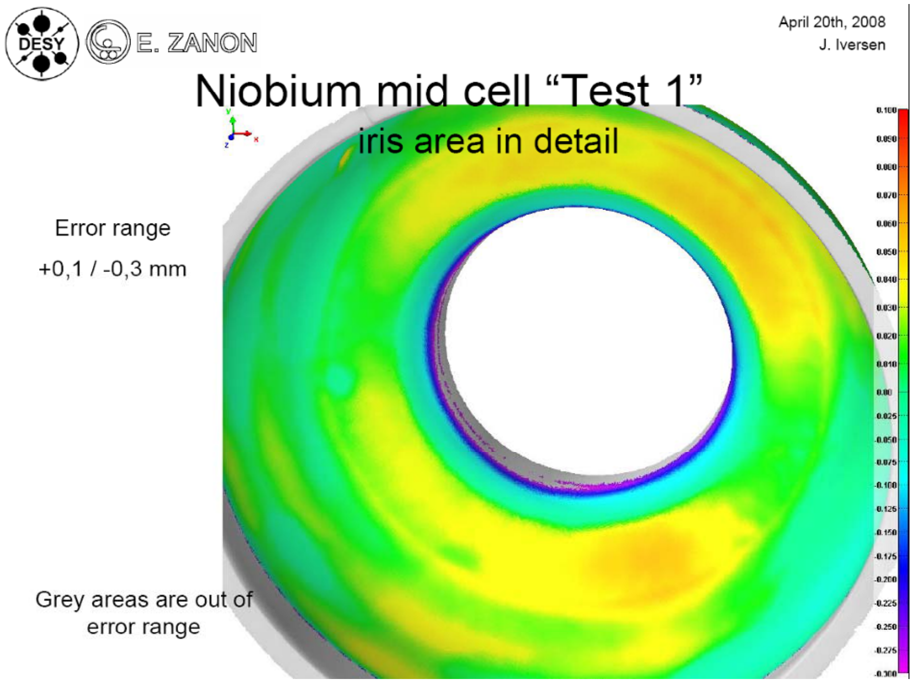

Laser 3D profile measurement

Dumbbell production steps

Cavity fabrication : Example dumb bell / Cavity

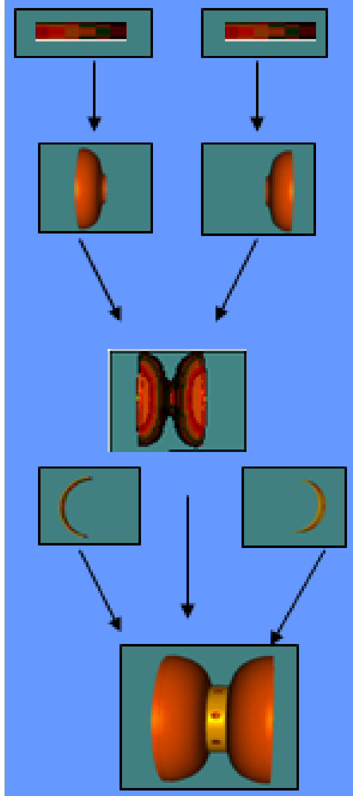

Dumb- bell

1. Mechanical measurement
2. Cleaning (by ultra sonic [us] cleaning +rinsing)
3. Trimming of iris region and reshaping of cups if needed
4. Cleaning
5. Rf measurement of cups
6. Buffered chemical polishing + Rinsing (for welding of Iris)
7. Welding of Iris
8. Welding of stiffening rings
9. Mechanical measurement of dumb-bells
10. Reshaping of dumb bell if needed
11. Cleaning
12. Rf measurement of dumb-bell
13. Trimming of dumb-bells (Equator regions)
14. Cleaning
15. Intermediate chemical etching (BCP /20- 40 µm)+ Rinsing
16. Visual Inspection of the inner surface of the dumb-bell

local grinding if needed + (second chemical treatment + inspection)

Dumb-bell ready for cavity

Rough BCP before welding

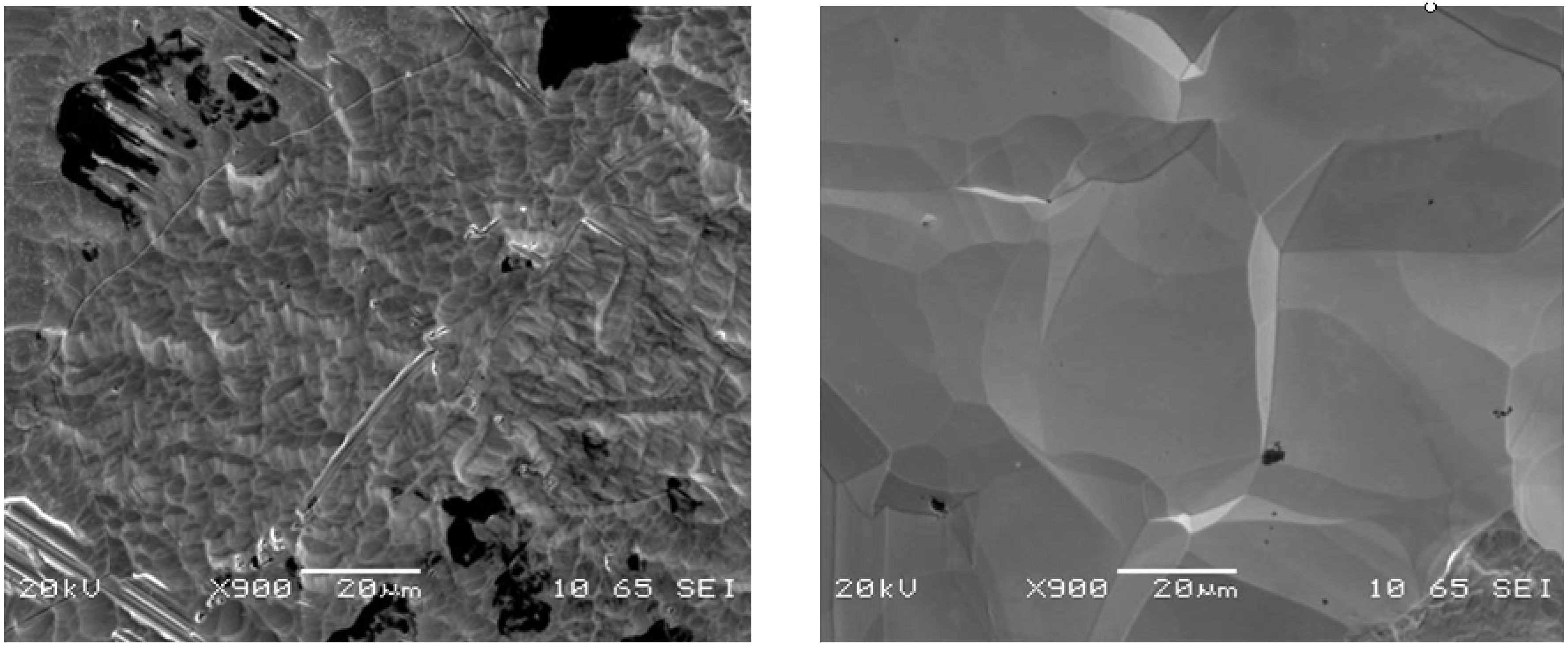

Chemical removal of contaminated and damaged surface layer of cavity components (~15 - 20 mm) via Buffered Chemical Polishing (BCP) prior to EB welding

Electron-beam Welding

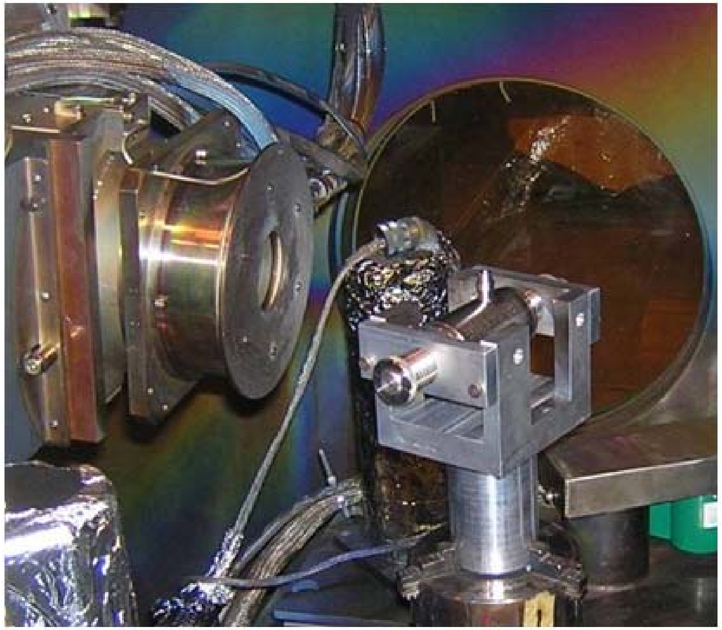

Clever fixture design is essential for quality welds

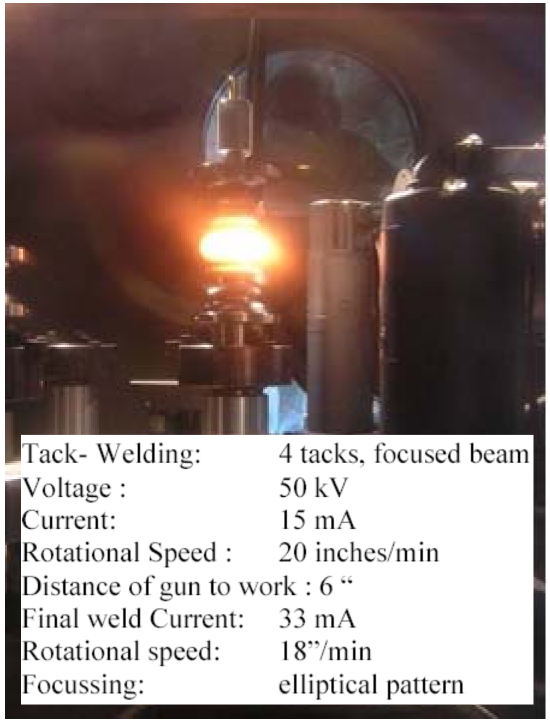

Vacuum pump. Cavity equator EB weld. must be cooled under vacuum to <200°F before exposing to atmosphere (45-60 min.). Cycle ~3-4 hrs.

EBW is expensive and time consuming process → TESLA/ILC mass production studies to reduce time and cost

Dumbbells

Dumbbell frequency measured and equators trimmed with allowance for weld shrinkage when combined into nine-cell

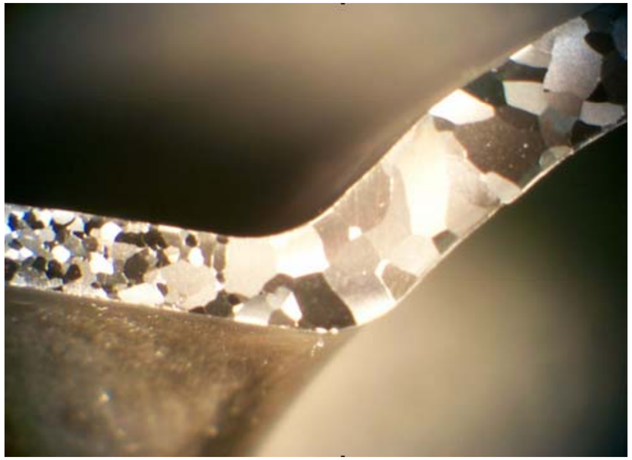

Grain growth in weld affected zone

Nominal (RF) length increases
~0.3 mm EBW shrinkage
0.25 mm lip joint

Dumbbell RF control

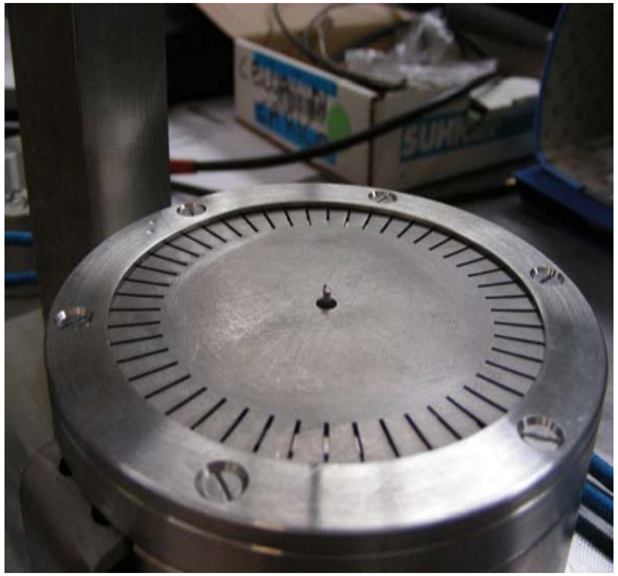

RF contact at equator

Frequency of individual half-cell ?

From frequency measured for dumbell: $F_1 = F_0$ and $F_2 = F_\pi$ we can define frequency of each cell:

$$F_{c1,c2} \approx \sqrt{\frac{2F_1^2 + 2\Delta F F_1 \pm \sqrt{(2F_1^2 + 2\Delta F F_1)^2 - 4(1-k^2)F_1^2(F_1+\Delta F)^2}}{2(1-k^2)}}$$

Taking $F_2 = F_1 + \Delta F$ we have:

$$F_{c1,c2} = \sqrt{\frac{F_1^2 + F_2^2 \pm \sqrt{(F_1^2 + F_2^2)^2 - 4(1-k^2)F_1^2 F_2^2}}{2(1-k^2)}}$$

or

$$F_{c1,c2} \approx \sqrt{F_1(F_1+\Delta F)}\sqrt{\frac{1 \pm \sqrt{1-(1-k^2)}}{(1-k^2)}} = \sqrt{\frac{F_1(F_1+\Delta F)}{1 \mp k}}$$

Dimensional measurements

Length and straightness of the cavities were measured by 3D-measurement machine.

	EBW shrinkage
iris	0.148+-0.044 mm
equator	0.424+-0.125 mm

Dimensional deviation of length (only 9-cell part: 1038.5 mm)

-10 mm (1st 9-cell ICHIRO cavity)

- 0.7 mm (2nd 9-cell ICHIRO cavity)

- 0.1 mm (3rd 9-cell ICHIRO cavity)

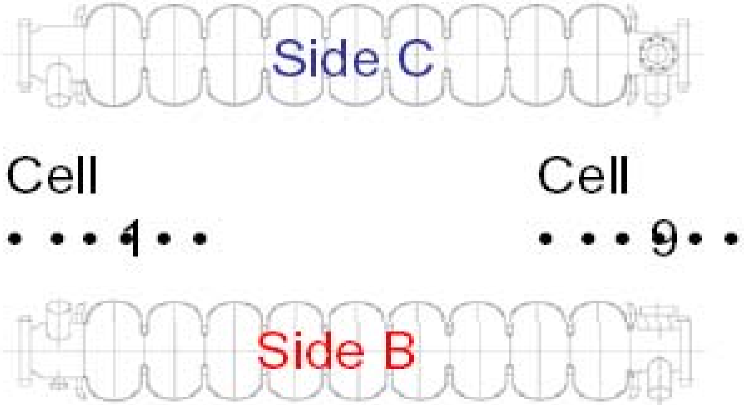

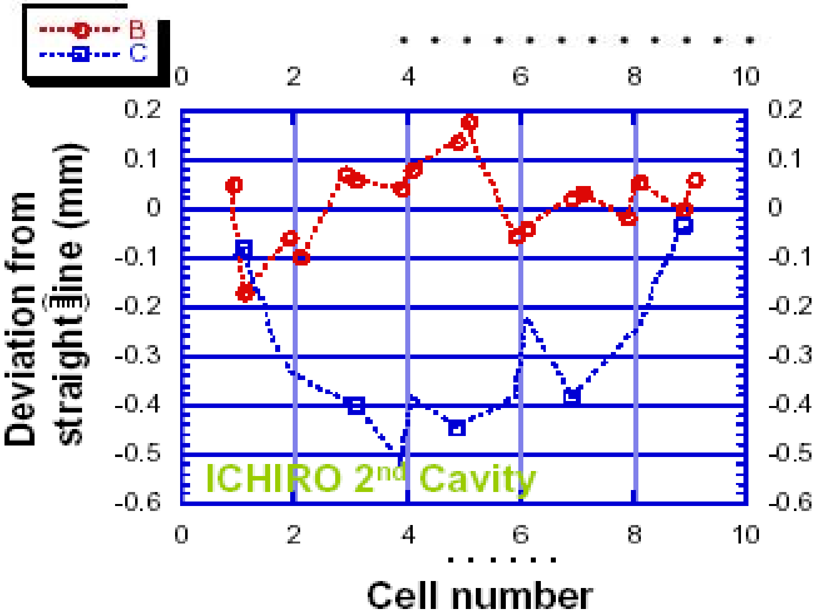

Frequency and field flatness tuning

Computerized tuning machine at DESY

- Frequency measurements
- Bead-pull measurements
- Mechanical cell alignment
  - Straightening of cavity
- measurement and tuning
- Field flatness tuning
  - Based on field measurements at each mode and frequency spetrum
  - Equalizing stored energy in each cell by squeezing or pulling

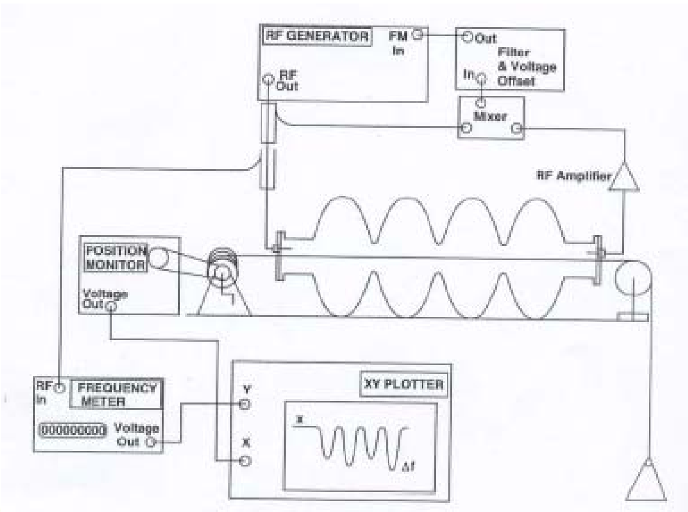

Set-up for field profile measurements:

a metallic needle is perturbing the rf fields while it is pulled through the cavity along its axis; (Slatter theorem)

the stored energy in each cell is recorded.

Field flatness tuning (FNAL)

- Based on bead-pull measurements of field distribution on operating mode. Amplitudes of E-field in the center of each cell used for frequency tune of individual cells. Perturbation of frequency of each cell df_i will change field distribution: $dA_i = K_{in} * df_n$
- Solution: $dA = K \cdot df \;\Rightarrow\; df = K^{-1} \cdot dA$

Where ***K*** - matrix of sensitivity coefficients is calculated from HFSS simulations.

- Goal - tuning operating mode frequency F. Tuning of cell #n by df_n shifts cavity frequency by $dF \sim df_n/9$. If design frequency is F_0 tuning of the cell should be done by shifting operating mode frequency by:

$$dF = (F_0 - F - df_n)/9$$

- This technique works best when field flatness of the cavity is close to ideal (based on small perturbations). Tuning is better to start with most perturbated cell. If field flatness still not acceptable the additional tuning cycle should be done.

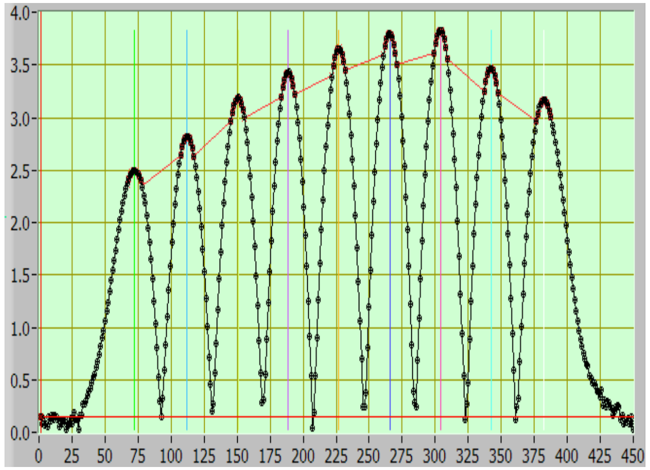

Cavity before tuning. Slope +28 %

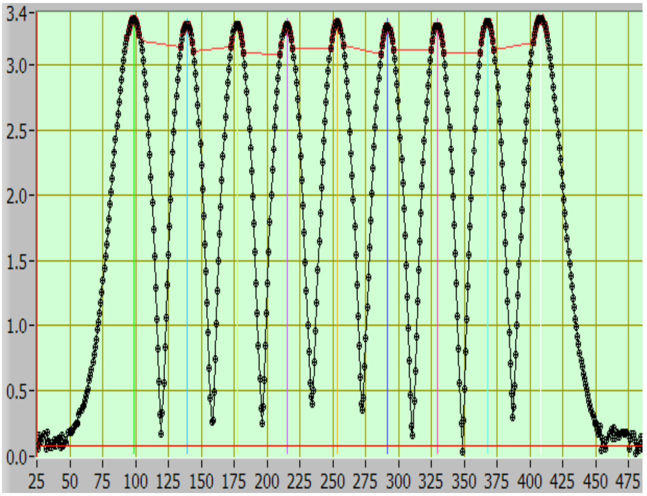

After tuning. F=3893.21 MHz. Slope +0.64 %

Bead-pull based alignment technique

1) Mechanical measurements (outside)
   - Time consuming
   - Impossible on dressed cavity

2) EM measurements based on bead pull measurements.
   - Calibration: E max in each cell
   - Five meas: -2d, -d, 0, d, 2d
   - Best fit to find Emax (X/Y plane)
   - Cavity rotates by 180 degree to exclude error of initial positioning of fishing line.

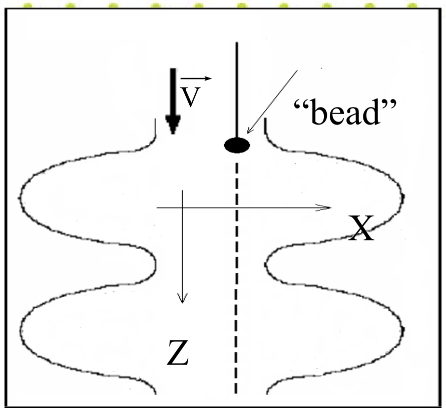

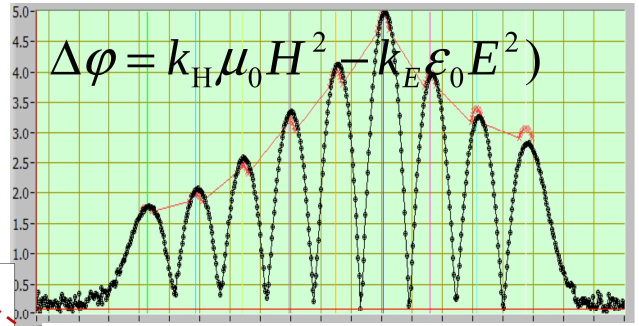

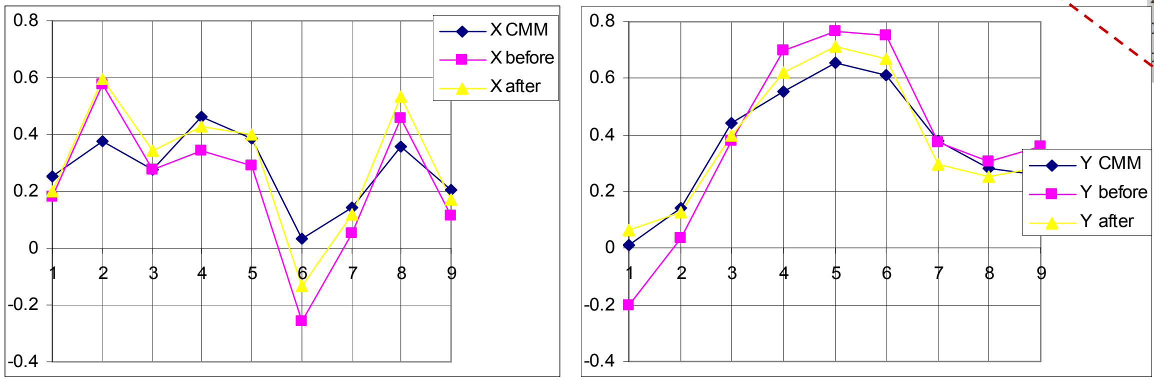

CMM and bead-pull cell center measurements of the cavity

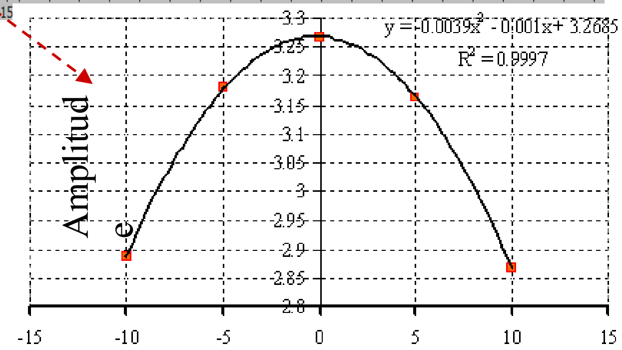

Experiences on cavity fabrication:

Deep drawing:

1. Reproducibility depends on tool design and tool material
   → specification – investigation in tooling
2. Dependency on Nb supplier found
3. Different shape from ingot to ingot found (Hardness / grain size)
   → Better quality control + specification ➔ reproducibility

Measurements:

1. Rf measurement of cups / dumb bells ➔ Time consuming
2. Mechanical measurements of sub units → Time consuming
   (F part HOM tube / flanges /dumb-bell 3 D measurement complex
   → combination of mechanical and rf measurement possible ?
   (3 D imaging of units)

Fabrication:

1. Sequences need to be adopted to the company hardware
2. Companies need to be trained an <u>stay trained</u>
   → learning curve to stable production
3. Control on subcontractors
4. Dependency on major products of company → training of personal

Surface Preparation

Four major steps of cavity preparation process

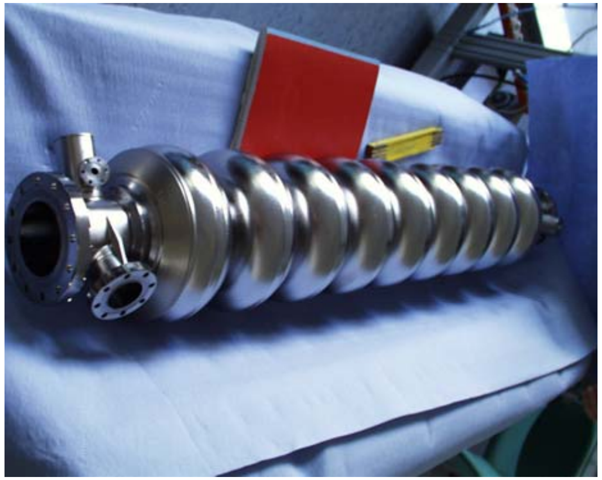

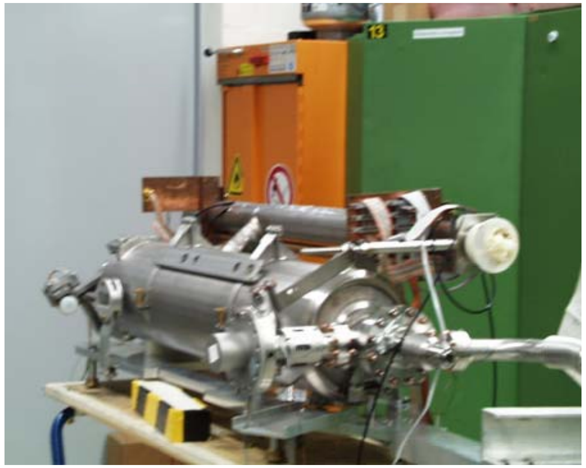

Preparation step A
Removal of damage layer / post purification / tuning

↓

Preparation step B
Final cleaning and assembly for vertical test. Testing in VST

↓

Preparation step C
Welding cavity to He vessel / He vessel welding

↓

Preparation step D
Final cleaning and assembly for module / horizontal test

Why surface treatment ?

Damage layers influences cavity performance

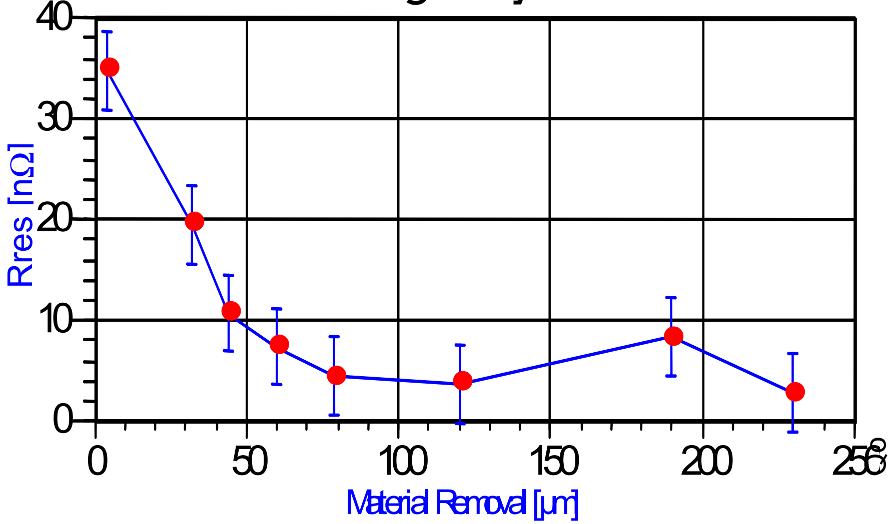

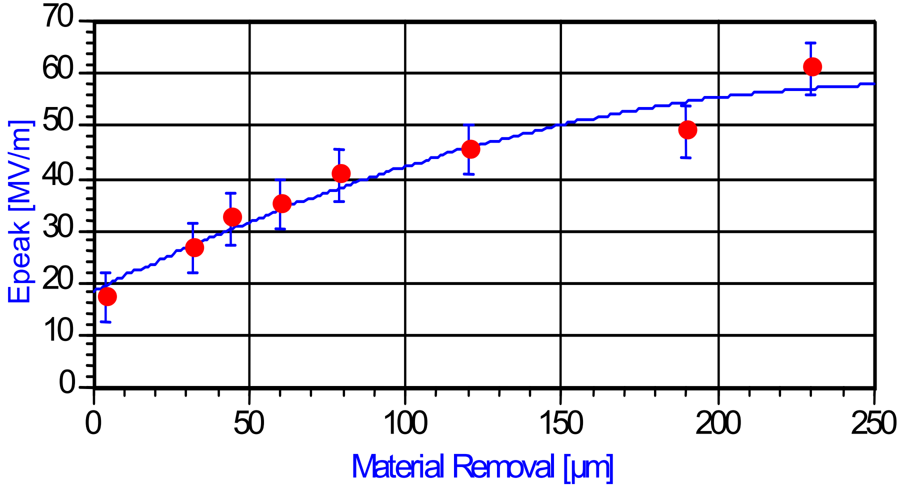

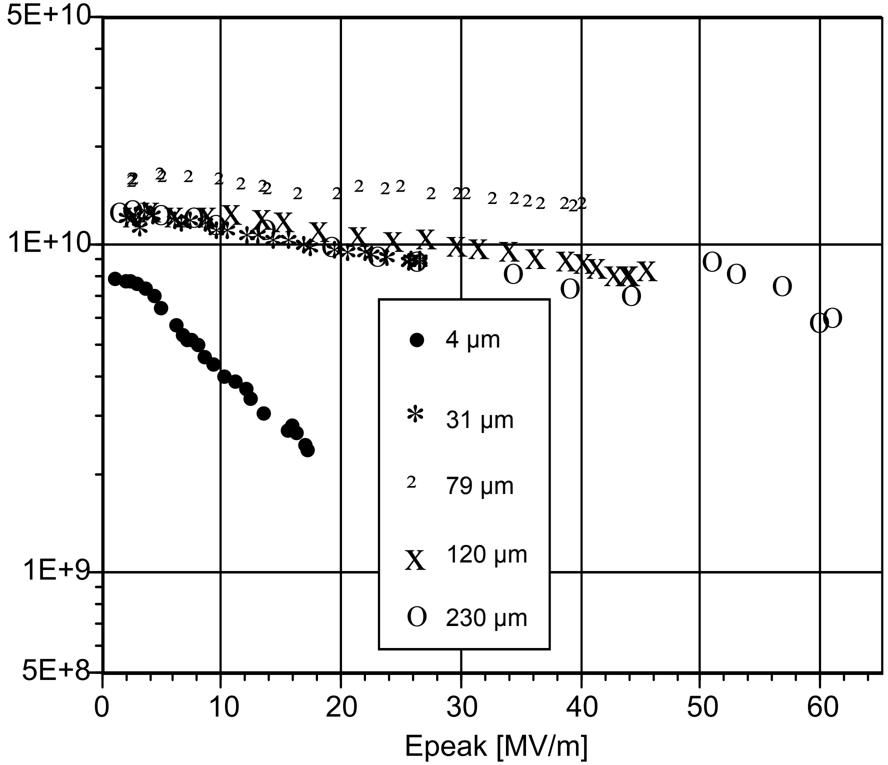

Removal of “damage” layer

Removal Method's

Mechanically by

Grinding

- Simple handling, low cost, mostly in use for removal of local defects non uniform abrasion !
- But: Abrasives, remain of C; Si ; glue; scratch size, produces a new damage layer of about 40 μm thickness!!!

Barrel polishing (tumbling)

Chemically by

- Chemical etching (buffered chemical polishing – BCP)
- Chemical polishing (electro polishing – EP)
- + few new solutions under development, etc.)
  - **Chemical-Mechanical Planarization technology**
  - **(Accel/poligrat)**

CMP of Nb (FNAL- Cabot Microlectronics)

Veeco **3-Dimensional Interactive Display**

Date: 08/29/2007
Time: 10:12:18

Surface Stats:

Ra: 471.30 nm

Rq: 603.60 nm

Rt: 8.22 um

Measurement Info:

Magnification: 20.21

Measurement Mode: VSI

Sampling: 415.64 nm

Array Size: 736 X 480

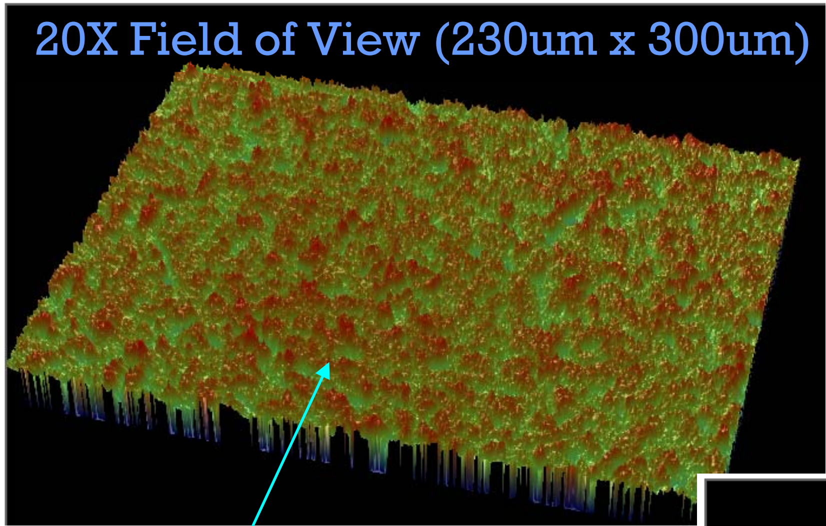

BEFORE: Rq = 603nm
Heavily cratered surface from machining

AFTER: Rq = 3.5nm
Small islands appear to be grains. Highest point to lowest point around 18.6nm.

BCP/EP uses hydrofluoric and sulfuric acid mixture:

- Complicated procedure, dangerous chemical, expensive
- Cause surface contamination (Sulfur)

CMP – no hydrofluoric and sulfuric acid

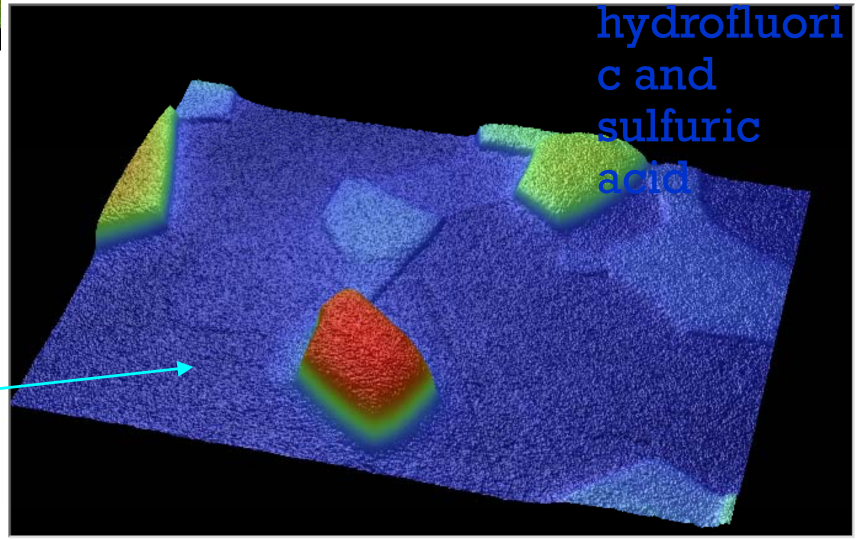

Tumbling

- Material :"Stones" made in different shape and material
- Effect: Smoothening and removal of local enhancement (Sparks from EB welding weld in area)
- Removal: Non uniform contact pressure, For optimum removal you need to design machines that make use of centrifugal forces to uniform the forces (Complicated design)

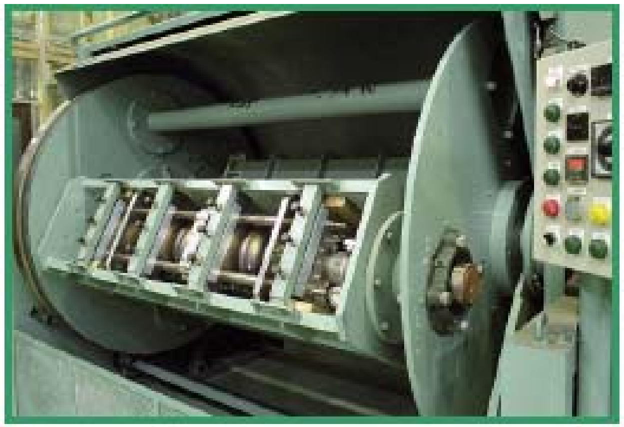

Chemical removal of "damage" layer

Two types chemical removal are most commonly in use

BCP - Buffered Chemical Polishing

Mixture of Hydrofluoric; Nitric and Phosphoric acid

- Mixed by volume from 1:1 HF(49%) /HNO3(70%) to (1:1:2 HF(49%):HNO3(70%) :H3PO485%)
- Removal rate:
  - **1:1 at 20C >20 μm/min; 1:1:2 at 20 C ~1μm/min**
- Mixture is self exiting ! Spontaneous reaction with Nb!!

EP – ElectroPolishing

Mixture of Hydrofluoric acid and Sulfuric acid

- Mixed by volume from 1:8 HF(45%) /H2SO4 (96%) to 1:10 (HF(45%)/H2SO4 (96%) (+ H_2O due to hygroscopic reaction of H_2SO_4)
- **Removal rate with 17 V applied:**
  - 1:9 at 20C 0,3-0,5 μm/min; 1:10 a t 20 C 0,3 – 0,4 μm/min
- No reaction on Niobium without voltage applied.

Cavity Preparation

Actually there are 3 general lines

BCP

Standard treatment used for TTF Modules 1-5 (BCP treatments + 1400 C titanium post purification)

EP / 1

Treatment sequence
<u>used for the first batch of cavities electro-polished in collaboration with KEK</u>
Combination of
BCP (80- 160 µm)+
EP (80- 100µm) at KEK+
EP (20-50 µm) at DESY
Part of production
1400 C titanium post purified

EP / 2

Treatment sequence
<u>under study at DESY</u>
No 1400 C Ti post purification
<u>Only EP</u> applied (**200** µm)
Improved handling sequences

BCP process

Chemical Polishing: BCP

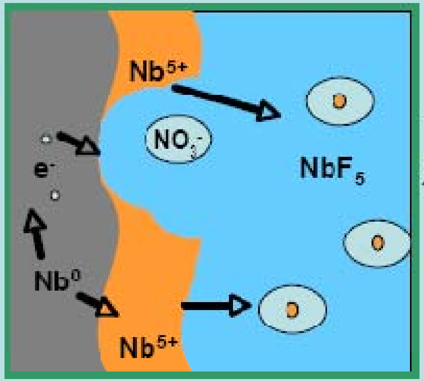

$Nb_2O_5 + 10HF_2 \longrightarrow NbF_5 + 5H_2O$

$2Nb + 10HNO_3 \longrightarrow 10NO_2 + 5H + Nb_2O_5$

$H_3PO_4 \longleftrightarrow H^+ + H_2PO_4$

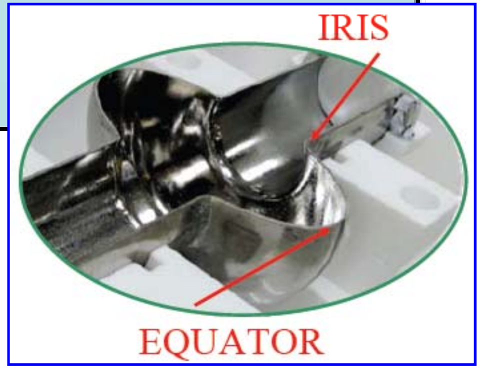

Pros:
- Set up simple and cheap
- Accelerating gradients below 25-30 MV/m in cavities made out of polycrystalline Nb
- Reliable results with very high reproducibility of cavity performances
- Average etching rate: 1 μm/min
- Accelerating gradients of 40 MV/m in cavities made out of single crystal Nb

Cons:
- High average roughness in polycrystalline Nb sheets (field enhancement)
- Etching rate is deeply affected by the local velocity and T of the acid <20C
- Differential etching: Lower removal at the equator (cell zone with lower radius) and a double removal at the iris zone.

Talk by K.Saito in JLAB on Oct. 2003

Electropolishing of Niobium

Current oscillation control: innovated by H.Diepers et al. in 1971

$2Nb + 10HF \rightarrow 2H_2NbOF_5 + 5H_2 \uparrow$

Metal complex salt

EP acid

H_2SO_4(>95%) : HF(46%) = 10 : 1 V/V

Very hazardous Acid

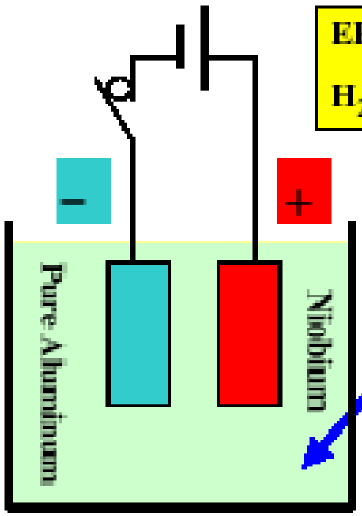

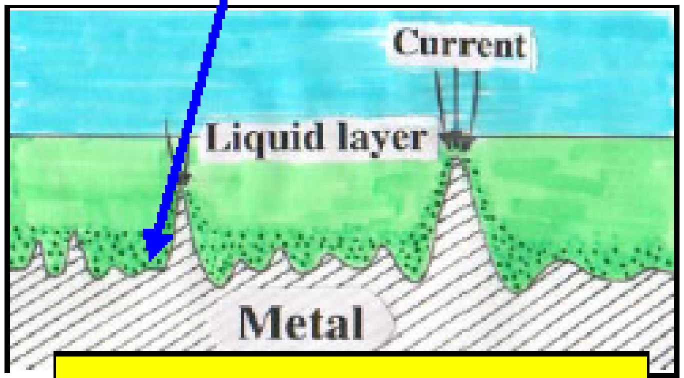

Leveling mechanism by P.A.Jaquet

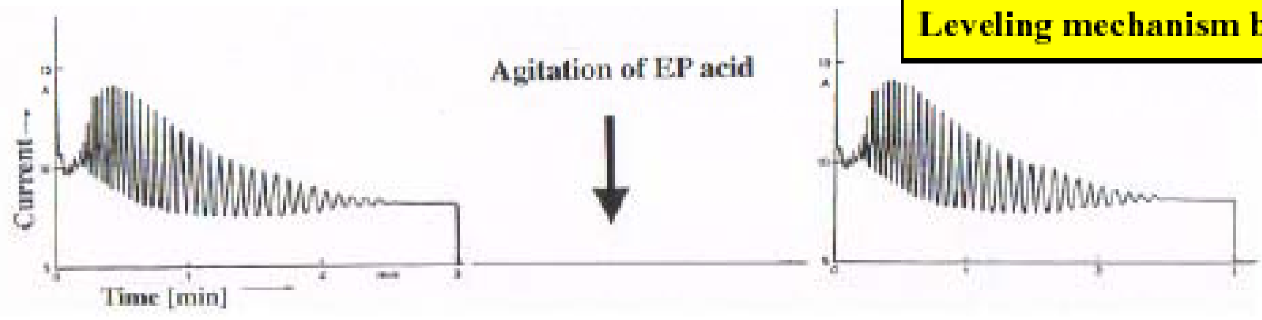

Chemistry

BCP

$$2\,Nb + 5\,NO_3^- \Rightarrow Nb_2O_5 + 5\,NO_2 + 5\,e^-$$

$$Nb_2O_5 + 6\,HF \Rightarrow H_2NbOF_5 + NbO_2\ 0.5H_2O + 1.5H_2O$$

$$Nb_2O_5 + 5\,HF \Rightarrow H_2NbOF_5 + NbO_2\ 0.5H_2O + 1.5H_2O$$

EP (electro chemical polishing)
Mixture by volume 1/9 HF/H2SO4

$$2\,Nb + 5\,SO_4^{2-} + 5\,H_2O \Rightarrow Nb_2O_5 + 10\,H^+ + 5\,SO_4^{2-} + 10\,e^-$$

$$Nb_2O_5 + 6HF \Rightarrow H_2NbOF_5(\text{l編.}) + NbO_2F \bullet 0.5H_2O(\text{unl編.}) + 1.5H_2O$$

$$NbO_2F \bullet 0.5H_2O + 4HF \Rightarrow H_2NbOF_5 + 1.5H_2O$$

EP- Systems

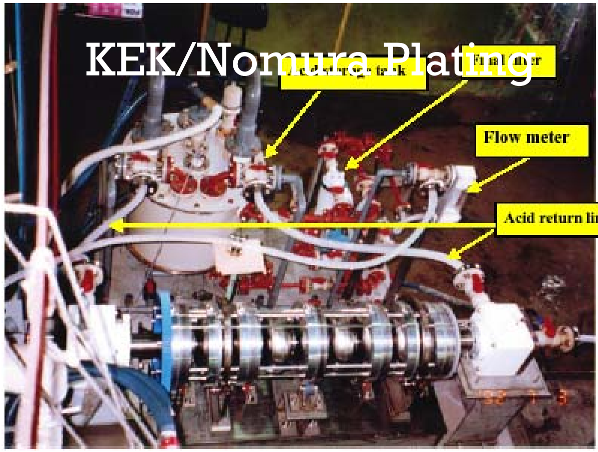
KEK/Nomura Plating
Flow meter
Acid return line

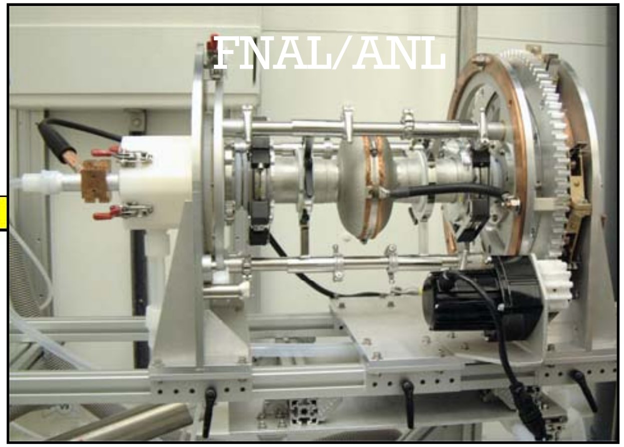
FNAL/ANL

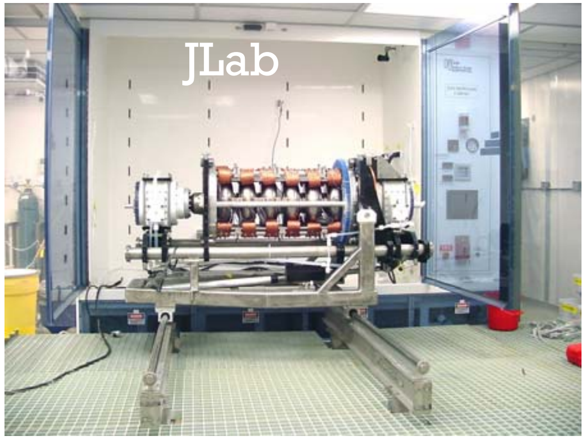
JLab


INFN

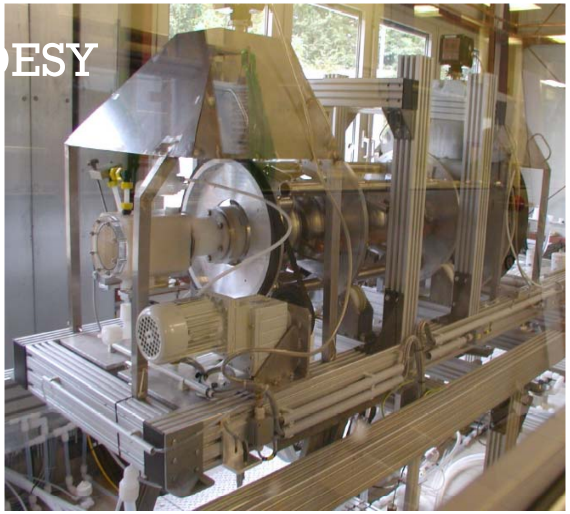
ESY

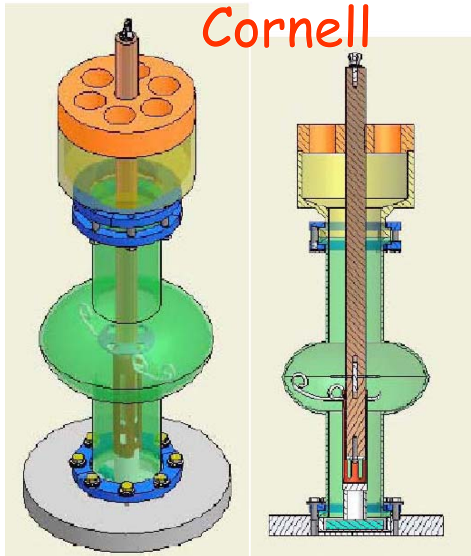
Cornell

Preparation for vertical test at 2K

1) "Car wash"
2) Degreasing and rinsing
2a) Prepare for EP and EP treatment
2b) or BCP treatment
4) Rinsing and 1st high pressure rinsing
5) Drying in class 10 (ASTM)
6) Assembly of accessories
7) Alcohol rinsing
8) Six times high pressure rinsing
9) Drying in class 10 (ASTM)
10) Assembly of test antenna
11) 120 C baking
vertical test

High pressure stand
in clean room

Alternative plasma cleaning

Plasma cleaning

ECR plasma and RF cavity

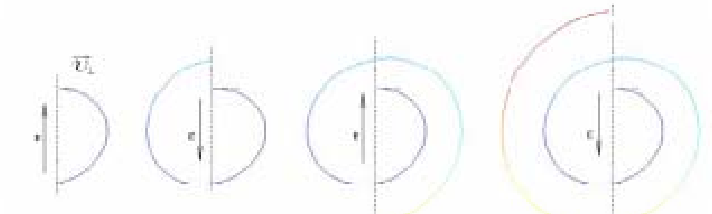

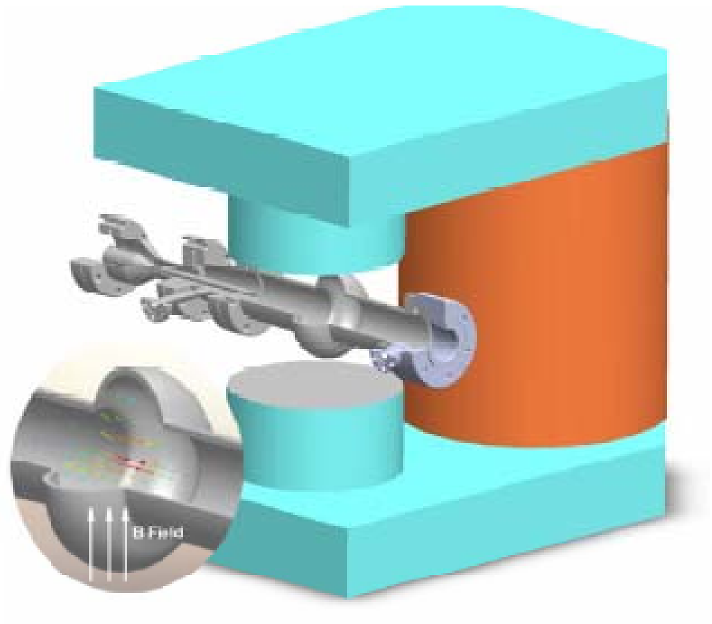

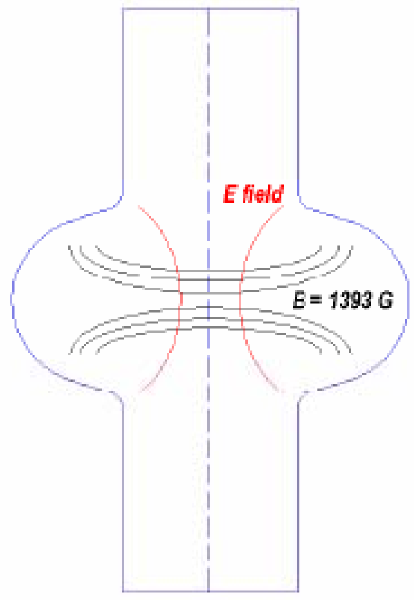

$$\omega = \frac{eB}{m}$$

- ECR = electron cyclotron resonance

G.Wu, FNAL

July 24, 2008 G. WU et al, TFSRF 2008, JLAB 8

Cavity Vertical Test Stand (VTS)

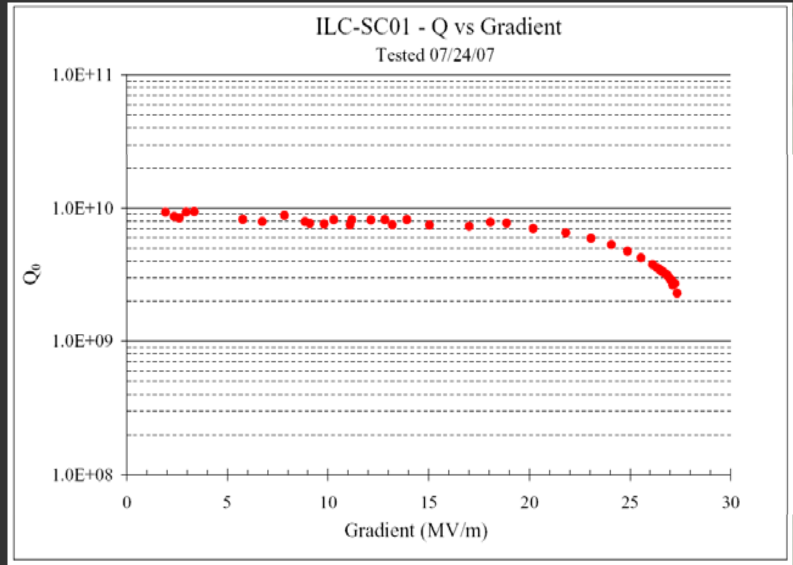

FNAL VTS

- Vacuum pumping
- Variable coupler
- Two cavity operation
- T-mapping

Q – Disease (Losses from Hydrides)

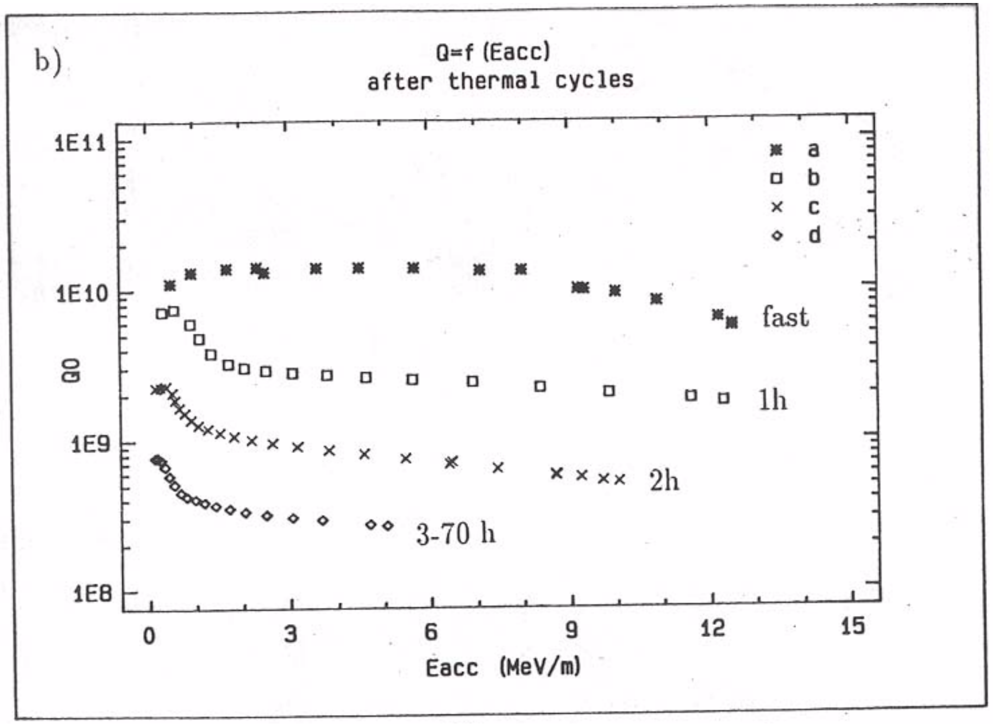

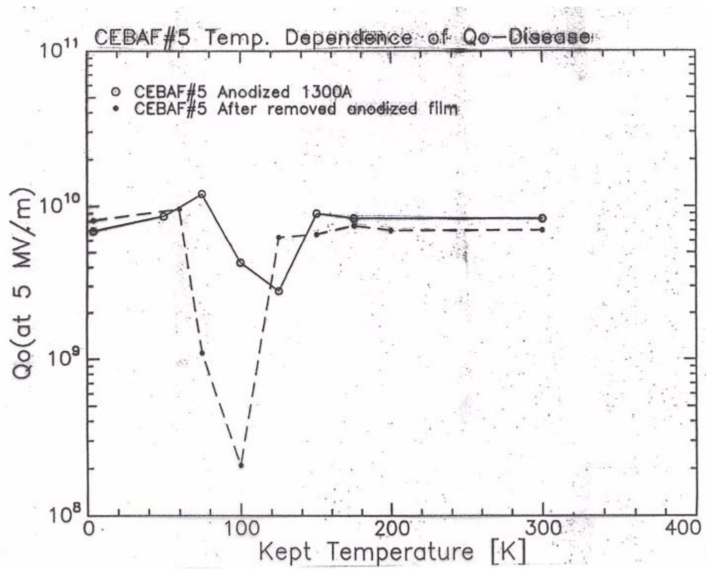

- Fast cool-down is essential (<1hr at T=120-170K)
- Nb with high oxigen (>100 wt ppm is not affected Q-disease problem)
- Effect depends on surface contamination, RRR, …

From vertical test to module

(Shortened version there are more steps than shown here necessary)

1. Back to clean room
2. Install FEM (in situ bead pull measurement)
3. Tank welding
4. Remove FEM
5. Install Antennas
6. High pressure rinse cavity
7. Install power coupler
8. Assemble of module

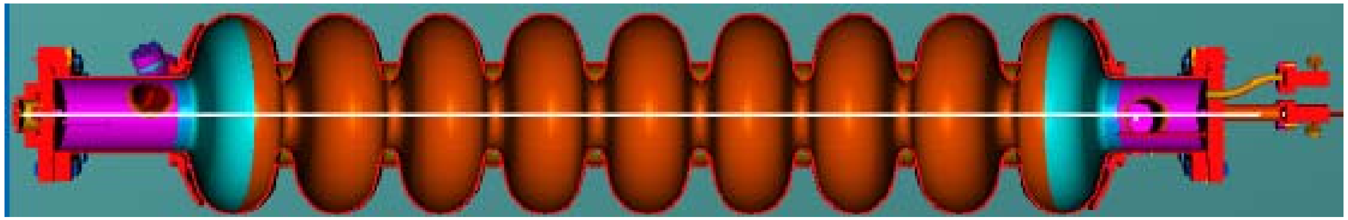

Bead-pull measurements after tank welding

Horizontal Test System (HTS)


HTS Cryostat

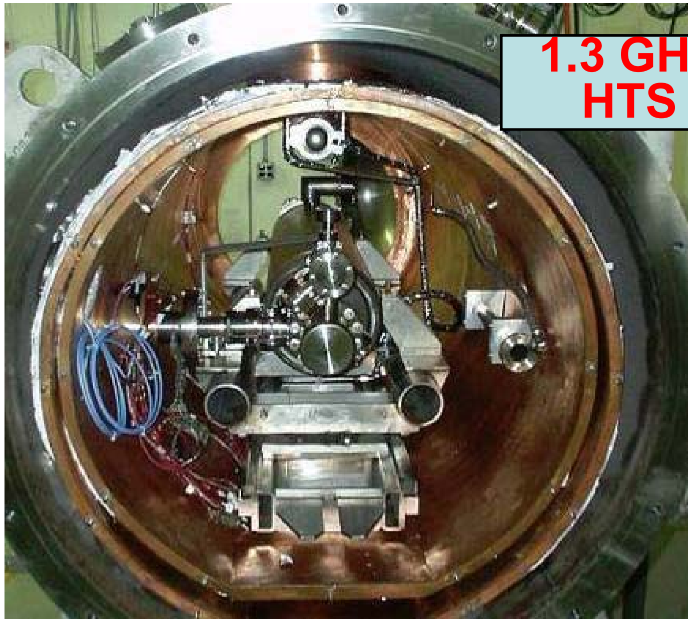
1.3 GHz Cavity in HTS Cryostat


2K Cryogenic


RF Power for HTS

Accelerating Gradient:

Limit and Spread

Limit of SRF Electric field

- No known theoretical limit
- 1990: Peak surface field ~130 MV/m in CW and 210 MV/m in 1ms pulse.
  J.Delaen, K.Shepard,"Test a SC rf quadrupole device", Appl.Phys.Lett,57 (1990)
- 2007: Re-entrant cavity: E_{acc}= 59 MV/m (E_{pk}=125 MV/m,Hs=206.5mT).
  (R.L. Geng et. al., PAC07_WEPMS006) – World record in accelerating gradient

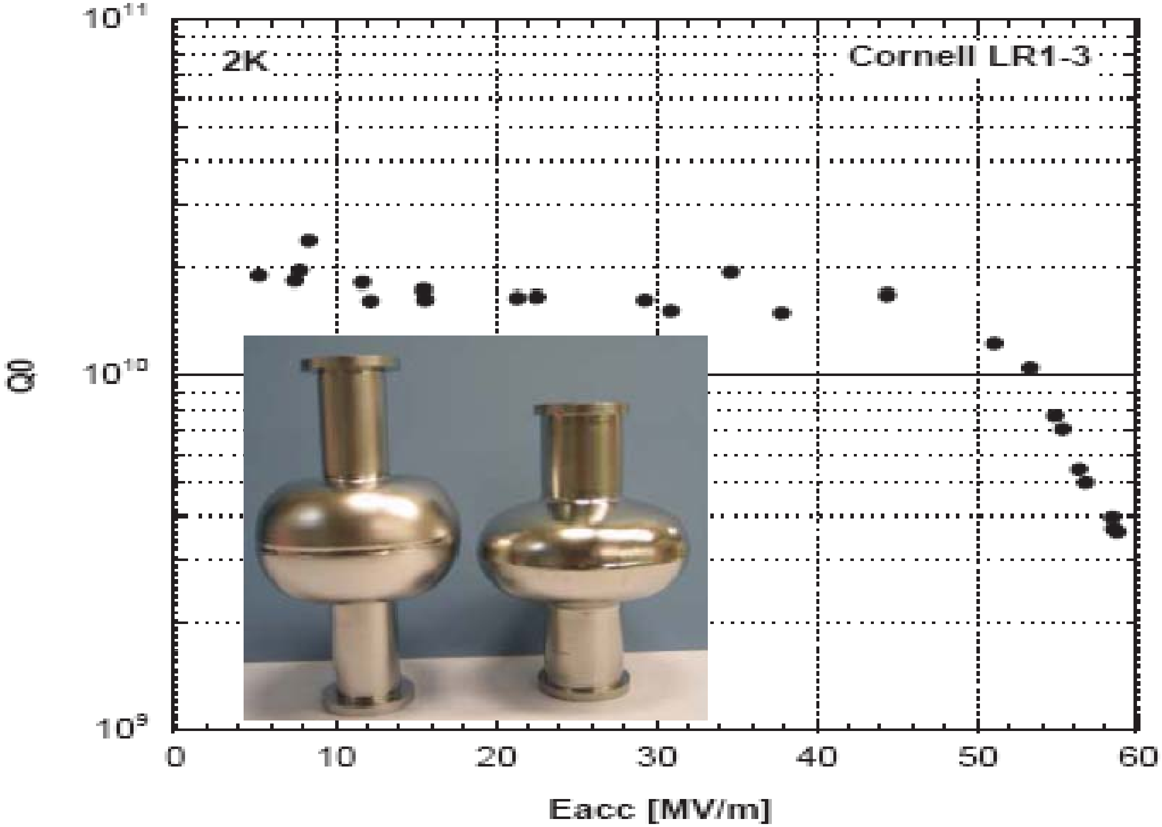

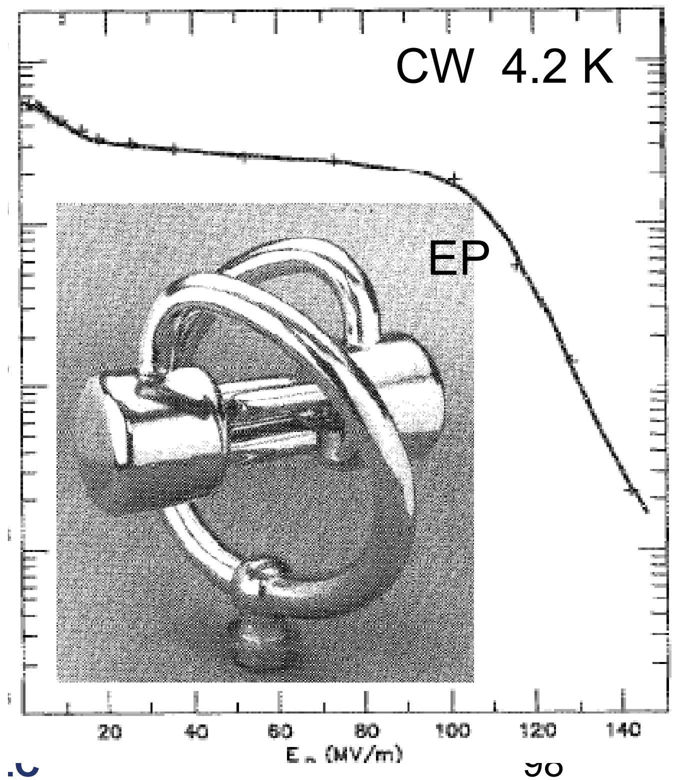

Gradient & Magnetic field Limits

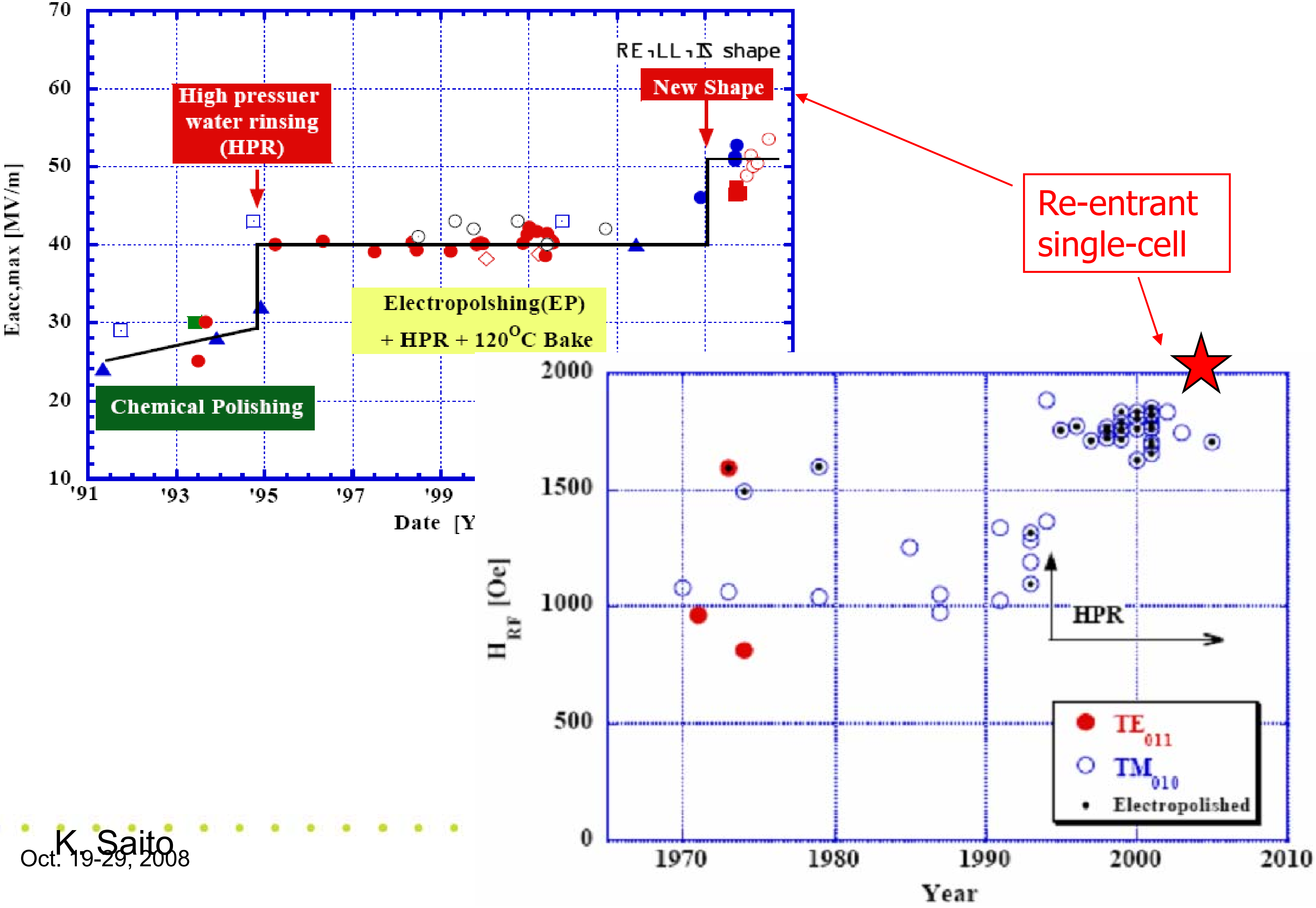

Reproducibility – Scattering of gradient

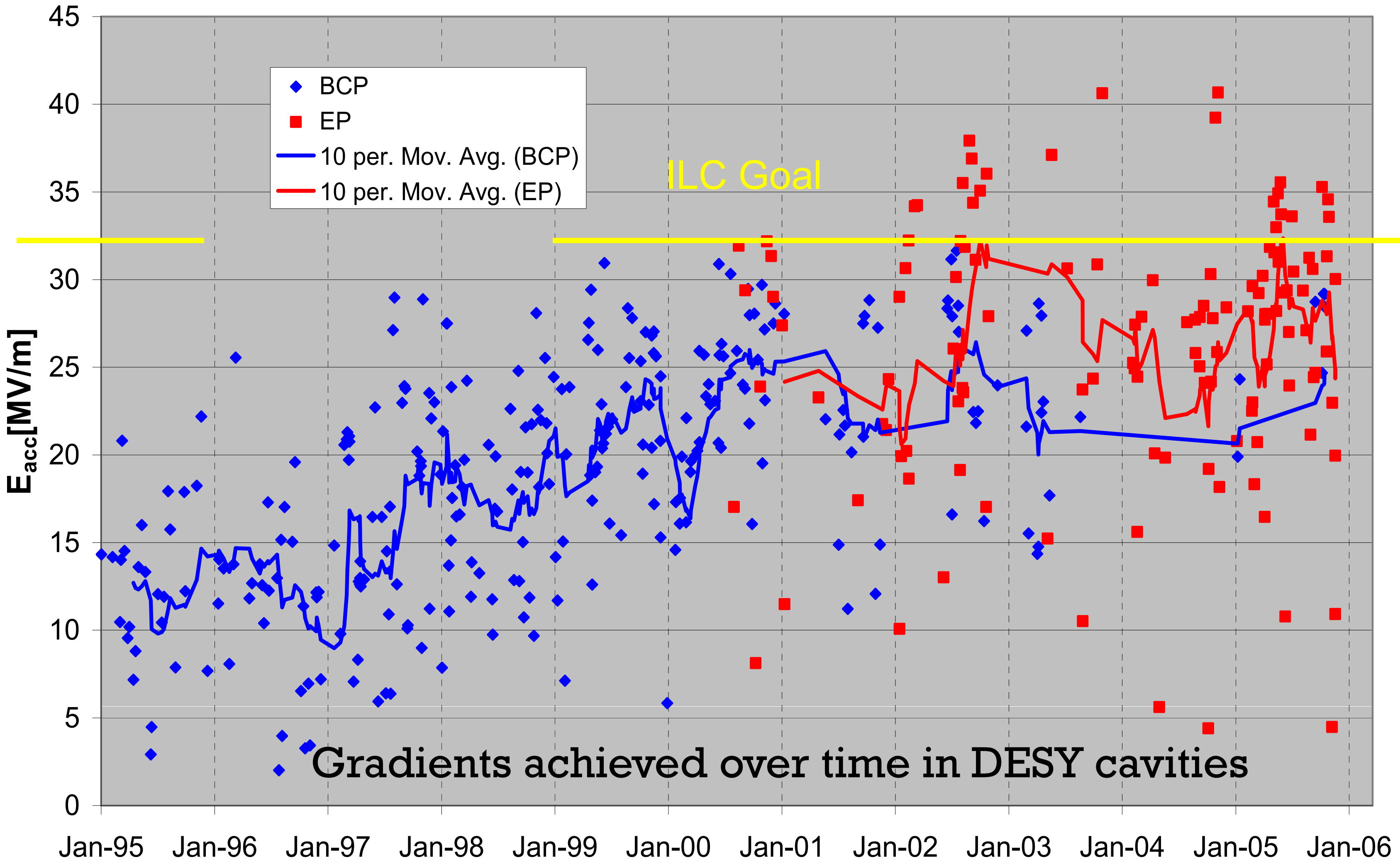

K.Saito

"Practical" gradient limitations for SC cavities

- Surface magnetic field – 200 mT (absolute limit?)
- Field emission, X-ray, starts at ~ 20 MV/m
- Thermal breakdown (strong limits for F>2GHz)
- Multipactoring (in cavity or couplers)
- Medium and high field Q-slopes (cryogenic losses)
- Lorentz detuning and microphonics (frequency change)

<u>Key issue:</u>

Quality of surface treatment and Assembly

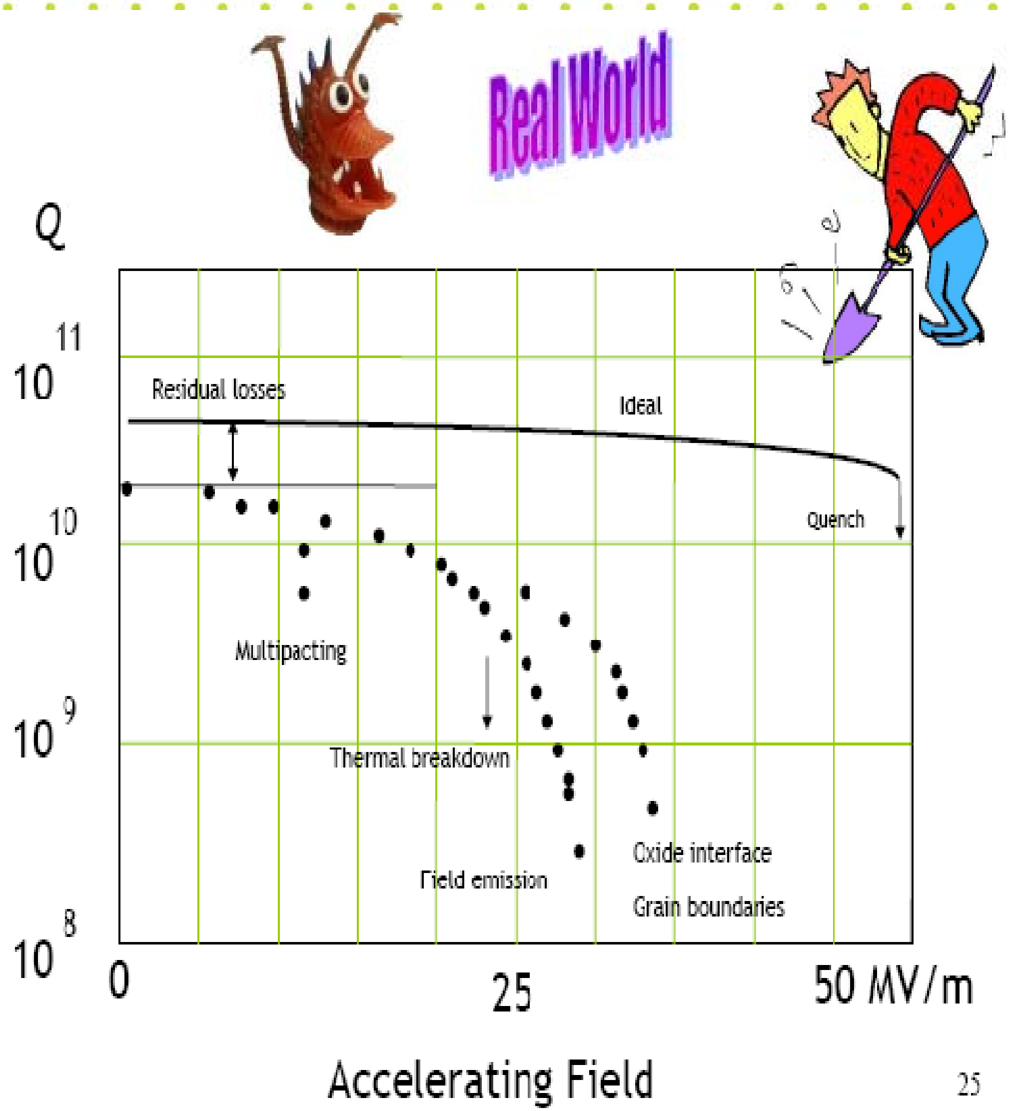

Field emission

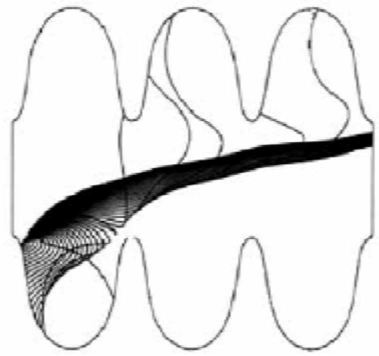

- Caused by macro-particles at the surface
- Some cavity FE limited. Starts typically ~ 20 MV/m
- Radiation→ heating of the wall → Q-drop
- Dark current
- Frequently disappear after HPR, but risk re-contamination (such as He tank d ressing) remains.
- Collective behavior in linac: affect other cavities (beam loading, heating, phase) - SNS
  - **Clean assembly**
  - **Understanding and improvement needed.**

Thermal Breakdown in pure Niobium

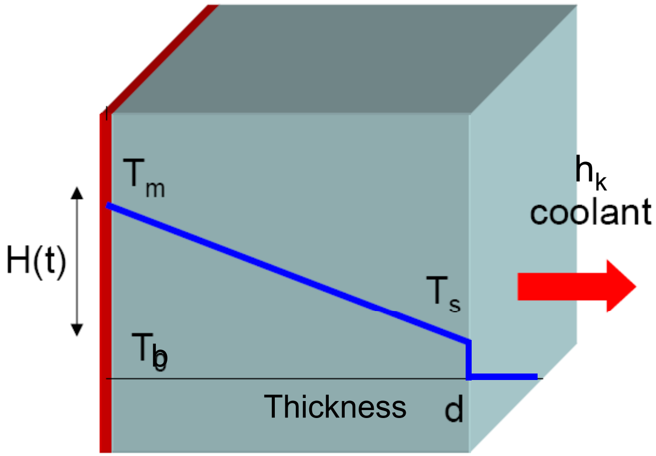

Power dissipation: $P_{diss} = \frac{1}{2} R_s(T_m, H_{RF}) H_{RF}^2$

$$\left\{ \begin{array}{ll} \text{Bulk:} & \frac{\partial}{\partial x} \kappa(T) \frac{\partial T}{\partial x} + P_{diss}(T_m, H_c, ..) \delta(x) = 0 \\ \text{Nb-He:} & \frac{1}{2} R_s(T_m, H_c, ..) H_{RF}^2 = h_K(T_s, T_b)(T_s - T_b) \end{array} \right\}$$

Run away solution for 2°K and

k(T_0)=30 W/(m•K); h(T_0)= 10^4 W/(m^2•K);

Solution:

$$\delta T = 0.137^\circ K$$

$$H_b = 140\ mT$$

Quality factor (an example)

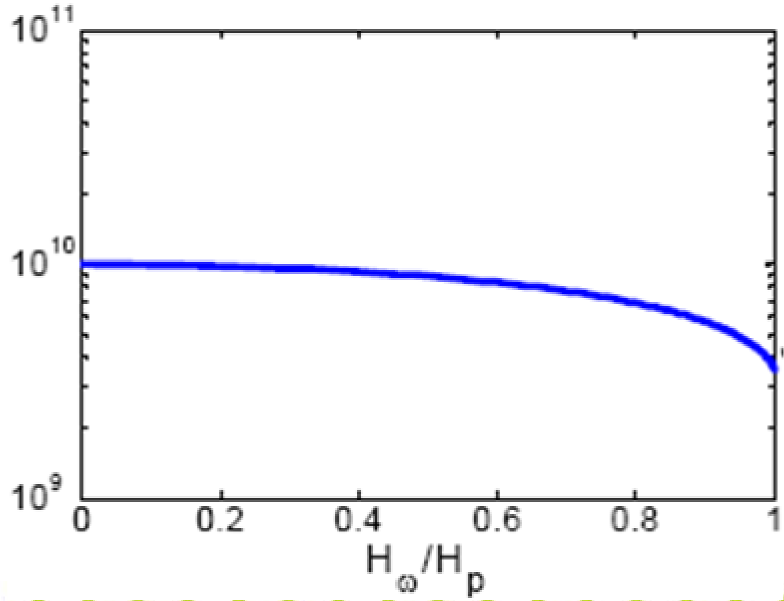

Example: 3.9 GHz accelerating cavity

- Final cavity preparation done at FNAL (BCP,HPWR)
- Residual resistance *R_res ~ 6 nΩ*
- Achieved: *H_peak = 103 mT, E_acc = 19 MV/m*

(Goal: H_{peak}= 68 mT, Eacc=14 MV/m)

Magnetic field is likely limited by thermal breakdown

- No Field Emission
- *Q ~ 8*10 ^{9} at E_acc =15 MV/m*
- Maximum accelerating field not depend on Temp

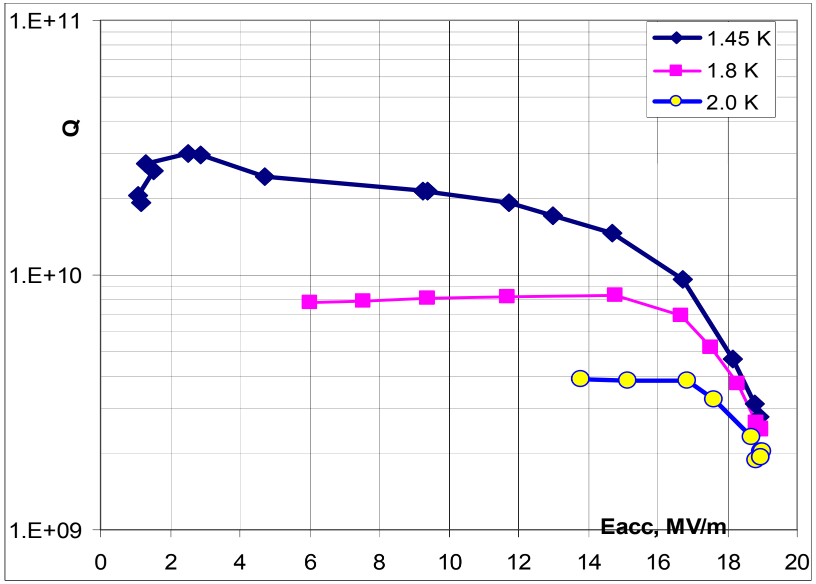

No Temperature dependence – why?

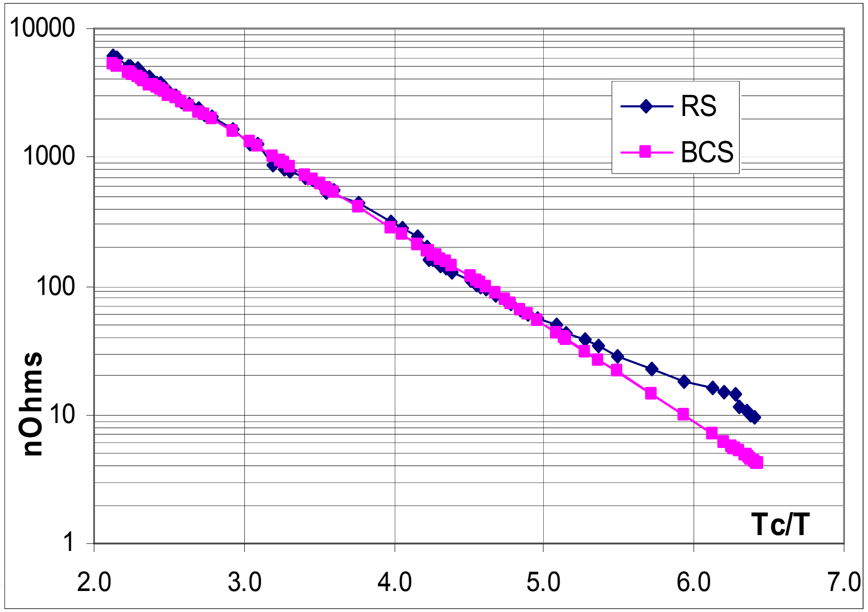

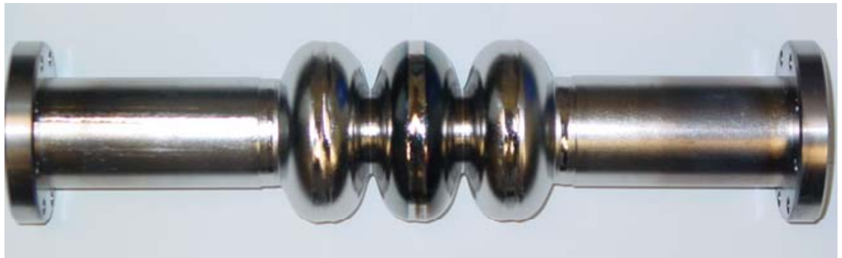

3-cell cavity built at FNAL

H = 103 mT ⇒ 9-cell/3.9GHz: → E_{acc} = 21 MV/m
TESLA: → E_{acc} = 24 MV/m

1. Non-linear Surface Resistance

The non-linear BCS resistance (RF pair breaking) in the *clean limit* is given by

$$R_s^{nlin}(T,B) = R_{s,bcs}^{lin}(T)\frac{2}{\pi}\left[\int_0^{\pi}\sin^2(t)\frac{\sinh[\beta(T)h\cos(t)]}{\beta(T)h\cos(t)}dt\right] + R_{res}$$

$$R_{s,BCS}^{lin}(T) = \frac{A(\Delta)\cdot f^2}{T}e^{-\frac{\Delta}{k_b T}}$$ - Linear BCS:

Δ ~1.5 meV is the superconducting energy gap

Where: $\beta(T) = \frac{\pi}{2^{3/2}}\frac{\Delta}{k_b T}$, $h = \frac{H_{RF}}{H_{c,0}}$

For 2 cases: β·h<<1 and β·h>>1 it gives:

$$R_s^{nlin1}(T,B) = R_{s,BCS}^{lin}(T)\left[1 + \frac{\beta^2}{48}\left(\frac{H_{RF}}{H_{c,0}}\right)^2\right] + R_{res}$$

$$R_s^{nlin2}(T,B) = R_{s,BCS}^{lin}(T)\left[\frac{4e^{\beta(T)\frac{H_{RF}}{H_{c,0}}}}{\beta(T)^{7/2}\sqrt{2\pi}}\right]\left(\frac{H_{c,0}}{H_{RF}}\right)^{7/2} + R_{res}$$

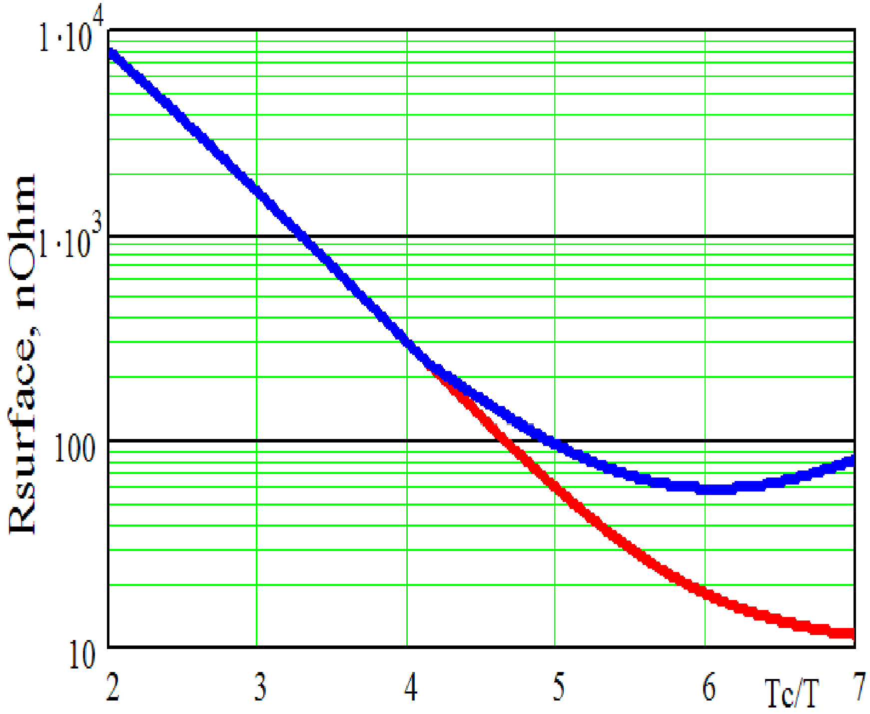

Surface Resistance used in models
Red-linear BSC; blue Non-linear case

*P.Bauer et.all, "Discussion of possible evidence for non-linear BSC resistance in SRF cavity", SRF 05 workshop

2. Thermal Conductivity and Kapitza resistance

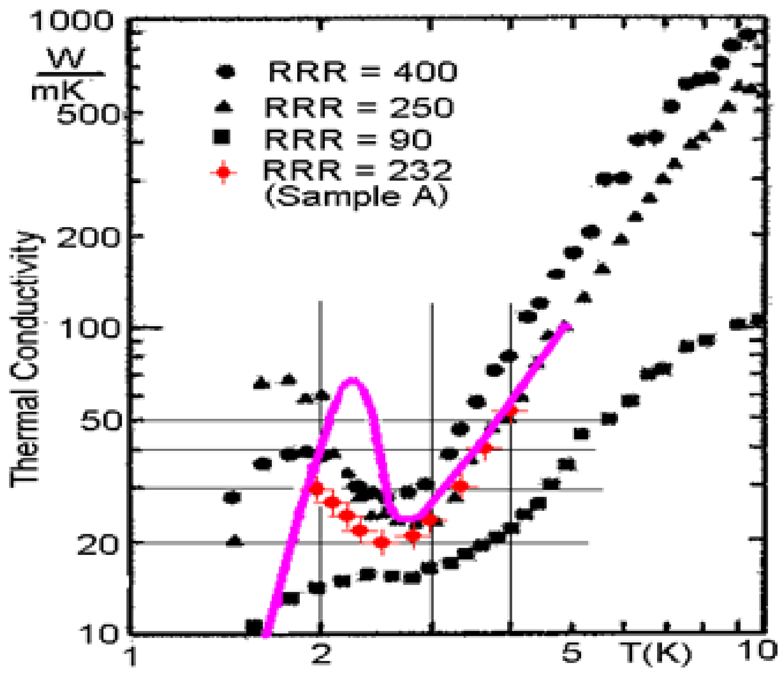

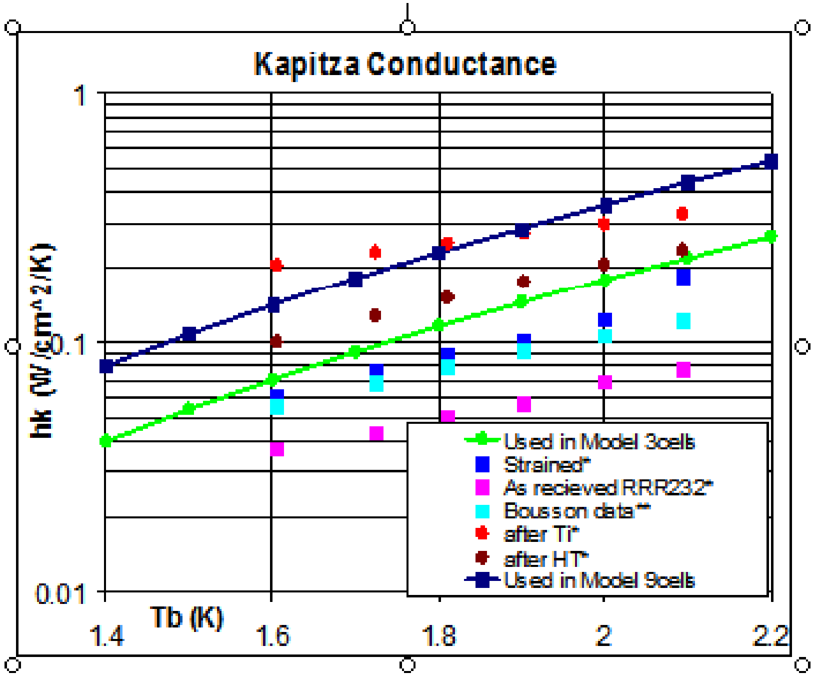

Measured thermal conductivity and values used in models (pink)

Measured values of Kapitza conductance and values used in model (solid lines)

A. Aizaz, "Improved Heat Transfer in SRF Cavities, NSCL, MSU, 2006

Bousson et. All, "Kapitza Conductance and Thermal Conductivity of Materials Used For SRF Cavities Fabrication", SRF workshop, 1999

Results for 3.9 GHz 9-cell cavity

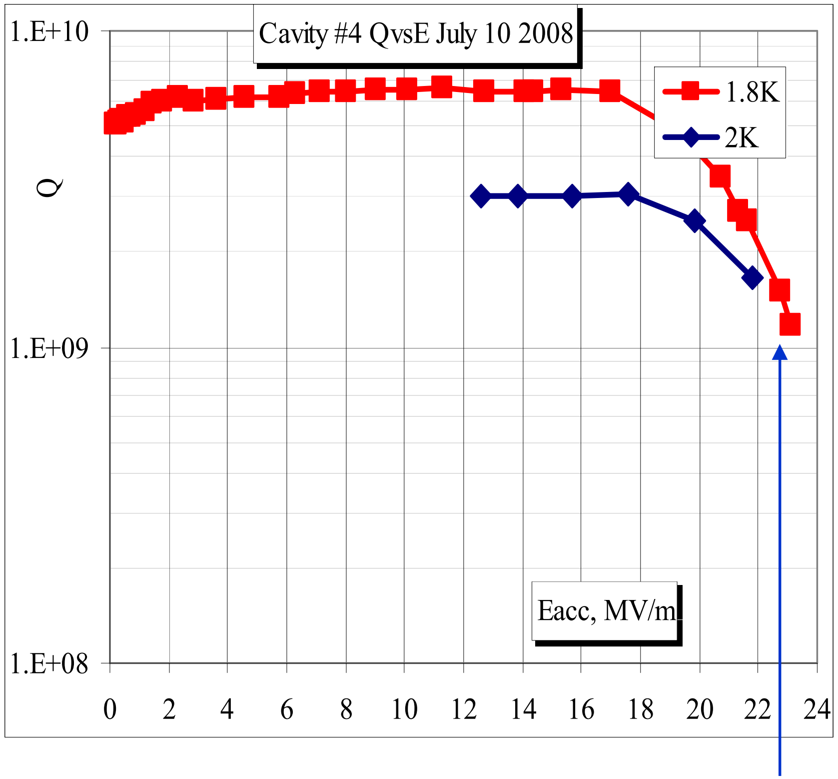

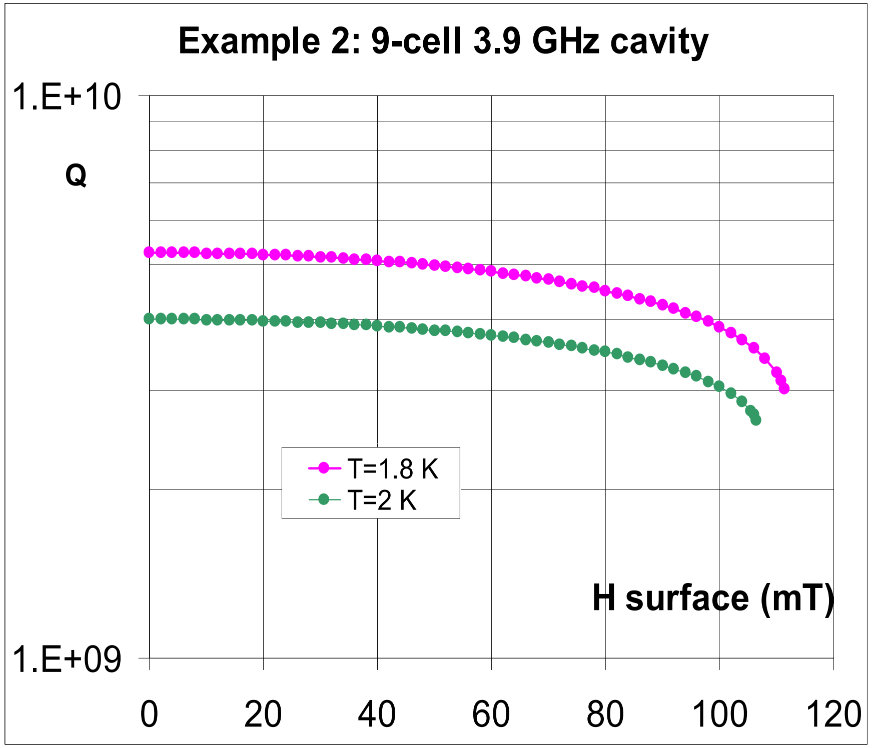

Experiment

Hs=120 mT

Simulations

I. Gonin - FNAL

Large Grain : Hot Spots

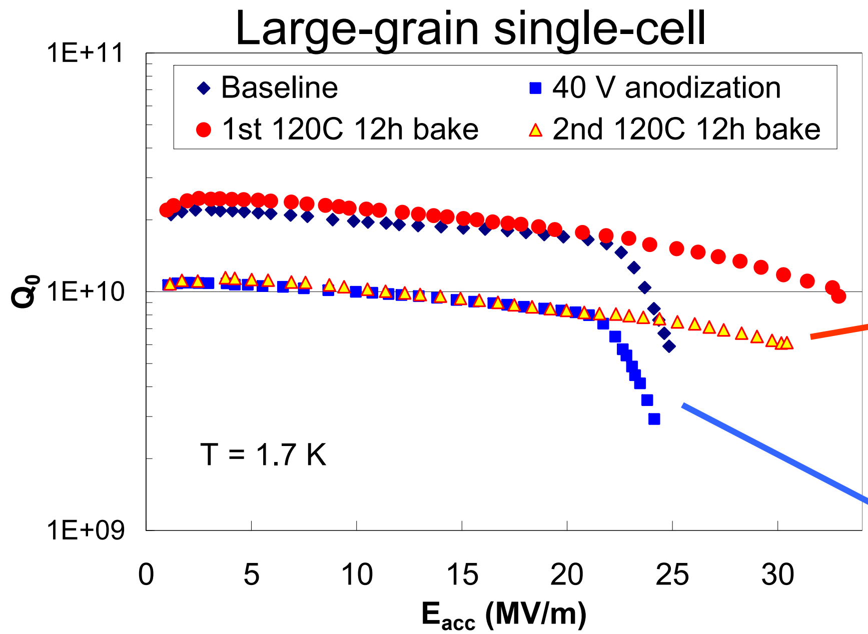

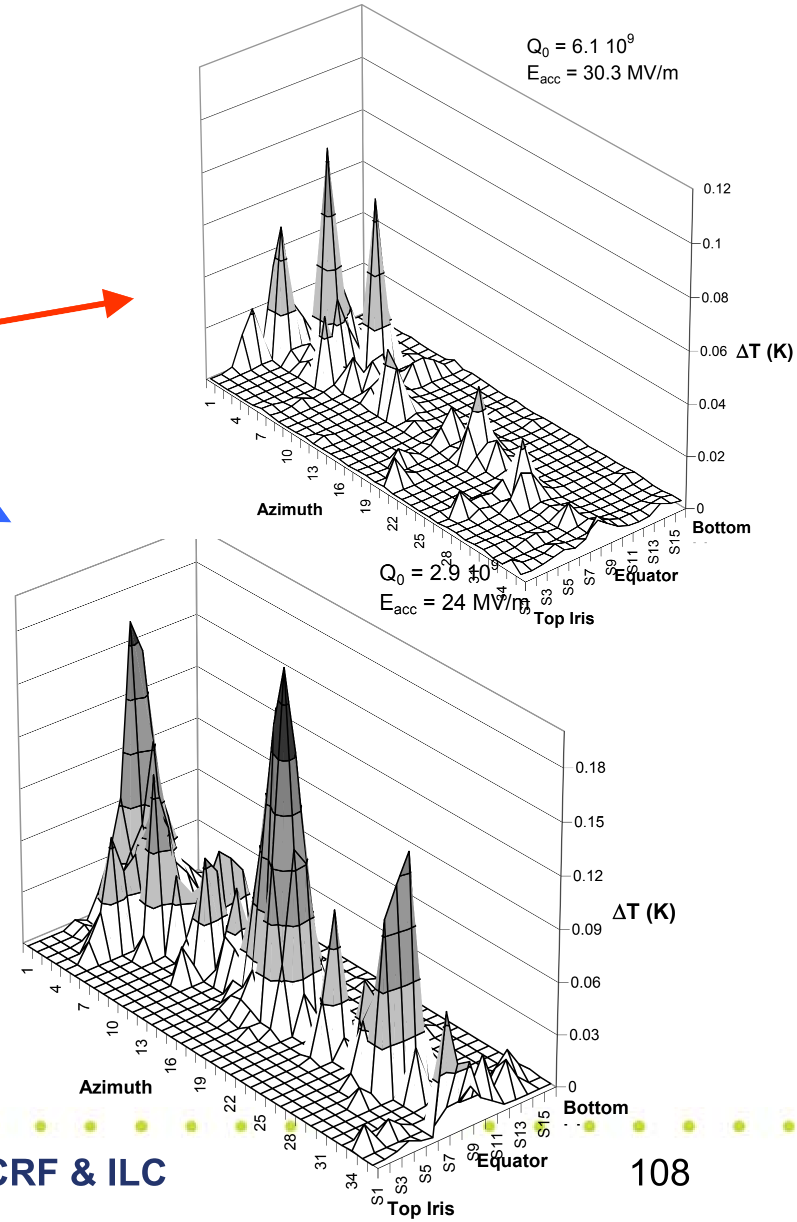

Hot spots (large grain cavity)

Reduced after baking

Q-slope restored by 40 V anodization

G. Ciovati - LINAC (2006)

T-mapping in cavity

Sub-mm size defects lead to quench

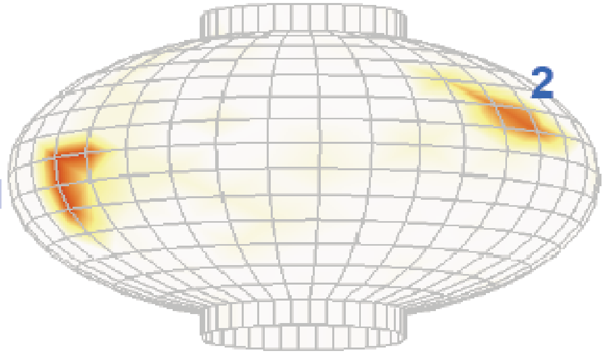

Temperature Mapping

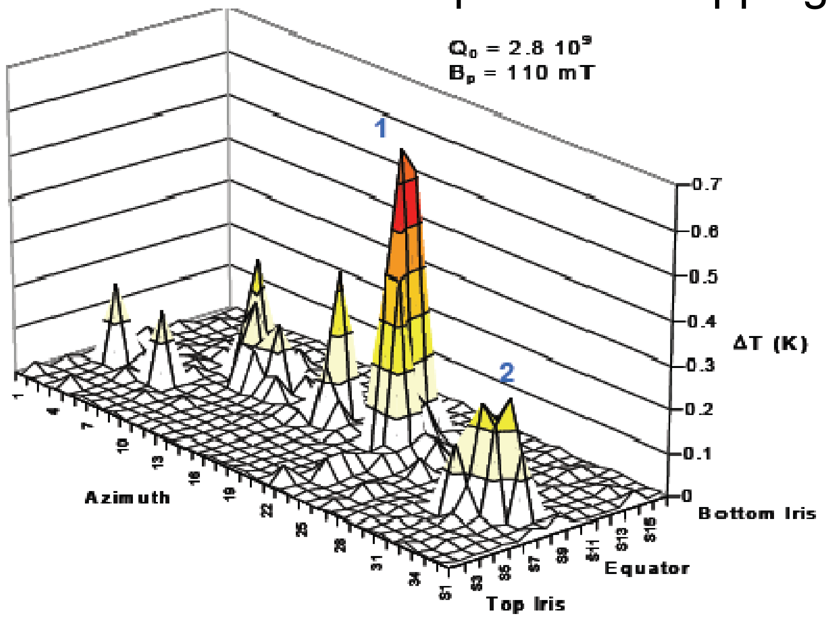

Thermometer array to detect hotspots, which ignite cavity breakdown

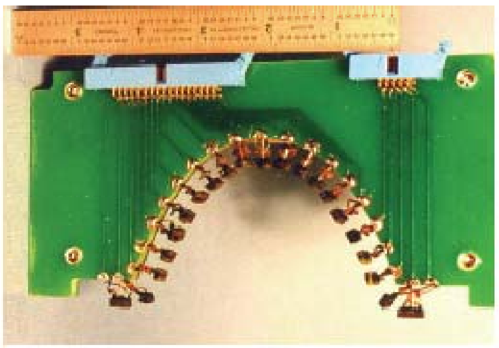

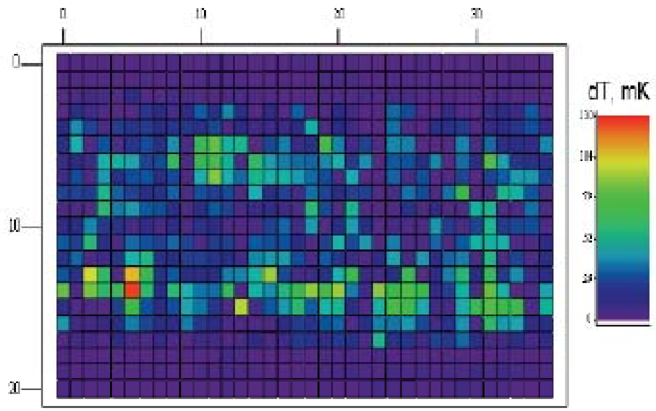

G. Ciovati - JLab - ODU

H. Padamsee - Cornell

Multipactoring in SC cavity

Theory of multipactor discharges

- The multipactor resonance condition for an electron in a parallel plate geometry can be determined analytically starting with the Lorentz force and the equation of motion,

$$\frac{d\mathbf{v}}{dt} = \frac{q}{m}(\mathbf{E} + \mathbf{v} \times \mathbf{B})$$

If v<<c and the equation of motion in 1-D then:

$$\frac{dv}{dt} = \frac{eE_o}{m}\sin(\omega t)$$

If the electron is born from an electrode at a time, $t = \frac{\alpha}{\omega}$, relative to the rf phase, α, with initial velocity v_o, the time dependent, 1-D velocity and position of the electron are given by

$$v = v_o + \frac{eE_o}{m\omega}(\cos(\alpha) - \cos(\omega t))$$

$$x = x_o + \frac{v_o}{\omega}(\omega t - \alpha) + \frac{eE_o}{m\omega^2}[\sin(\alpha) - \sin(\omega t) + \cos(\alpha)(\omega t - \alpha)]$$

In the simplest example, the multipactor resonant condition specifies the electron must traverse the electrode spacing, d, and impact the opposing surface near the time the electric field changes direction. The electric field changes direction at $\omega t = N\pi + \alpha$, where N is a positive odd integer. Invoking this condition of $\omega t = N\pi + \alpha$ the multipactor condition for the voltage in a parallel plate geometry is given by

$$V_o = E_o \cdot d = \frac{m}{e}\frac{\omega d(\omega d - v_o N\pi)}{N\pi\cos\alpha + 2\sin\alpha}$$

For simplicity, if the electron is born at the x=0 electrode with $v_o = 0$, and $\alpha = 0$

$$V_o = \frac{4\pi m}{e}(f \cdot d)^2$$

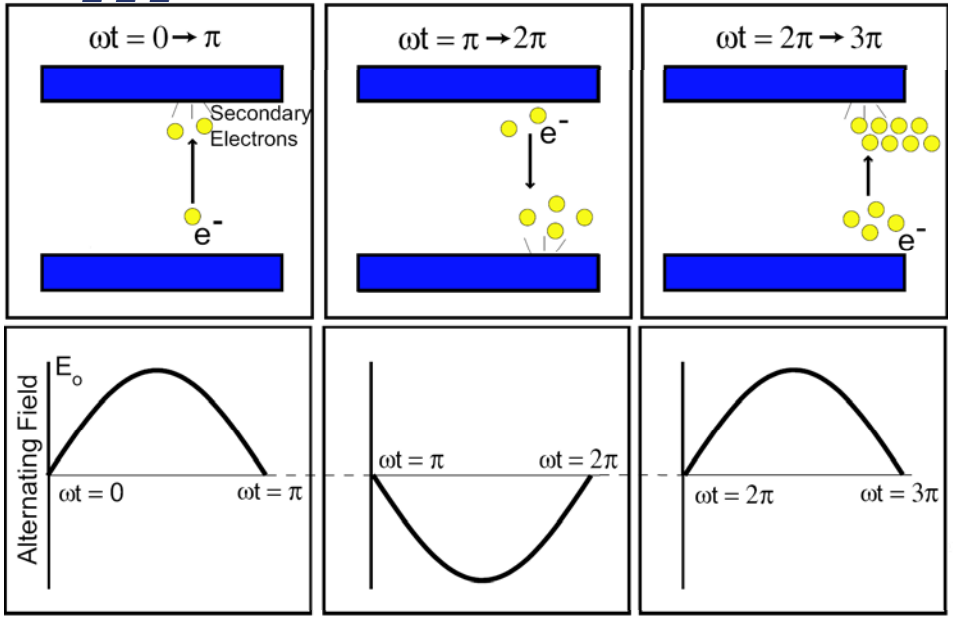

Multipactor discharge with an electric field oscillating between two metal electrodes.

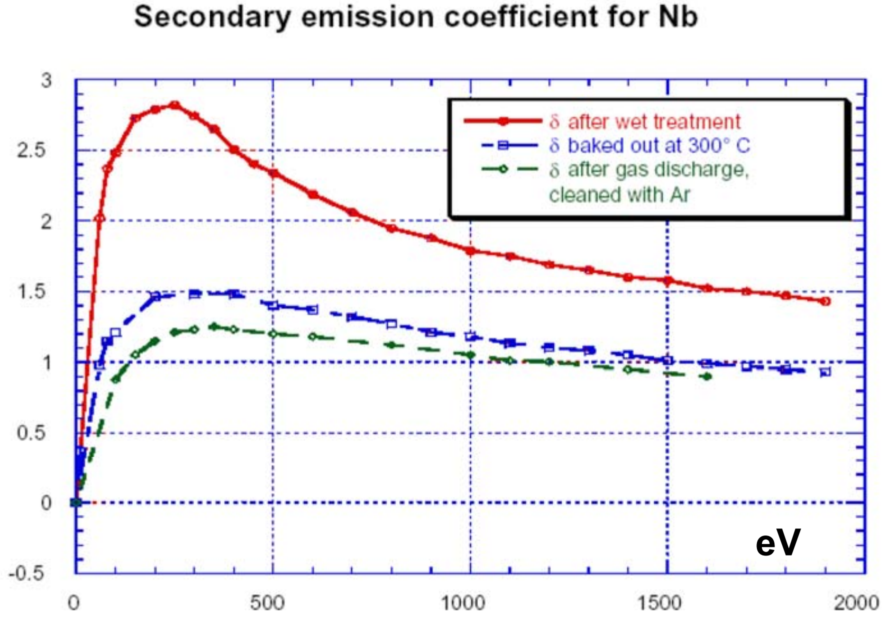

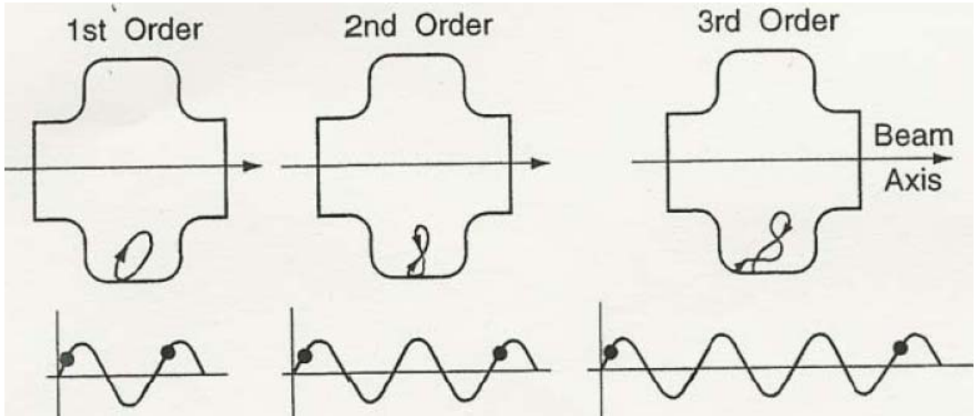

Typical one-point multipactor trajectories for orders 1, 2 and 3.

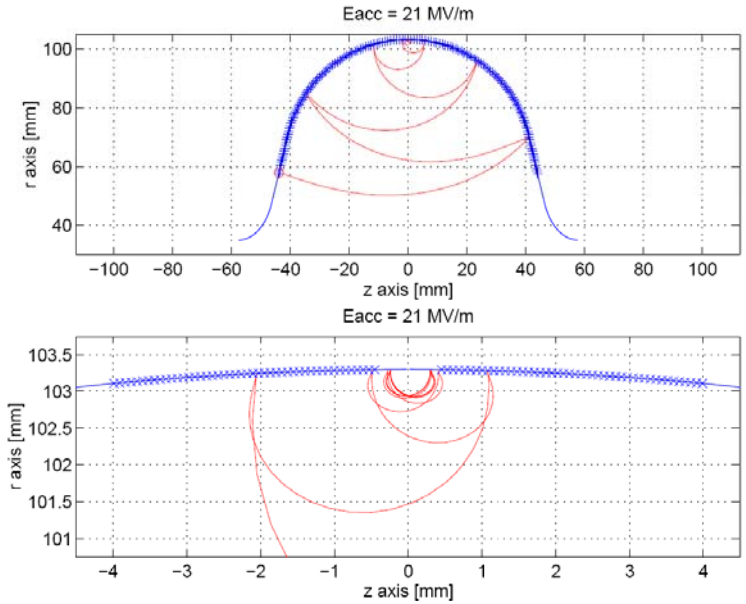

Two point MP in 1.3GHz TESLA cavity. 2D simulations

Ex: Multipactor in HOM Couplers of 3rd harm. cavity

3D simulation

Omega 3P(Analyst)

MP in notch gap 0.6 mm

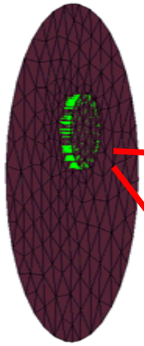

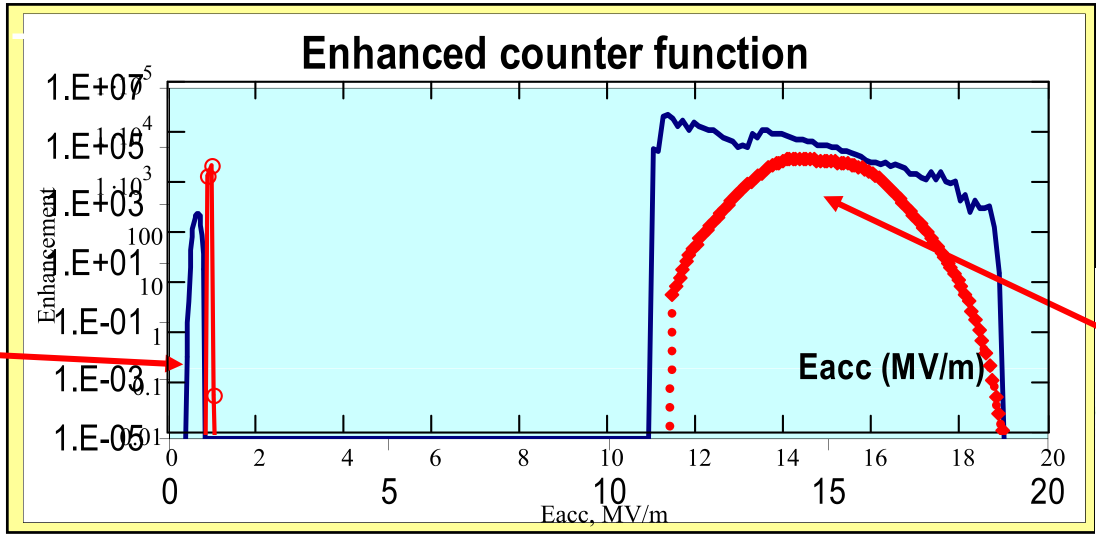

MP in 2 mm Leg-wall gap

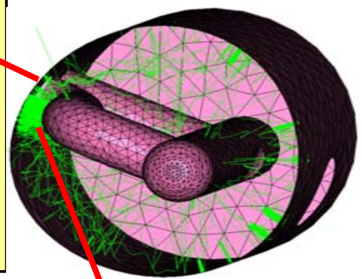

Cavity No.3. Results of vertical test: MP observed at Eacc~0.7MV/m (Q drop). Quench at Eacc~14MV/m.

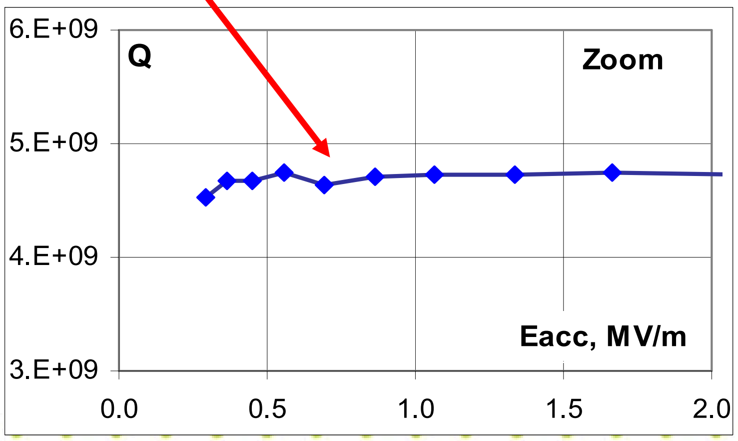

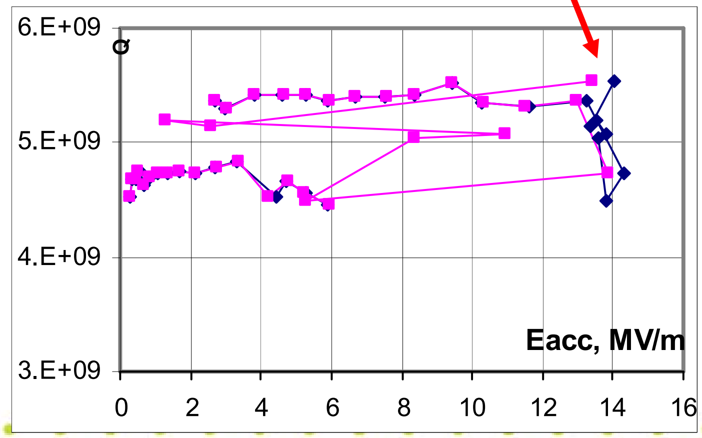

Multipactor in Cavity HOM Couplers

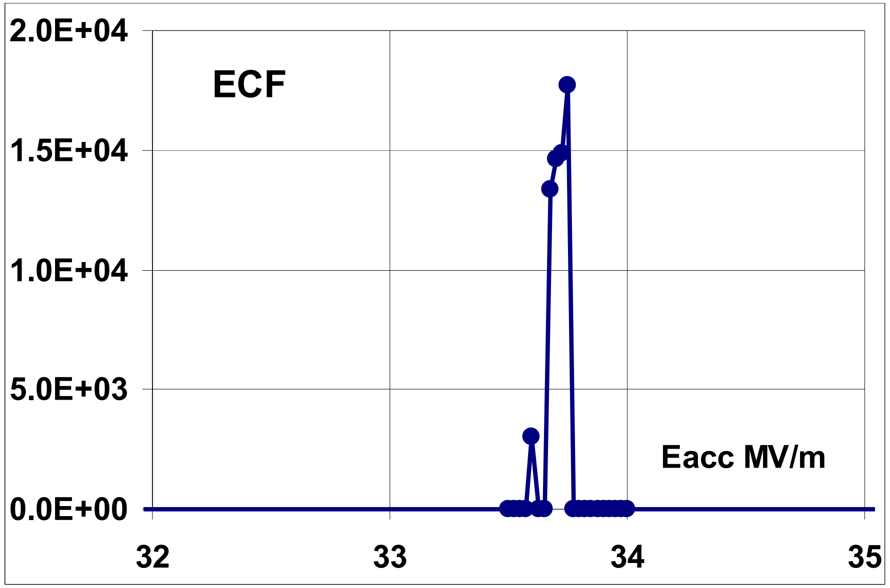

ANALYST predict MP at E_{acc}~1 MV/m and E_{acc}~ 33.7 MV/m

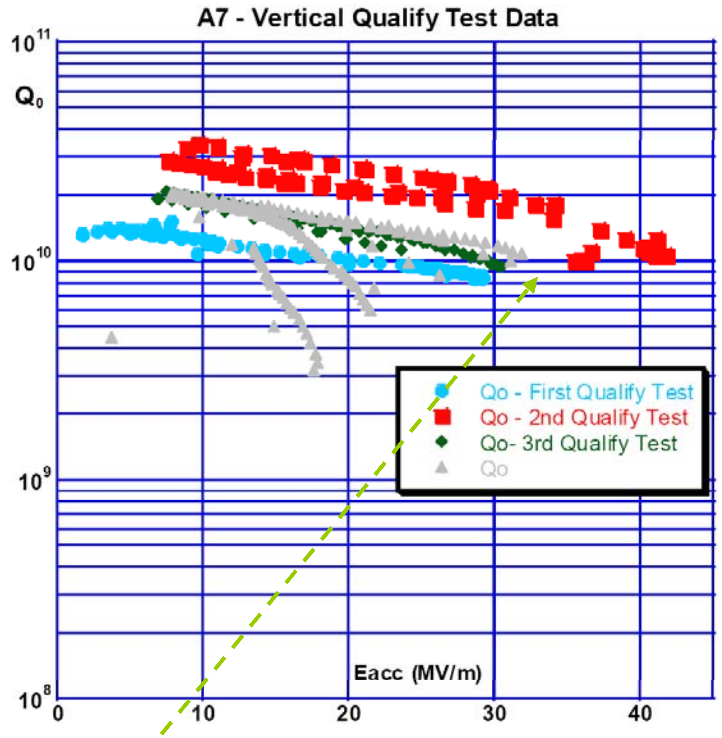

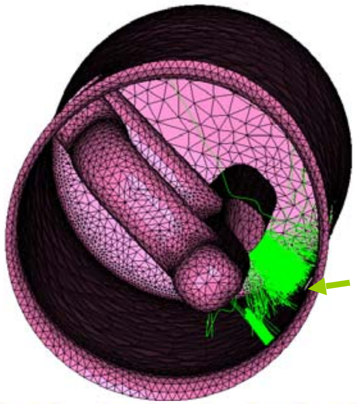

MP explains Q-drop during vertical test at JLab and localize the place of MP. ILC operating gradient E_{acc}= 31.5MV/m is close to MP level.

Possible HOM coupler design modification needed!

Problems in Ichiro 9-cell cavity

(Superstructure Version)

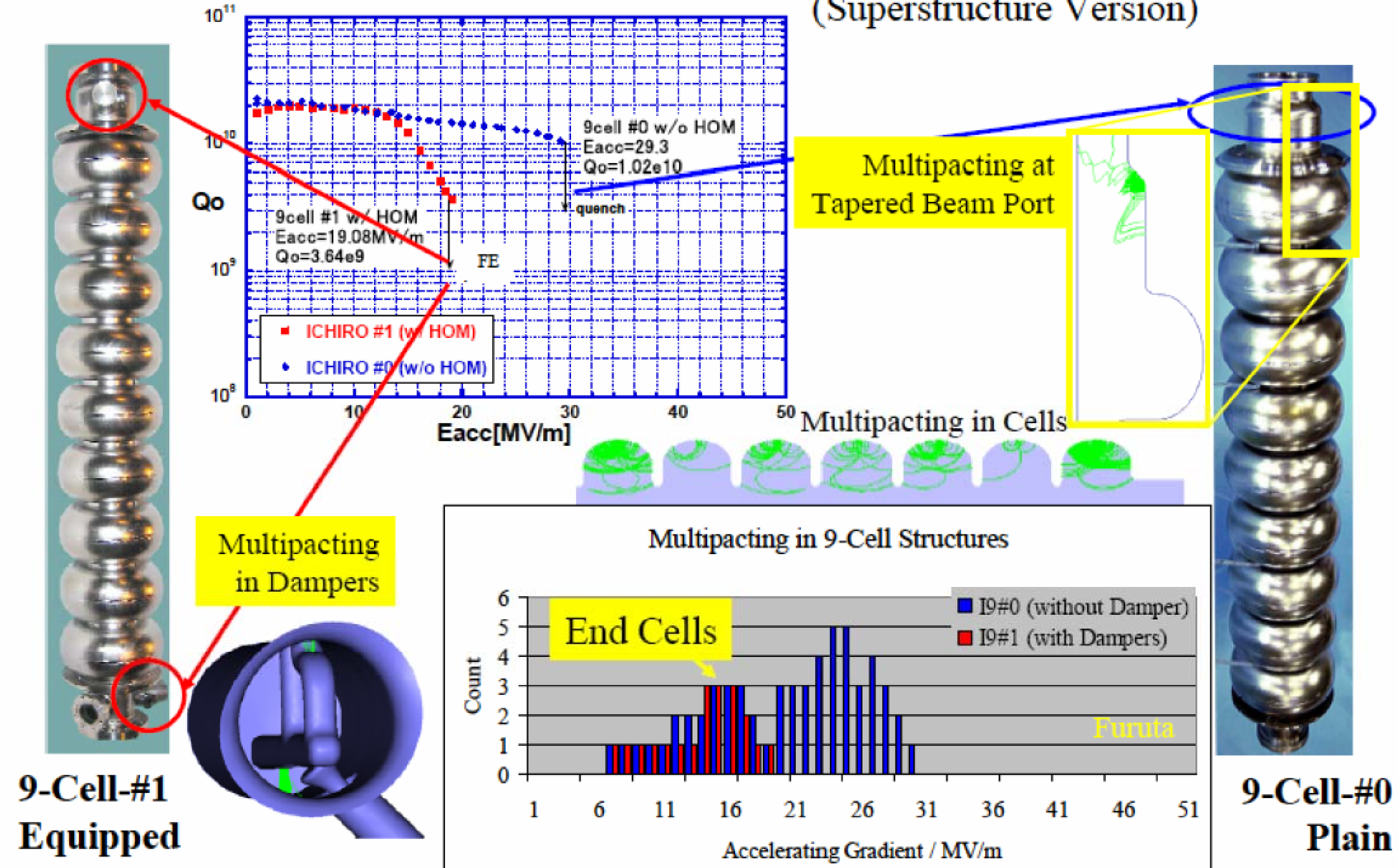

S0/S1 ILC R&D programs

Goal: develop procedure which will provide >85 % acceptance yield in cavity performance

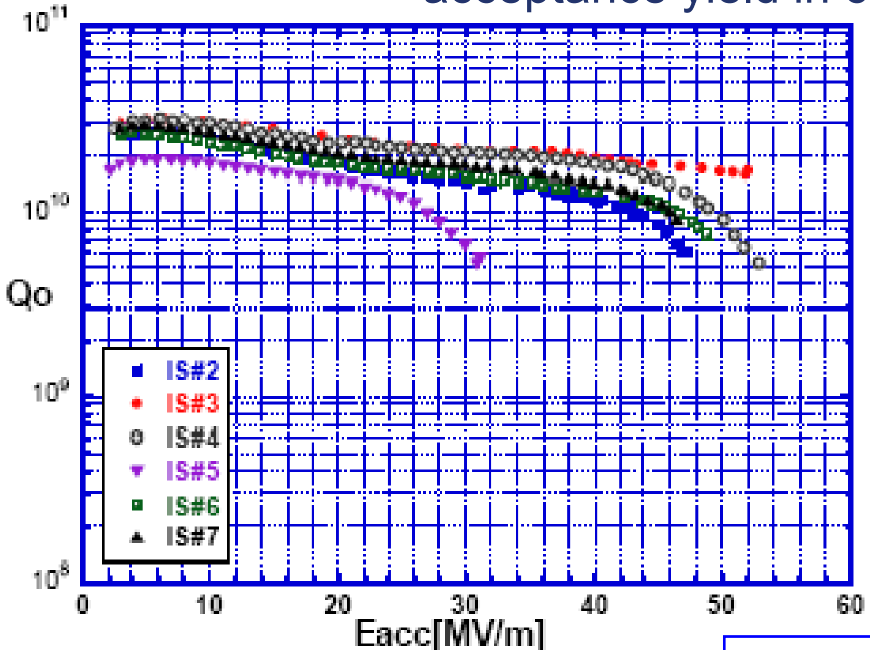

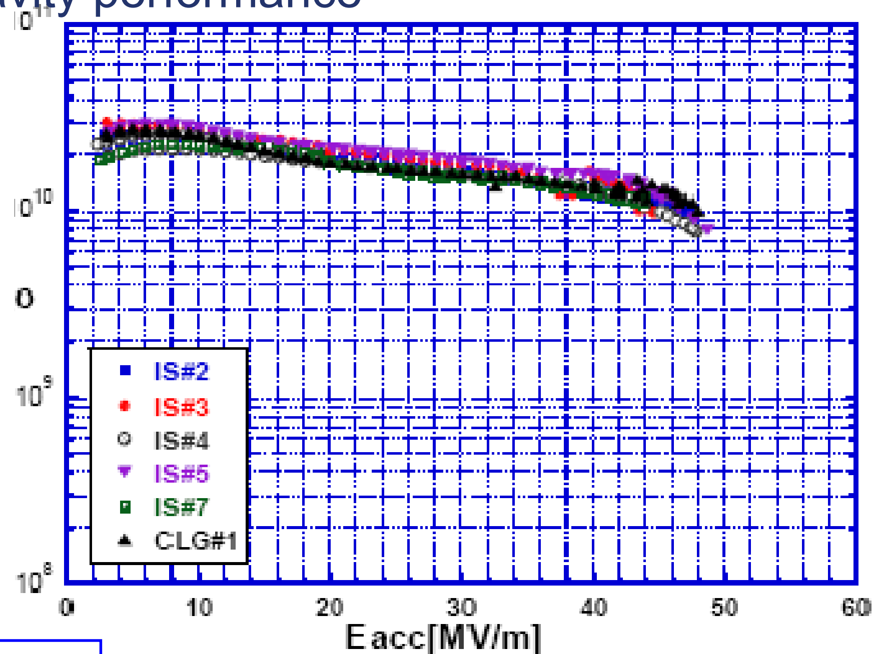

KEK results

ILC Baseline receipt

- Final EP (~20μm) after a heavy material removal (> 100μm)
- HPR (70kg/cm2,1hr
- Bake (120OC,48hr).

Eacc = 46.5± 8.0 MV/m (17%)

EP Flush receipt

- Final EP(20μm) + EP(3μm, fresh acid)
- HPR (70kg/cm2,1hr)
- Bake (120OC,48hr)

Eacc = 46.7±1.9 MV/m (4%)

Pushing up SRF gradient limit

New Geometry

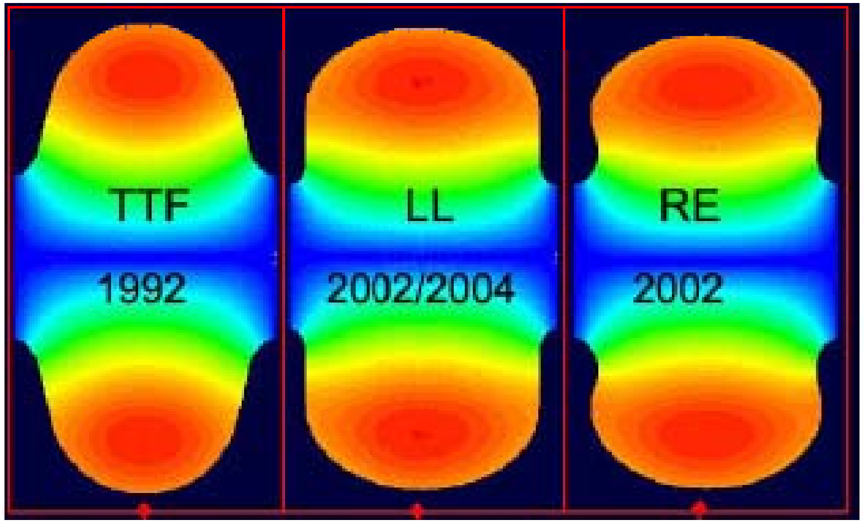

Table 1: Cavity RF parameters

	TESLA	LL	RE	IS
Diameter [mm]	70	60	60	61
Ep/Eacc	2.0	2.36	2.21	2.02
Hp/Eacc [Oe/MV/m]	42.6	36.1	37.6	35.6
R/Q [W]	113.8	133.7	126.8	138
Γ [W]	271	284	277	285
Eacc max [MV/m]	41.1	48.5	46.5	49.2

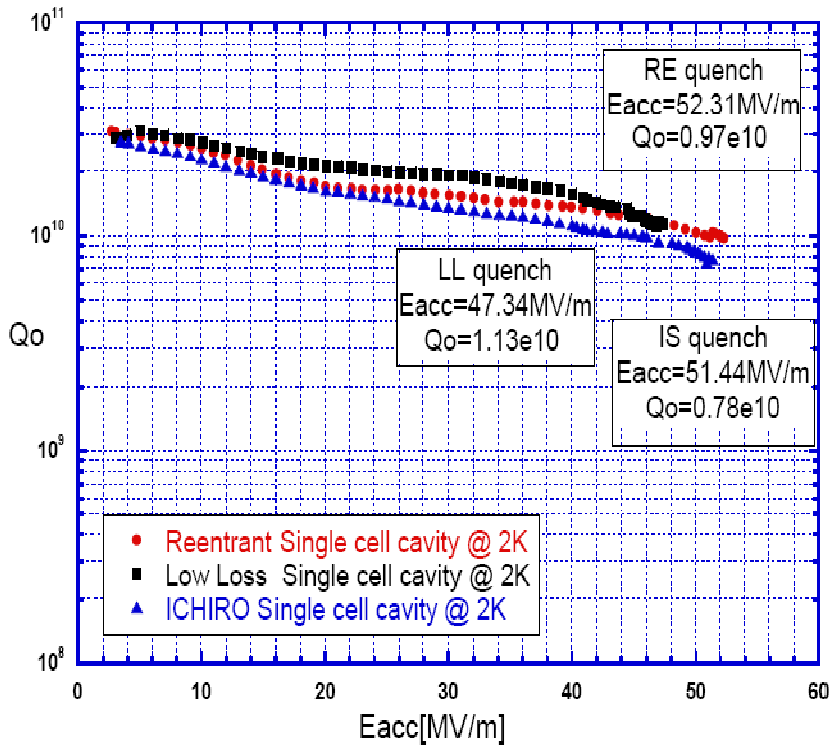

Figure 3: The results of high gradient measurements.

J.Sekutowicz, V.Shemelin, K.Saito

Single-crystal or large grain cavity

Studies also underway using single or large grain Nb – could eliminate need for Electro-Polishing (EP)

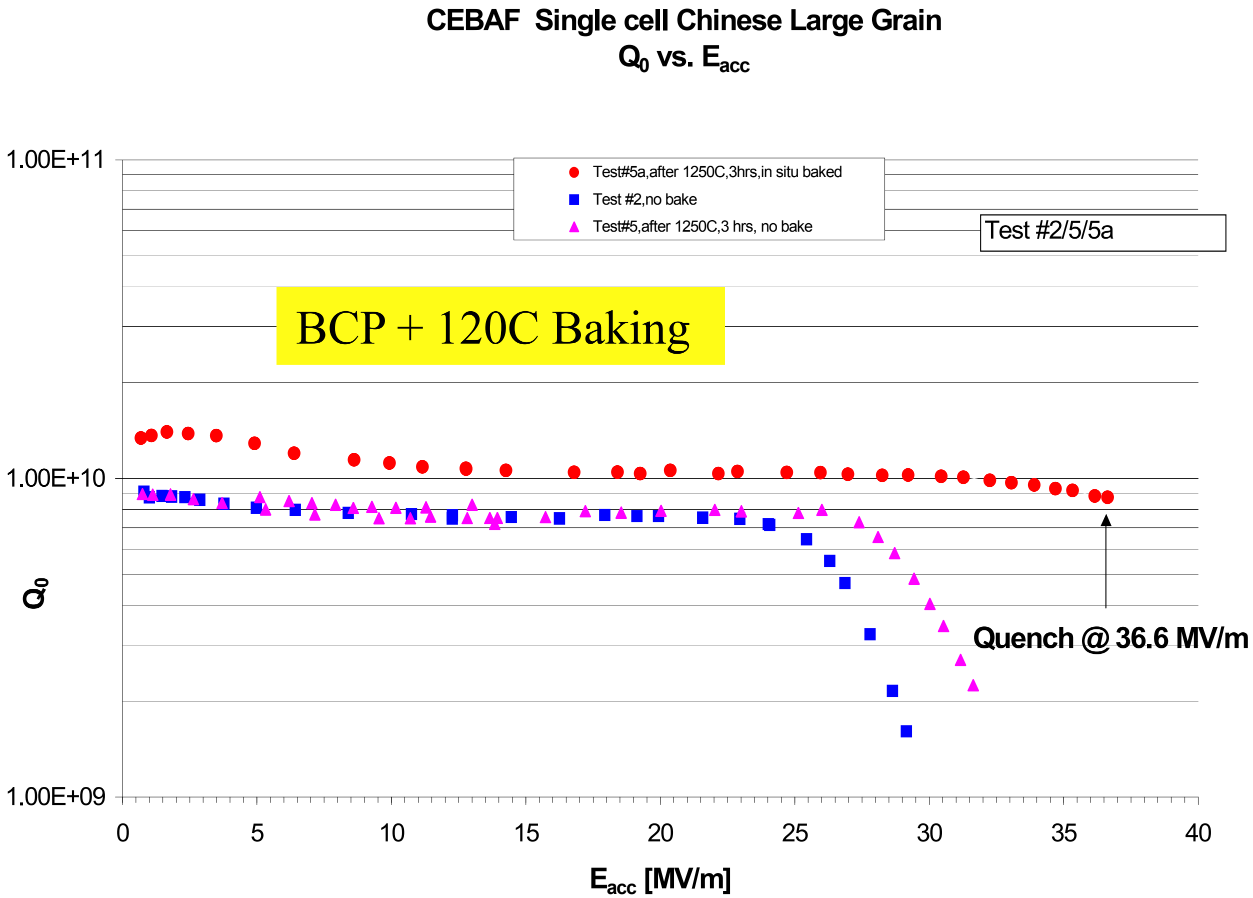

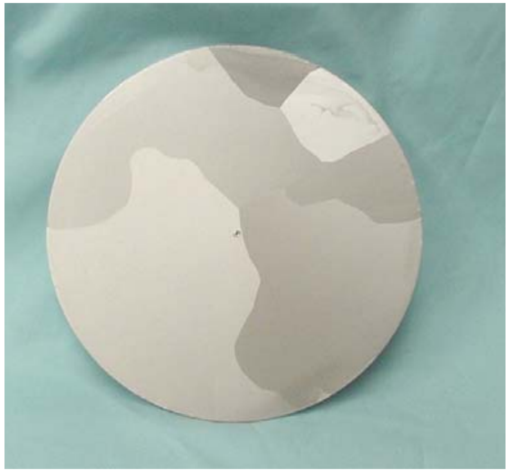

Traveling Wave Structure (TWS)

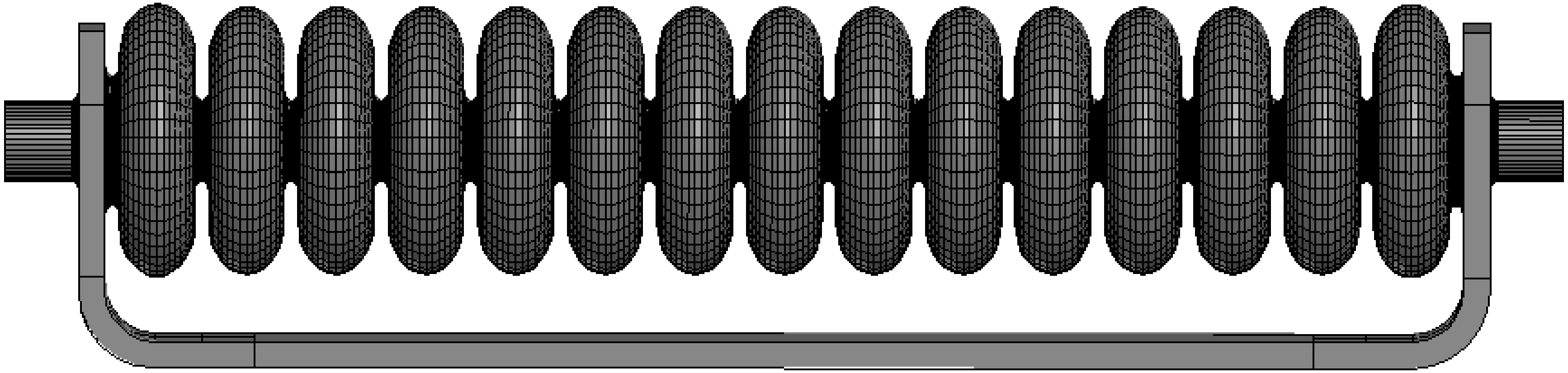

~ 25% (max 42%) higher accelerating gradient (vs. TESLA cavity) – SBIR project phase II

- Shorter cells (105 deg phase advance) to improve transit-time factor
- No limitation (up to 10m) in cavity length
- One, two or more input couplers
- Need tuning to cancel reflected wave

A.Kanareykin, S.Kazakov, N.Solyak, V.Yakovlev, P.Avrakhov

Beyond the Nb technology

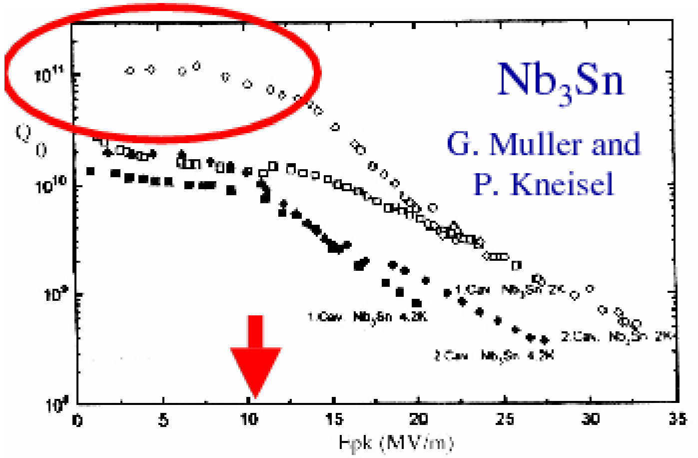

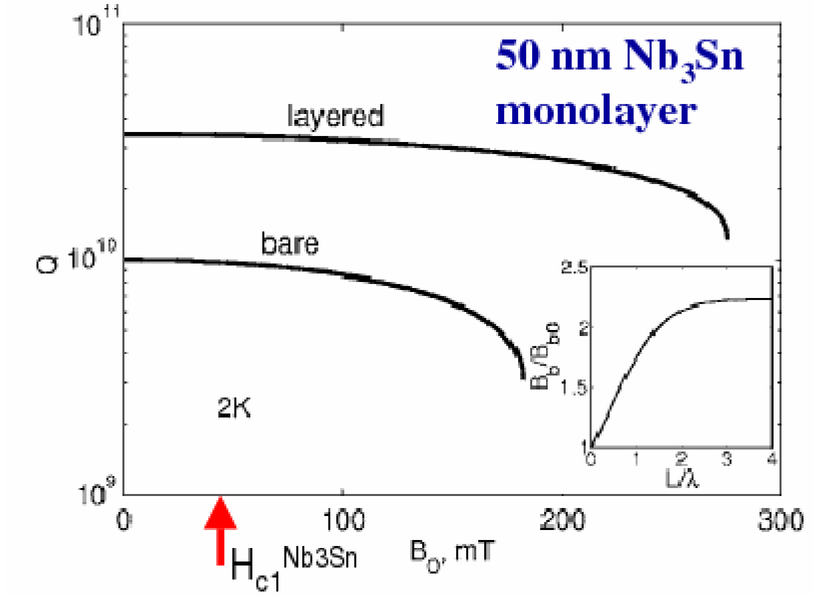

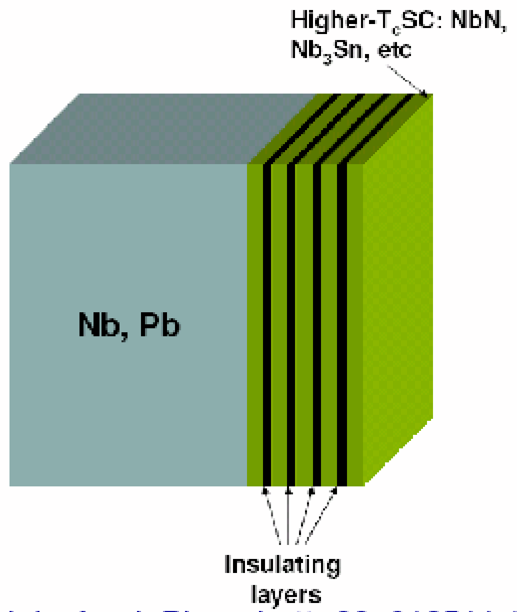

A. Gurevich, Appl. Phys. Lett. 88, 012511 (2006)

- Thin high-H_c layers ($d < \lambda$) separated by insulating layers increase H_{c1} well above the bulk H_{c1}.

- Nb_3Sn thin film coating may triple the breakdown field of Nb and increase **$Q \sim \exp(\Delta/k_BT)$,** by 3-10 times because **$\Delta_{Nb3Sn} \approx 1.8\Delta_{Nb}$**

Project Cost -vs- Linac Gradient

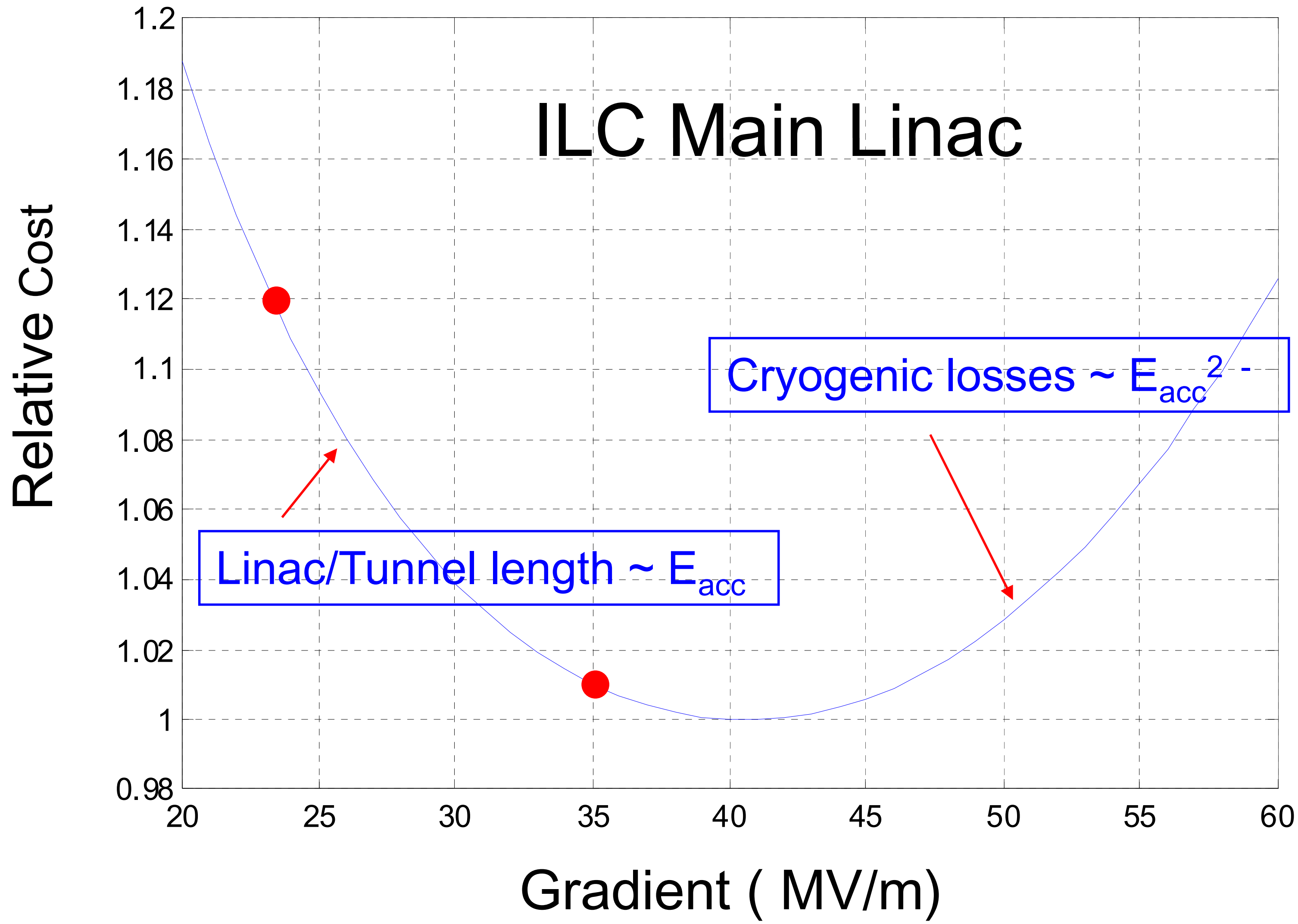

Lorentz Force Detuning,
Microphonics,
Fast and Slow Tuners

- Introduction and design parameters
- Designs of the slow tuners
  - Sac lay I and Saclay II tuners
  - Blade-tuner
- Fast Tuners
  - Piezo-tuner
  - Magneto-strictive tuner
  - SC electro-magnetic tuner

Lorentz Force Detuning

- Electromagnetic fields in the cavity cause the cavity wall to distort
- Distortion changes the resonance frequency of the cavity
- Effect proportional to the square of the field strength

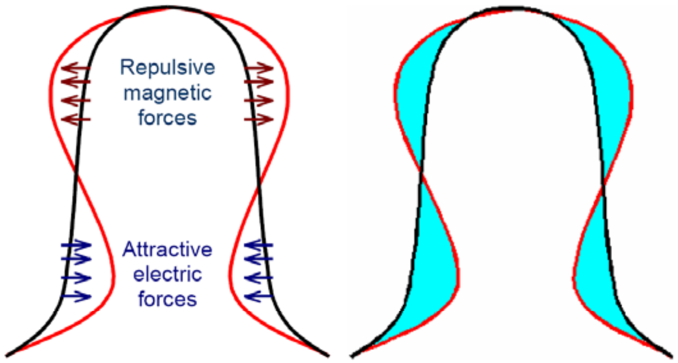

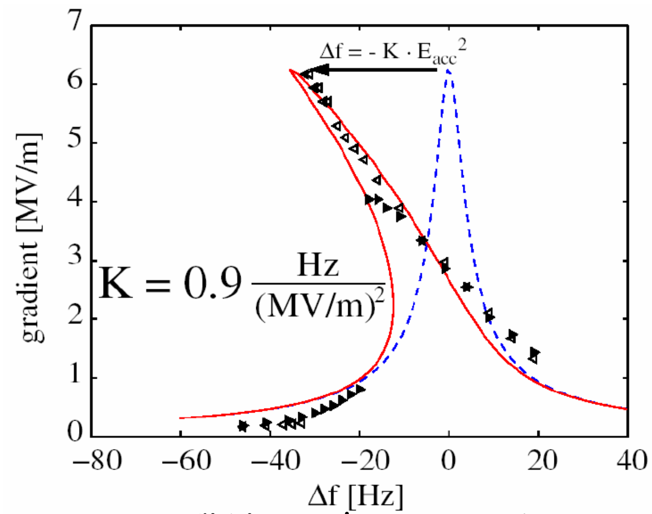

CW-mode operation

Lorentz Forces Detuning

1. Static Analysis

RF power produces pressures that act on the cavity wall

$$P = \frac{1}{4}\left(\mu_0 H^2 - \varepsilon_0 E^2\right)$$

The pressure deform the cavity wall, tending to act outward near the equator and inward near the iris. The cavity cell deformations produce a frequency shift.

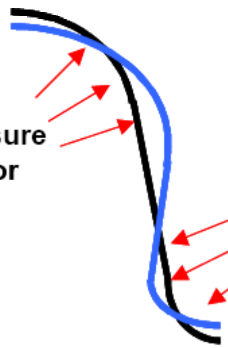

Lorentz pressures

$$\frac{\Delta f}{f_0} = \frac{1}{4W}\int_S \left(\varepsilon_0 E^2 - \mu_0 H^2\right) \cdot d\vec{S}\,\Delta\vec{l}$$

Finally: $\Delta f = -K_L \cdot E_{acc}^2$

K_L= 1.53 (Hz/(MV/m)^2): ILC cavity without stiffening

K_L= 0.9 (Hz/(MV/m)^2): with stiffening rings

Equilibrium equations for cell deformation

To get the deformation of cavity wall due to Lorentz forces, ANSYS solves the equilibrium equation with pressure as a boundary conditions and calculates the strain and stress tensors:

$$(1-2\sigma)\Delta\vec{u} + grad\left(div\,\vec{u}\right) = 0$$

$$\sigma_{ik} = \frac{E}{1+\sigma}\left(u_{ik} + \frac{\sigma}{1-2\sigma}u_{ll}\delta_{ik}\right)$$

$$u_{ik} = \frac{1}{2}\left(\frac{\partial u_i}{\partial x_k} + \frac{\partial u_k}{\partial x_x}\right)$$

Where :

σ – Poison ratio (for Nb σ=0.38), E – Young modulus (for Nb E=1.05GPa)

u – displacement vector

u_{ik} and σ_{ik} are strain and stress tensors

Static Simulations for mid-cell

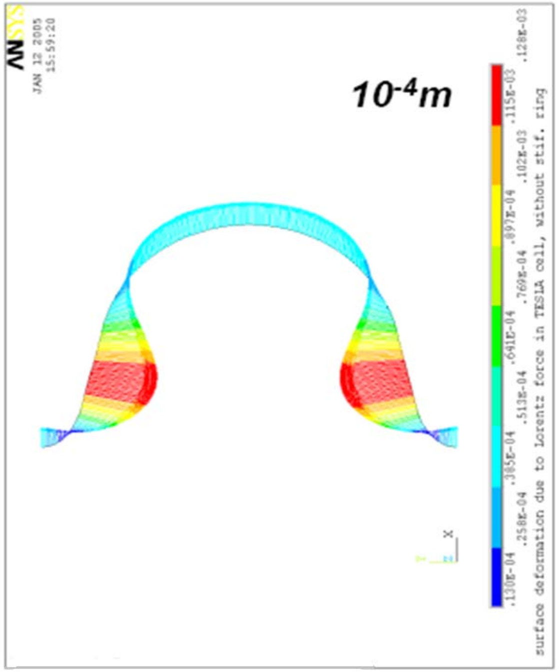

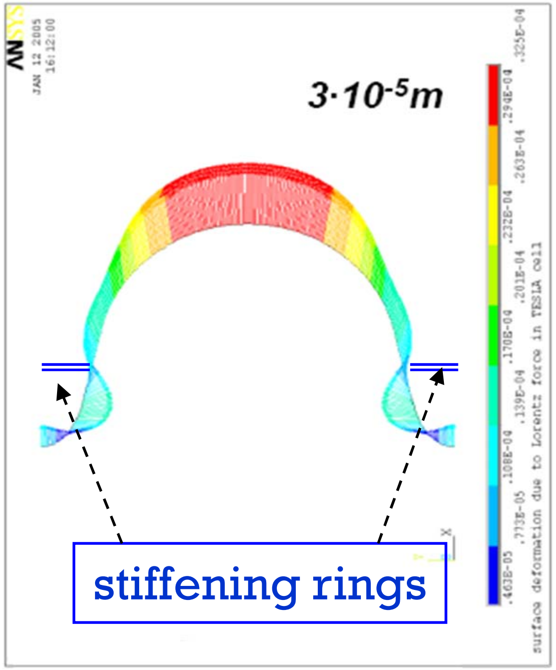

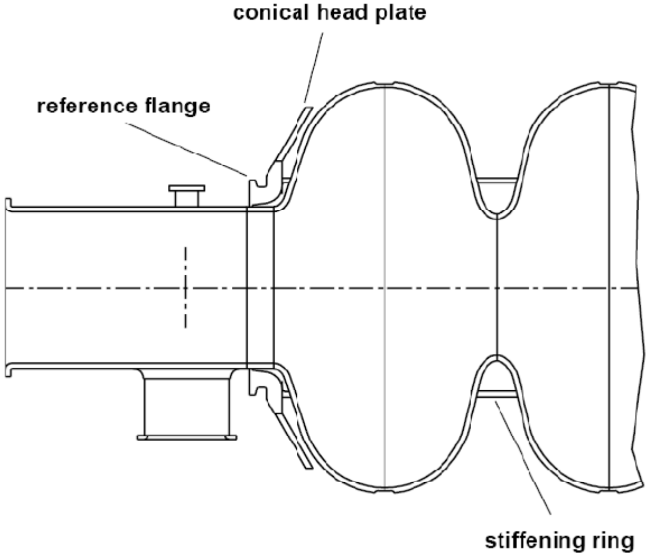

Stiffening Rings in cavity and end-group of the TESLA cavity

Results of ANSYS simulations of TESLA single cell deformation due to Lorentz forces without (left) and with the stiffening ring (right). **Both Ends are Fixed**

$K_L = 1.26\ Hz/(Mv/m)^2$ - without stiffening ring

$K_L = 0.74\ Hz/(Mv/m)^2$ - with stiffening ring

For free boundary conditions at the ends, the detuning coefficient is one order higher

Static Lorentz Force Detuning (2)

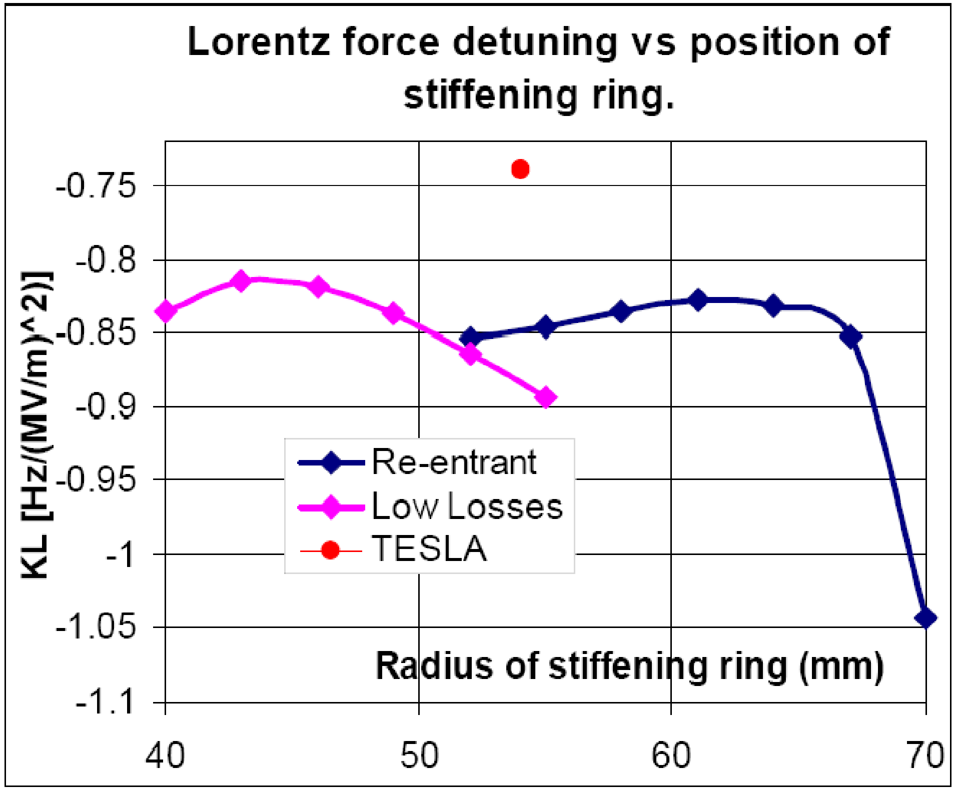

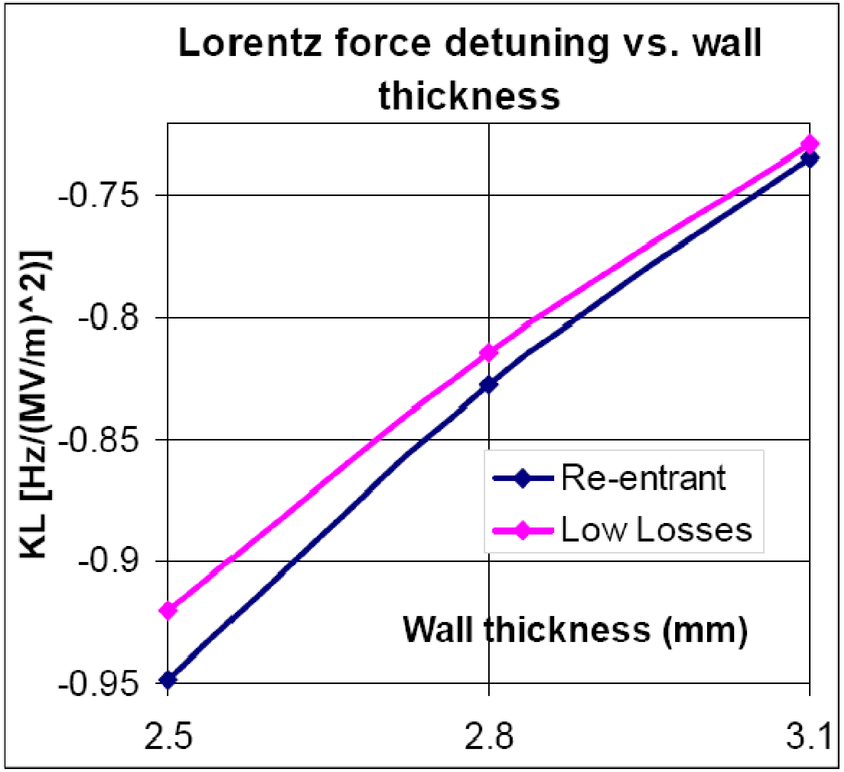

TESLA(wall=2.8mm)	ΔF(wo/w ring) = - 801/-463	Hz for 25 MV/m
Low Losses(2.8mm)	ΔF(wo/w ring) = - 871/-509	Hz for 25 MV/m
Re-entrant(2.8mm)	ΔF(wo/w ring) = - 860/-517	Hz for 25 MV/m

Resonances in ILC cavity

Dynamic model include the possible resonant behavior of cavity detunung Δf . *Corresponding to each mechanical eigenmode with frequency ω_m and quality factor Q_m we use the equation*

$$\frac{d^2\Delta f_m(t)}{dt^2} + \frac{\omega_m}{Q_m}\frac{d\Delta f_m(t)}{dt} + \omega_m^2 \cdot \Delta f_m(t) = -k \cdot \omega_m^2 \cdot E_{acc}^2(t)$$

To describe the contribution Δf_m of mt^h mode to the cavity detuning. In the equation, k_m is the dynamic Lorentz coefficient of m^{th} mode. The total cavity detuning is

$$\Delta f(t) = \sum_{m=1}^{N} \Delta f_m(t)$$

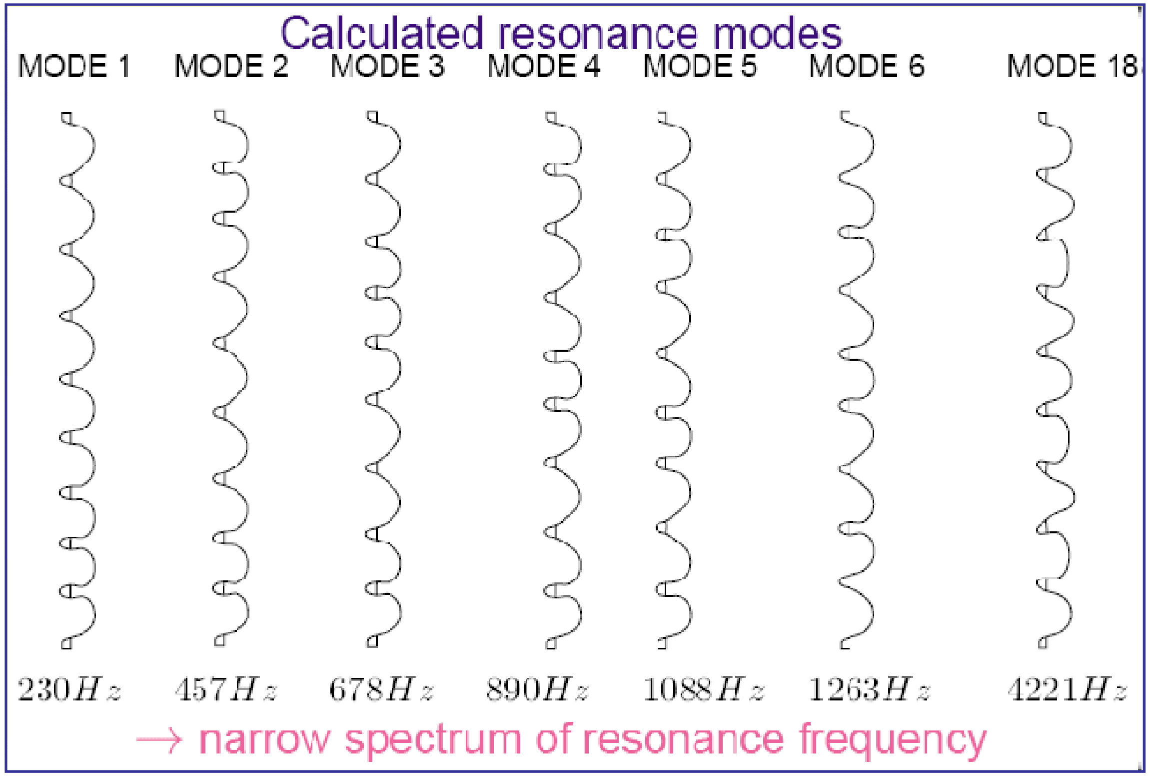

Results

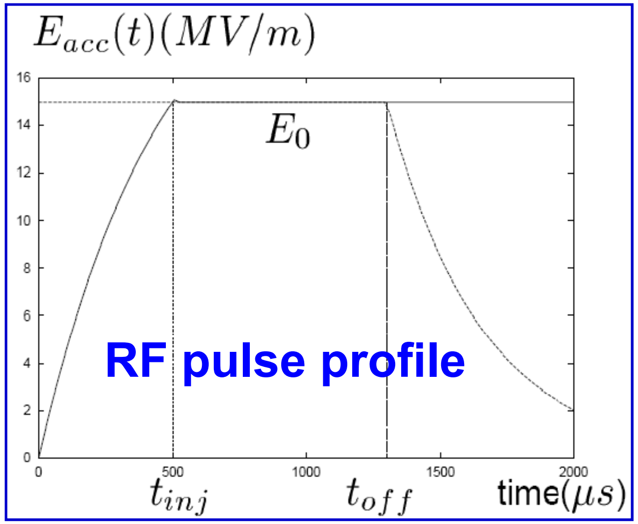

Simulations (left) vs. measurements (right) of frequency detuning for TESLA cavity

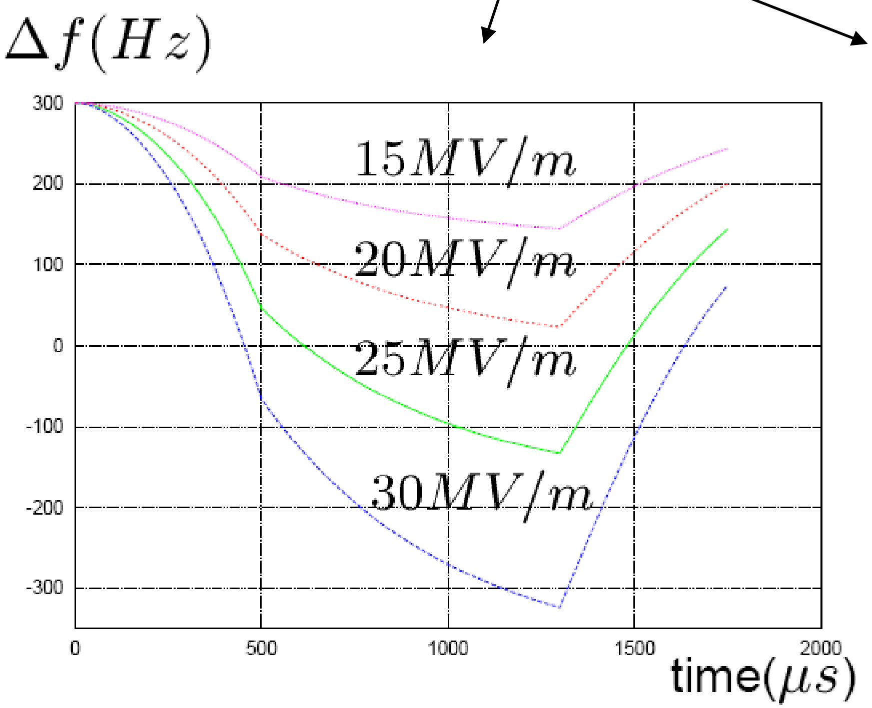

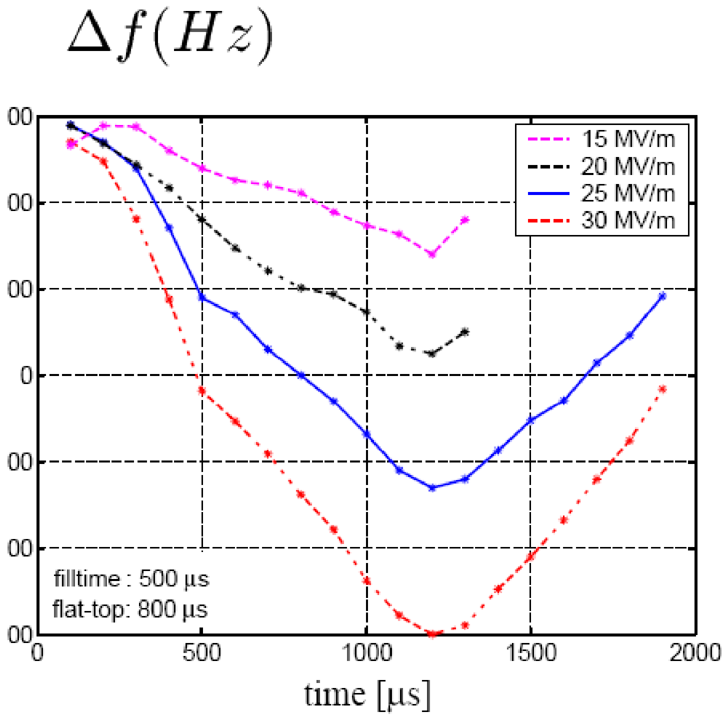

Scattering of Lorentz detuning in cavities

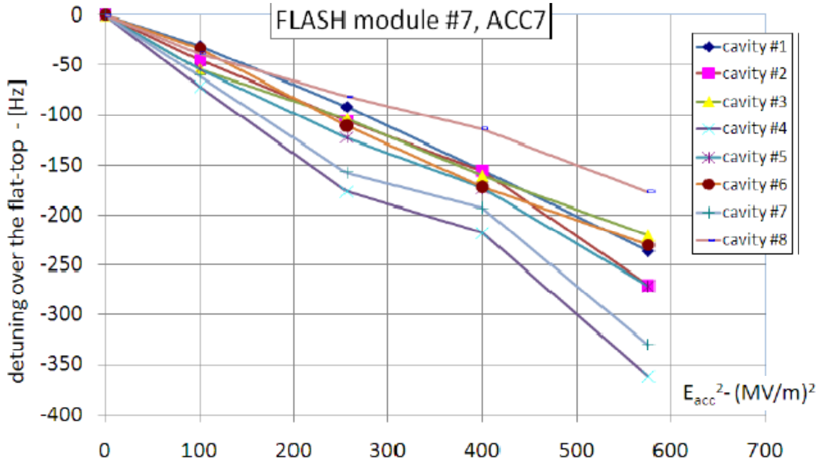

LFD showed during the flat-top for ACC7 cavities, plotted vs. the square of accelerating field

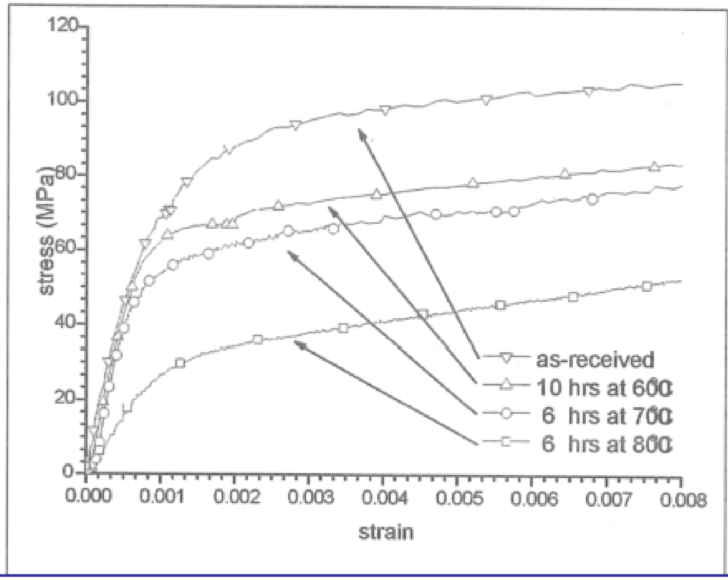

Stress-strain plots of the high RRR Nb subjected to different heat treatment, the 800°C annealed sample shows a decrease in Young's modulus

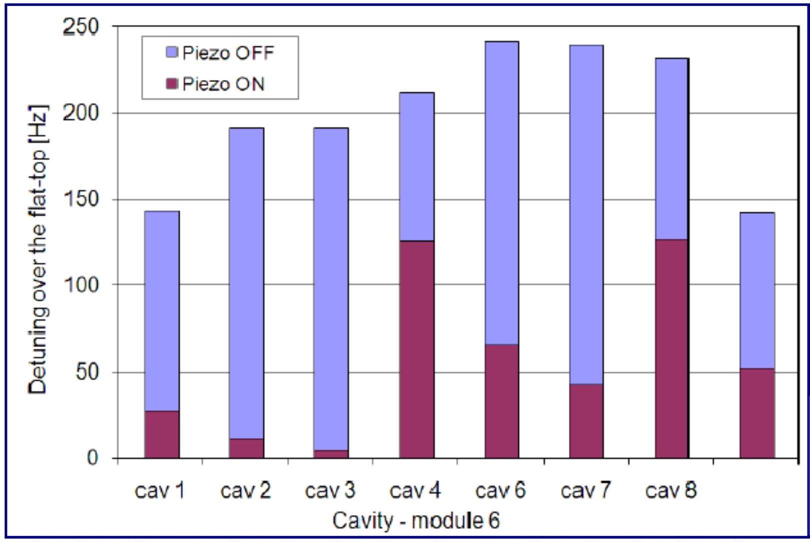

Detuning with and without proper piezo pulse for each cavity in ACC6

Lorentz Force Detuning & RF Power Requirements

$$\frac{\Delta P}{P_0} = 0.25\left(\frac{\Delta f_{FT}}{f_{1/2}}\right)^2$$

$$\Delta f_{FT} = -K_{FT} \cdot E_{acc}^2$$

$$\Longrightarrow \quad \frac{\Delta P}{P_0} = \frac{1}{4}\left[\frac{K}{f_{1/2}}\right]^2 E_{acc}^4$$

$-K_{FT} \approx 0.5$ (for FlatTop~800us)

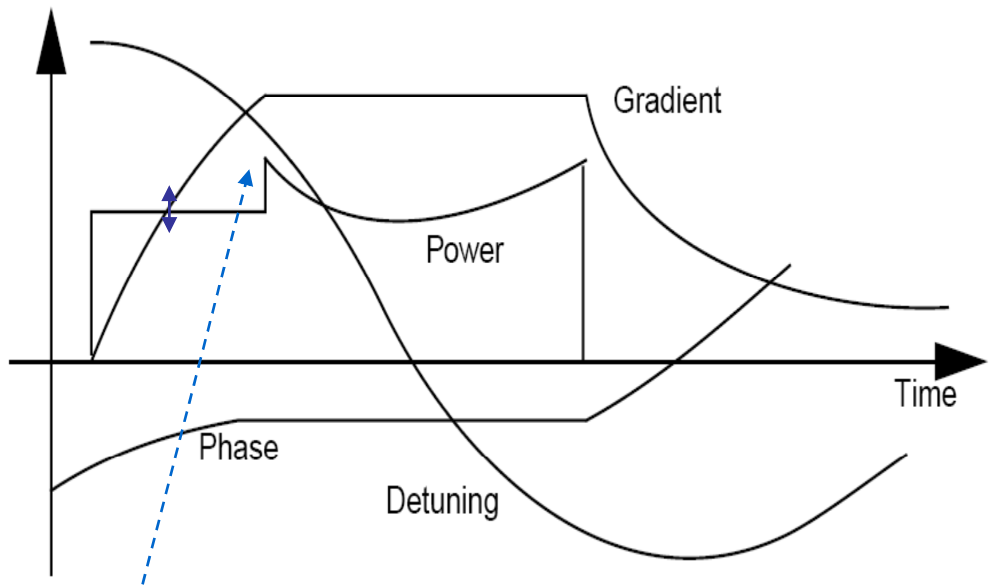

- Peak power increases with the **fourth** power of accelerating gradient:
  Example: for Eacc=35MV/m up to 100-150% extra RF power:
  - Over-sized Klystron
  - More difficult control of RF (LLRF)

Vibrations (Microphonics)

- Noise sources (.e.g. pumps, cryo-system; seismic waves, etc.) excite cavity vibrations

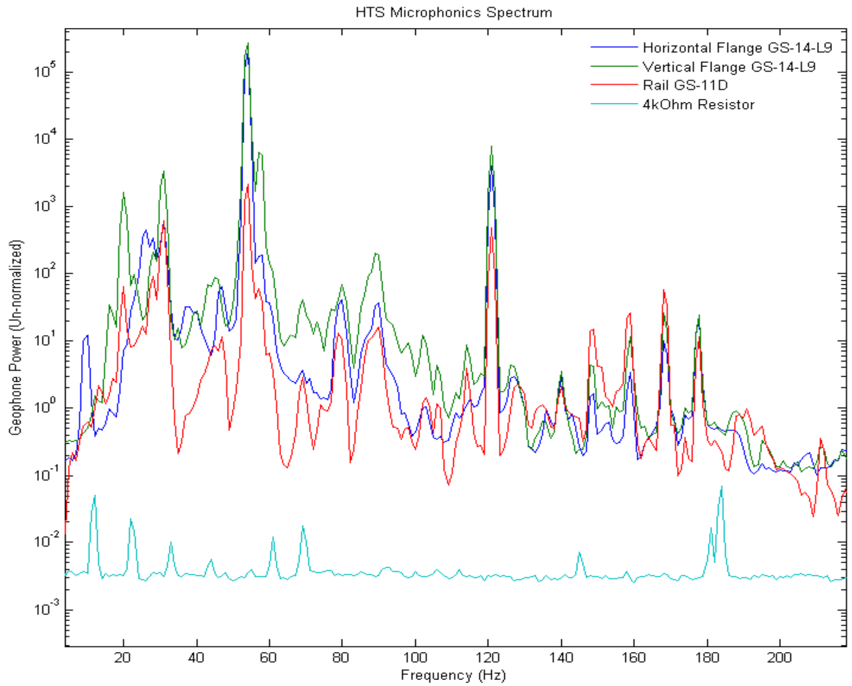

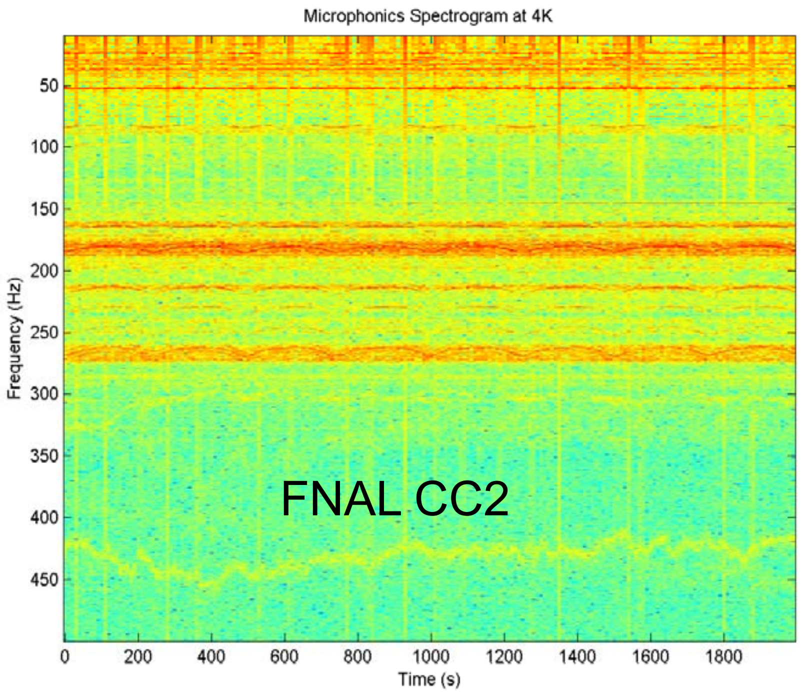

Important for CW operarion (ERL)

Beam loading small

- High loaded Q, small cavity bandwidth

> *Any small shift in the cavity frequency requires signficant increase in power to maintain E=const, produces phase errors that affect the beam*
>
> *Understand expected microphonics level*
>
> *Choice of cavity-tuner system to be able to compensate for the microphonics*

Resonance Control in SCRF Cavities

- SCRF cavities are designed with thin walls to maximize heat transfer to liquid He bath
- The thin walls lack stiffness making the cavities susceptible to mechanical oscillations
- Longitudinal oscillations can change the resonance frequency of the cavity
- Oscillations can be excited
  - **Deterministically (Lorentz Force)**
  - **Non-Deterministically (Microphonics)**

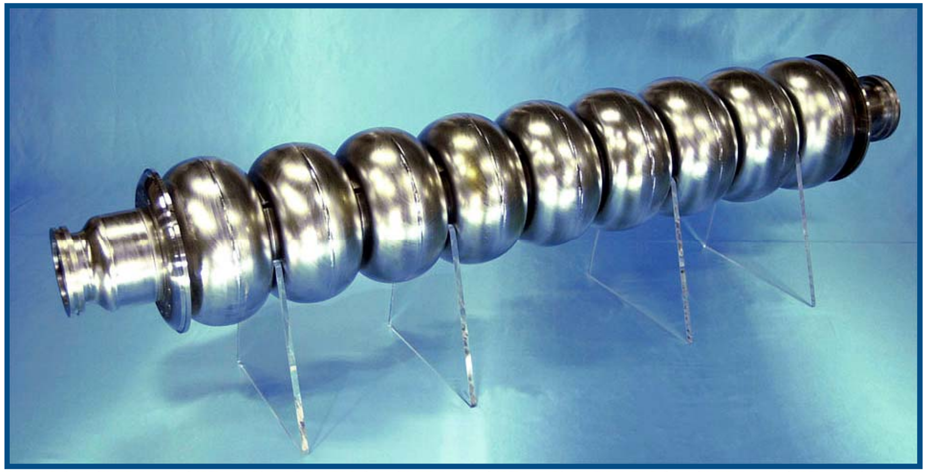

Frequency Tuners

- **Slow Tuner**

  Stepper motor changes length of the cavity to bring it to the desired resonance frequency)

  - Compensates
    - Static Detuning Forces
  - Techniques:
    - Saclay tuners
    - Blade-Tuner

- **Fast Tuner**
  - Compensates
    - Lorentz Force Detuning & Microphonics
  - Techniques:
    - Piezoelectric actuators
    - Magnitostrictive actuators
    - Electromagnetic (superconductive)

Piezoelectric Fast Tuner

The current tuner design has been developed with the insertion of two fast piezoelectric actuators. Required preloading – 20-50% of blocking force

Examples of piezo actuators:

Low voltage piezo stack with ceramic coating (left)

Packaged version with integrated mechanical preloading (right)

PROPERTIES	PI P-888.90	Unit
Material	PZT-PIC 255	
Case/preload	No	
Length	36	mm
Cross section	100	mm^2
Young modulus	48,3	kN/mm^2
Stiffness	0,105	kN/um
Max. stroke	35	µm
Blocking force	3600	N
Res. frequency @ no load	40	kHz
Density	$7{,}8 \times 10^3$	kg/m^3
Min. voltage	-20	V
Max. voltage	120	V
Capacity - nominal	12,4	µF
Capacity - measured	13,6	µF
Loss Factor	0,015	Tanδ

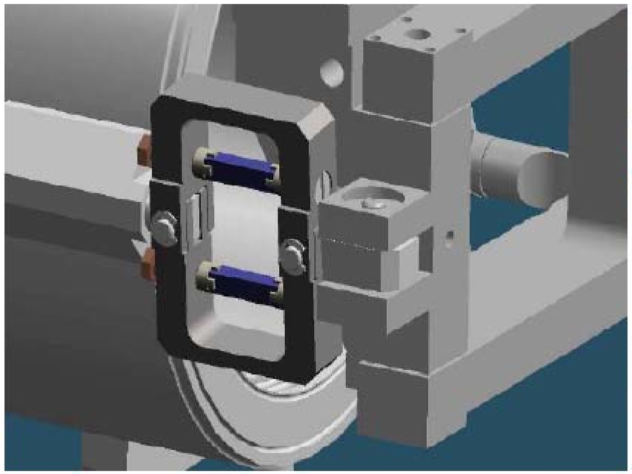

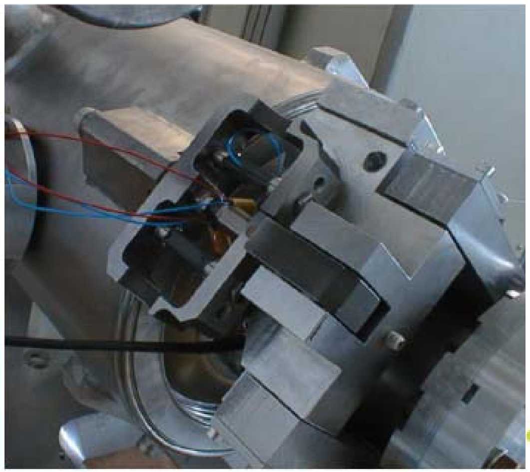

The piezo frame with 2 actuators installed in the TTF tuner CAD model (left) and first prototype (right)

Response time <1ms

ILC 9-cell cavity = 300 Hz/um

Fast Tuner Technologies

PIEZOELECTRIC ACTUATORS

- *Commercially available from multiple sources*
- *Typically used at room temperature (stroke~30μm for 40mm long Piezostack at RT)*
- *Work at cryogenic temperatures with reduced stroke (6-10% of RT stroke ~ 4-5mm at 4K)*
- *Deliver high forces ~5000N for 10*10mm^2 cross-section*
- *Actuator of main choice at many labs for detuning compensation studies*

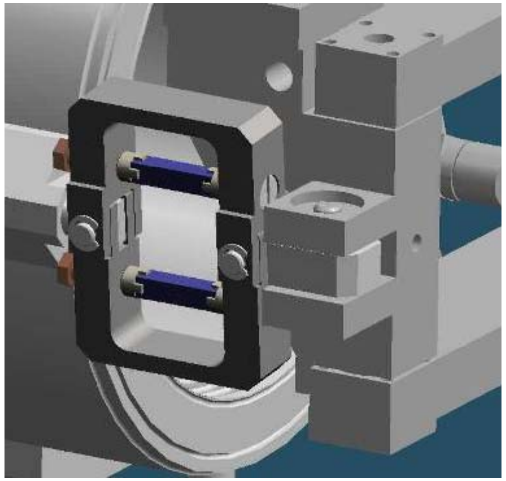

Double Piezo (DESY)

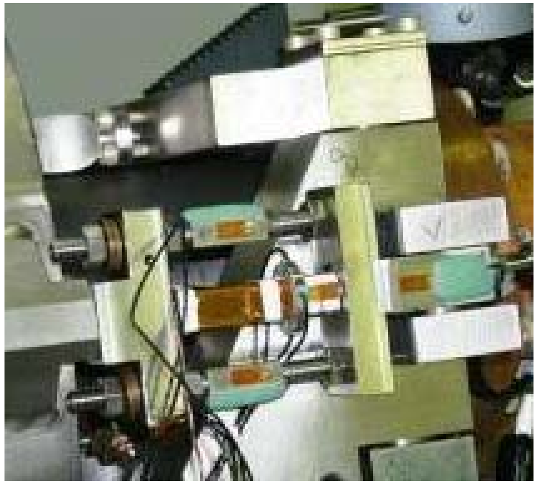

Single Piezo (FNAL)

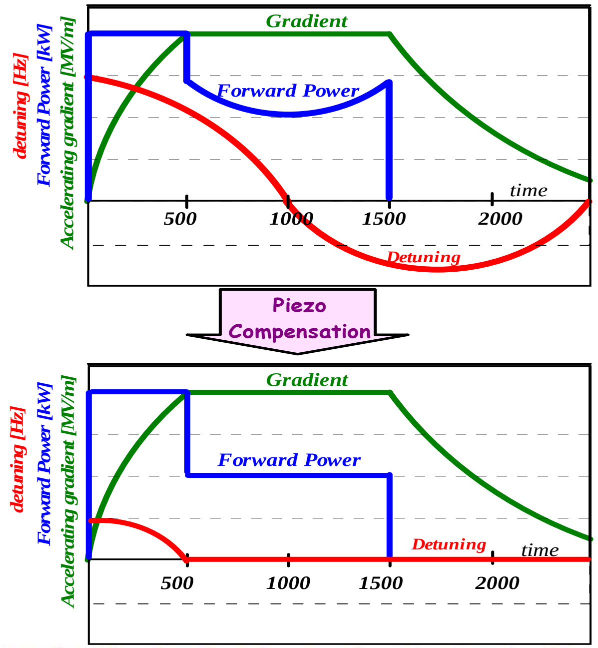

Detuning Compensation

Resonant Excitation Method

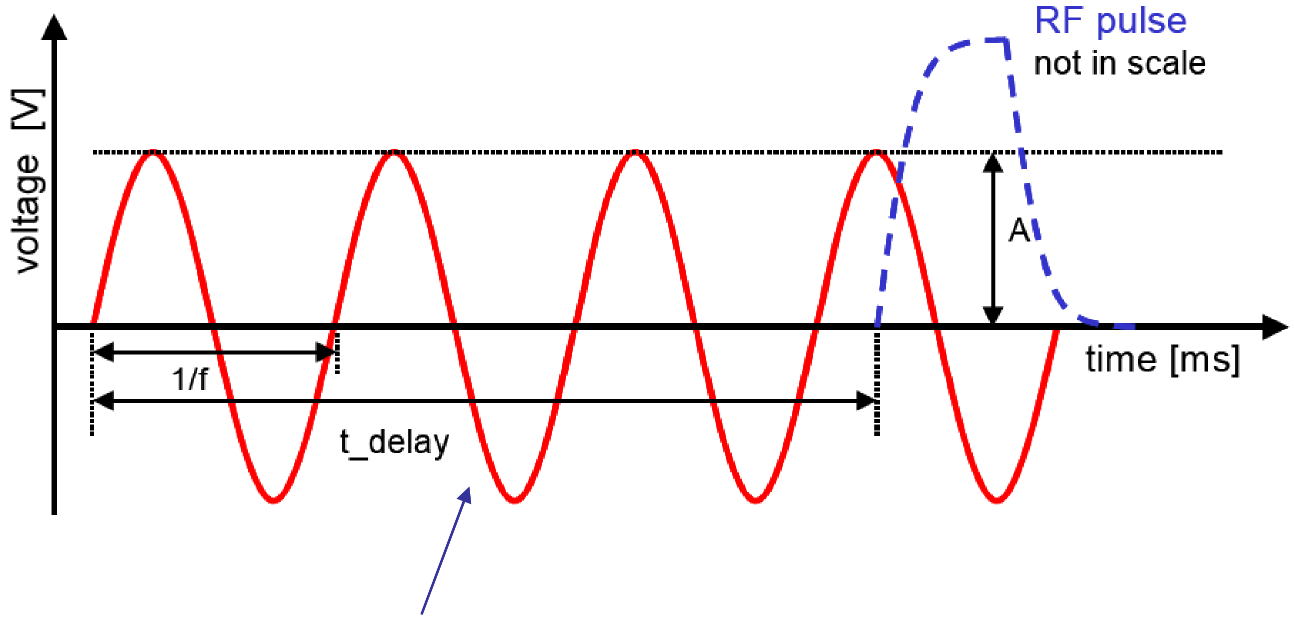

Excitation electrical pulse on the piezoactuator
(control of in-advance timing and amplitude)

Advantage: small piezo stroke amplified by mechanical resonance

How it's work ?

TESLA Capture Cavity: E_{acc}=26.2 MV/m

(Pre-detuning = 230Hz)

Frequency Detuning Monitor - Phase Detector

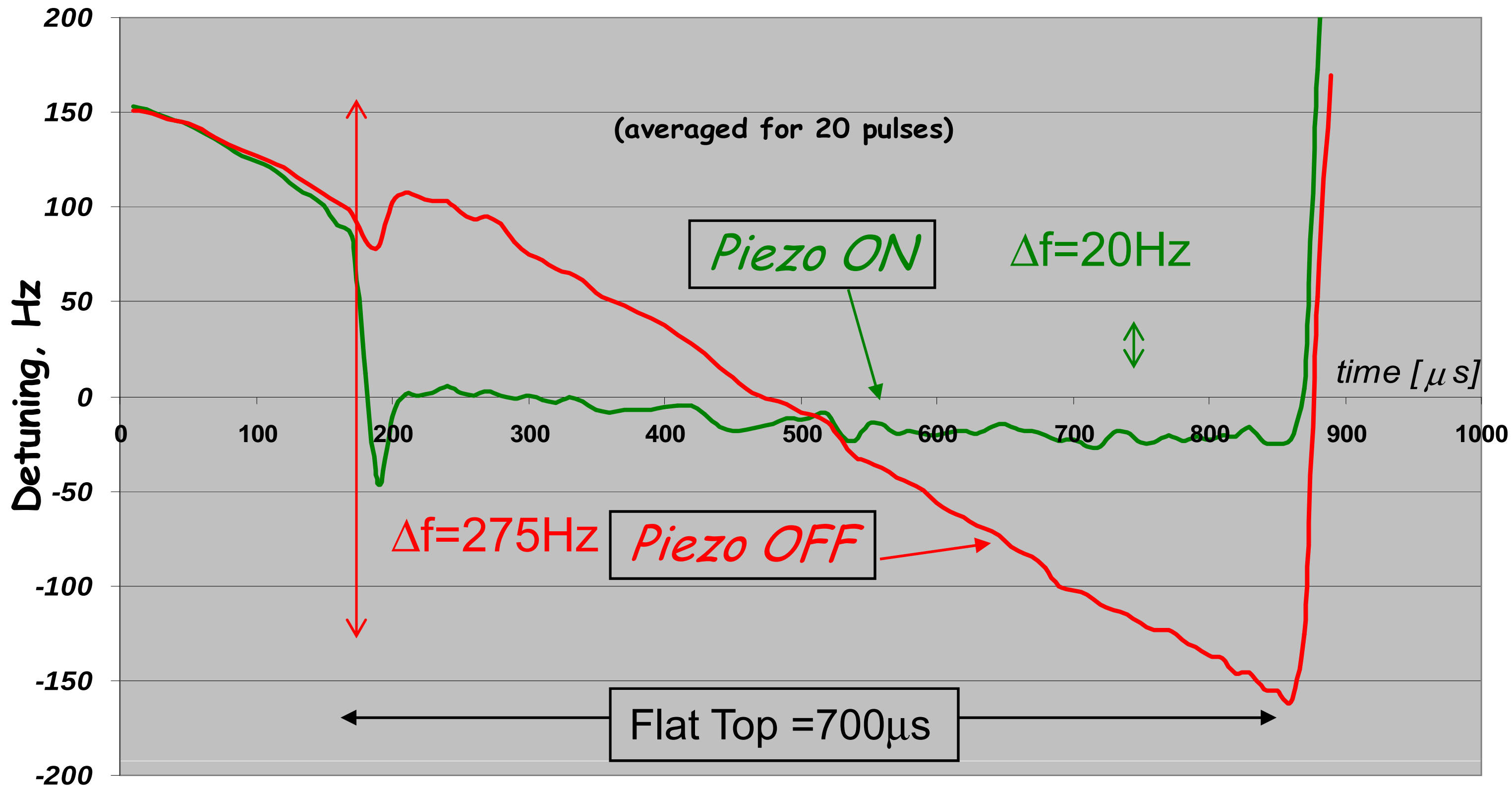

Summary of Lorentz Force Detuning Compensation at FNAL (CC2)

	Detuning (Hz)		Additional Forward Power at FT (pick)		Piezo Voltage, [V] (max=120V)
	Piezo OFF	Piezo ON	Piezo OFF	Piezo ON	
26.2 MV/m	275	20	29%	2%	20V
31.2 MV/m	350	50	92%	28%	40V

Detuning (Hz)

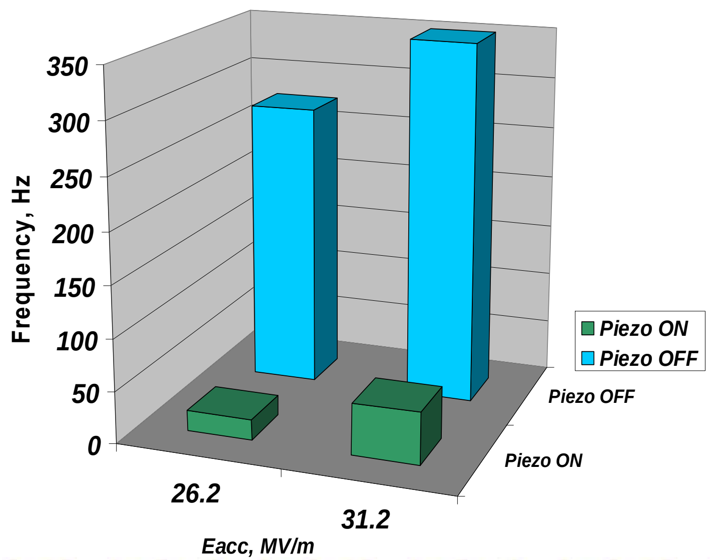

Additional Forward Power at FT (pick)

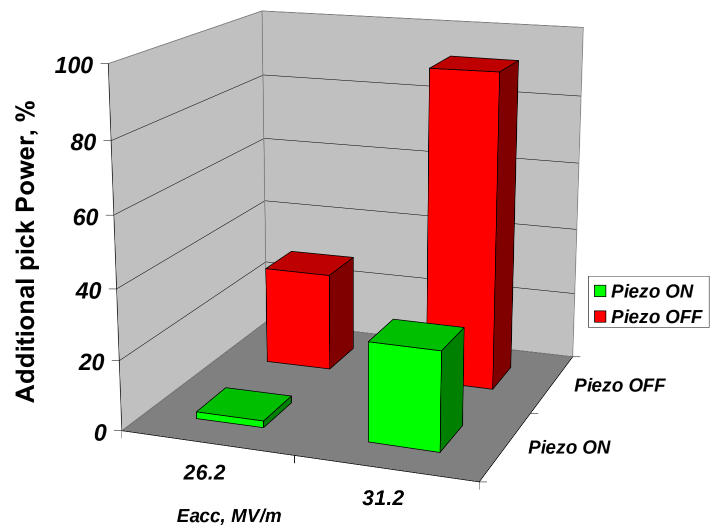

Fast Tuner Technologies

Actuator body

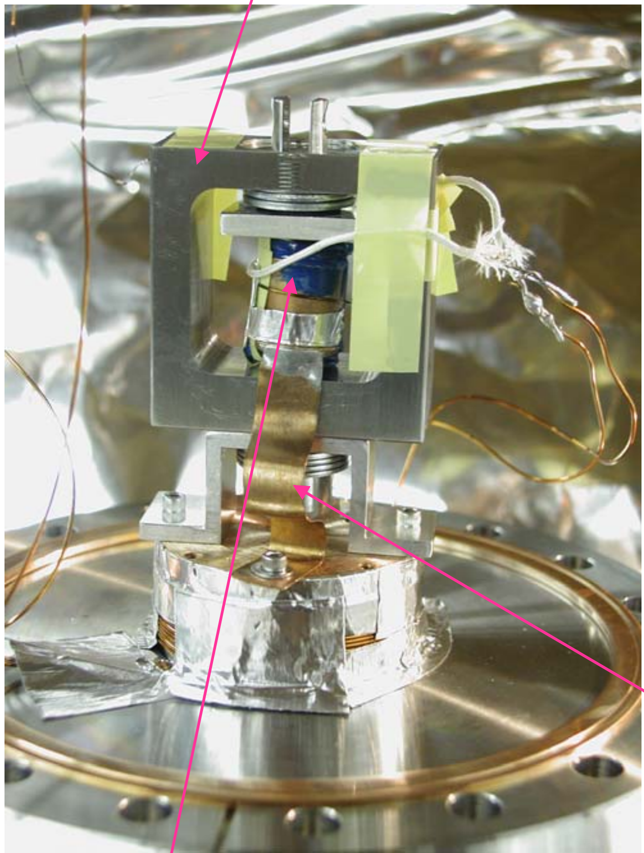

Thermal strap

Nb_3Sn coil

MAGNETOSTRICTIVE ACTUATORS

Special Ceramic Core increase size in the presence of strong Magnetic Field
(SCRF cavity working at 2-4K… magnetic field generated by SC coil

- *Being introduced as an alternative to piezoelectric actuators for SCRF fast tuning*
- *Advantage: could maintain large stroke at cryogenic temperatures*

Fast Tuner Technologies (3)

Idea Proposed and Prototyped at FNAL (B.Foster)

Loudspeaker with Superconductive Coils

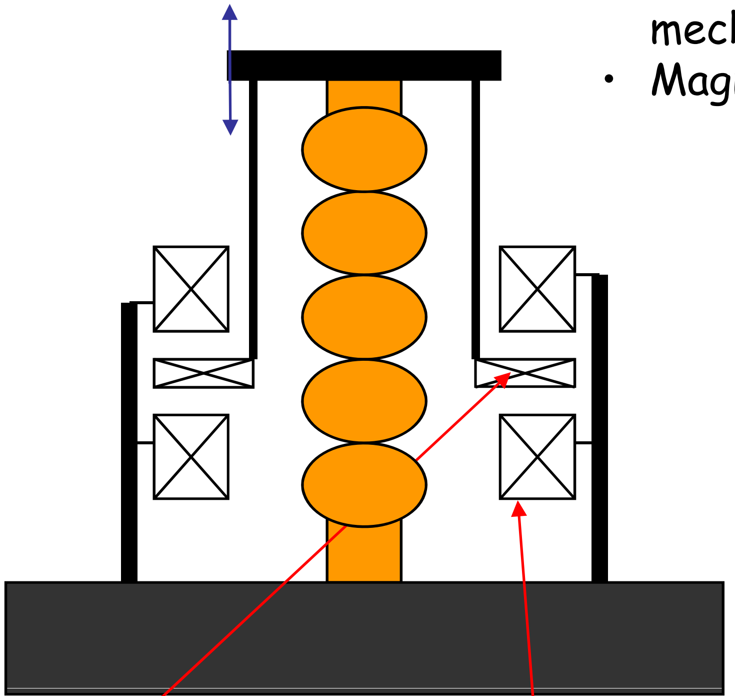

First test of SC_EM Tuner illustrated promising results in FAST TUNING MODE for SCRF.

Advantage of SC_EM Tuner:

Large stroke= 100's of kHz RF frequency shift in wide dynamic range of mechanical motion

Question for concerns:

- Need to study design which allowed quickly (0.1 sec) dump mechanical resonances
- Magnetic Field in the surface of SCRF cavity ?

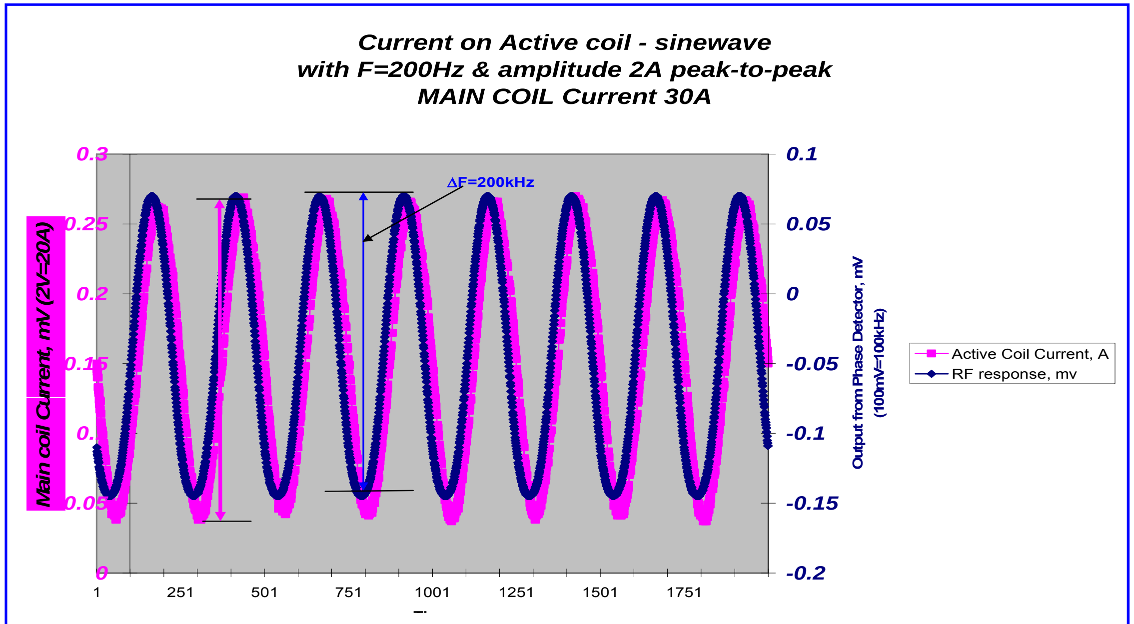

Cavity resonance change ~200KHz

Ex: Microphonics Compensation with Piezo Tuner

Illustration of Single Resonance Compensation for CC2 *(f=92Hz)*

(Algorithm: Narrow Band Filter Bank)

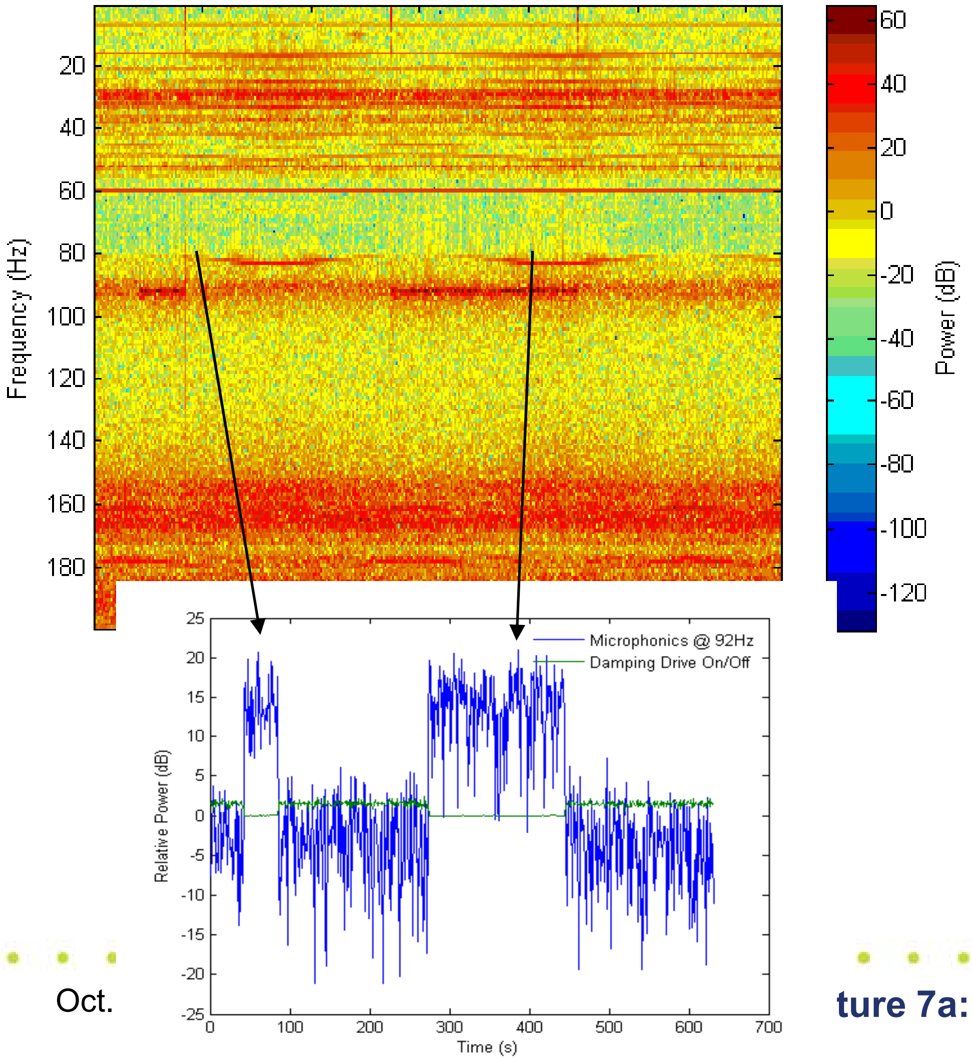

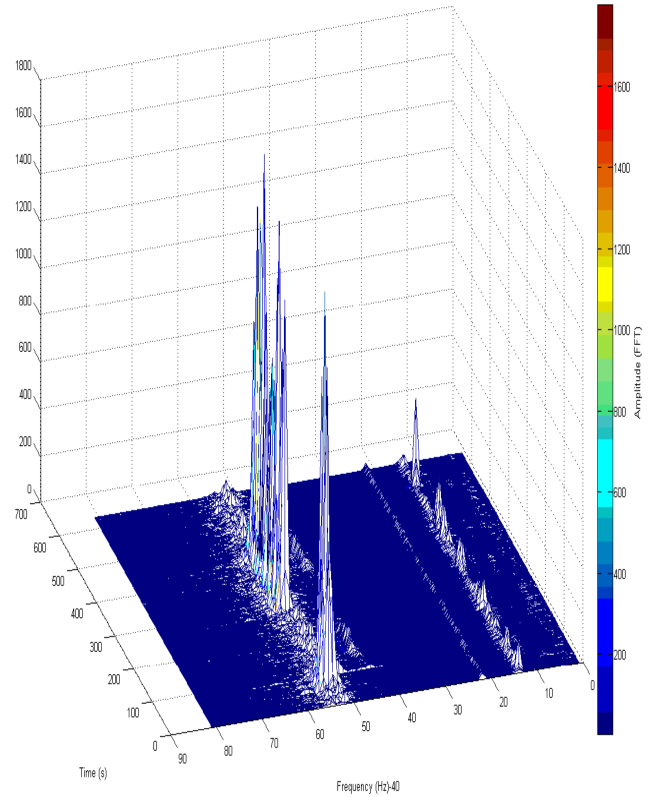

Few examples of slow tuner designs

Requirements for Slow Tuner

- Tuning Range
- Hysteresis
- Group delay small
- High Stiffness
- Boring transfer function
- Resolution

Saclay I tuner

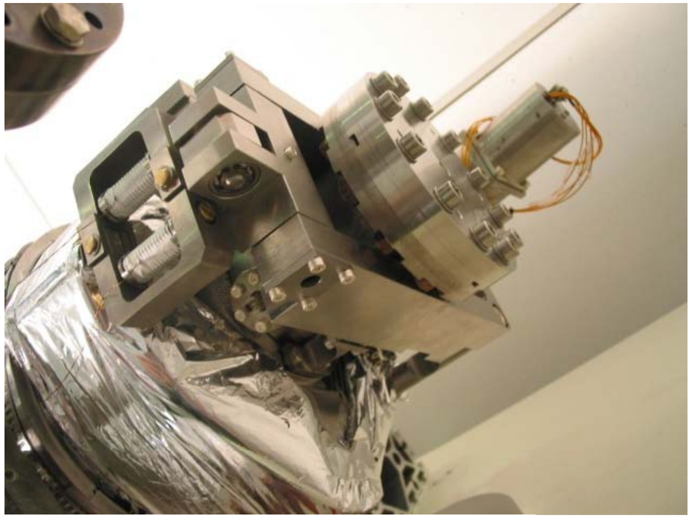

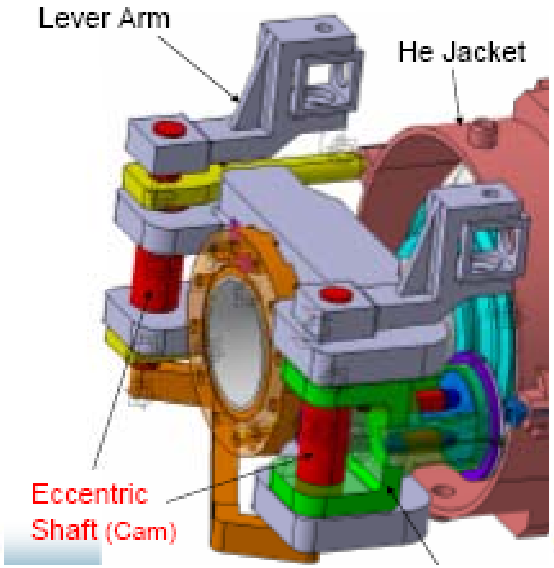

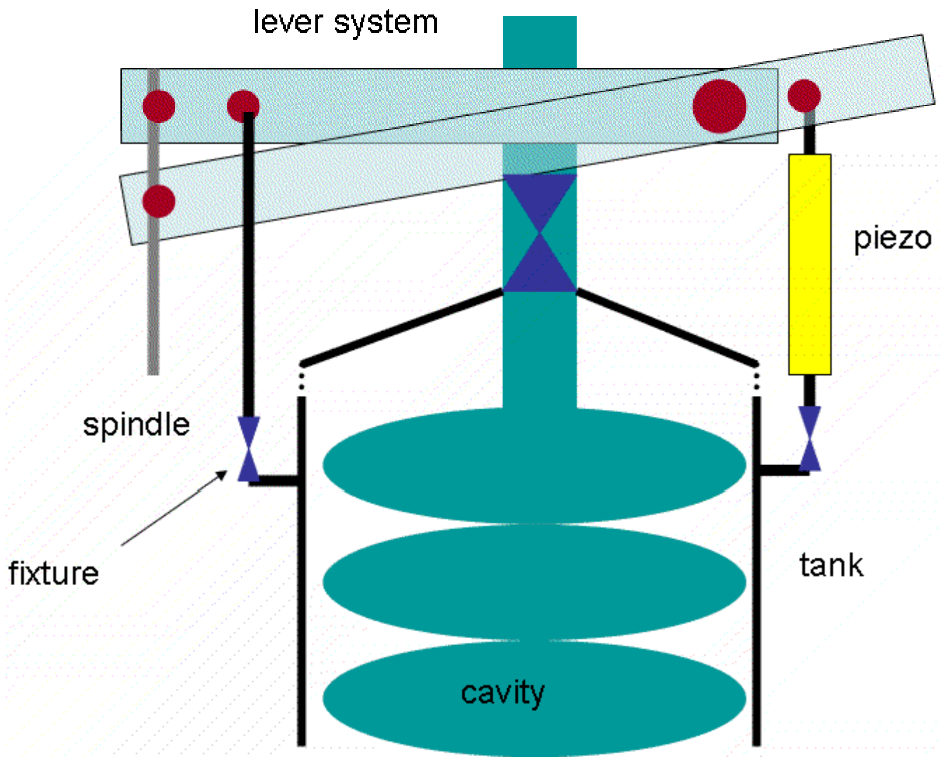

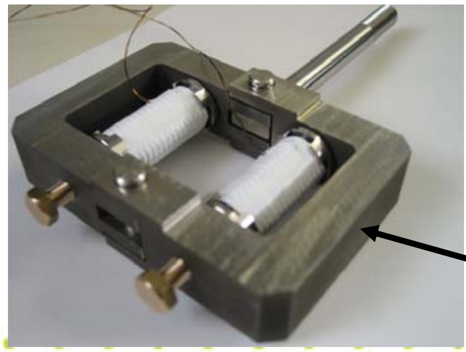

Modified piezo holder frame:
Higher wall thickness

Saclay I tuner

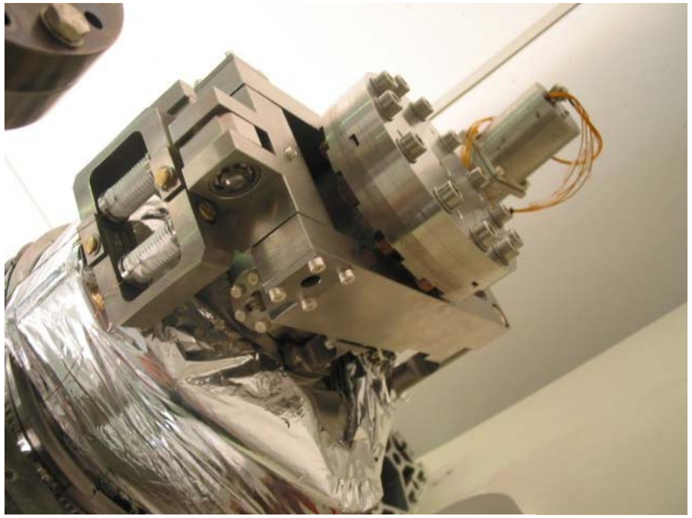

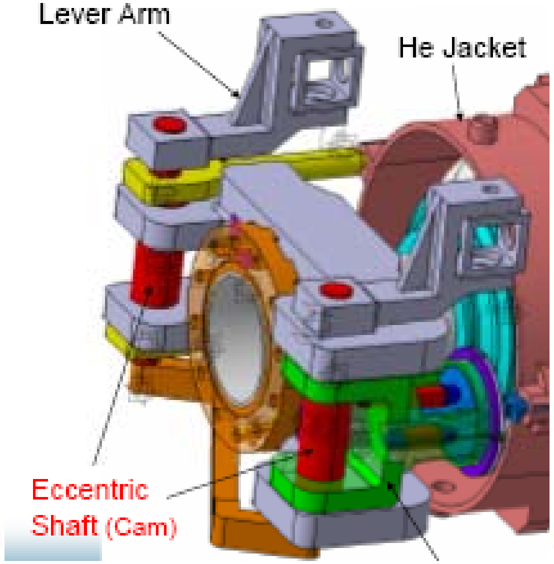

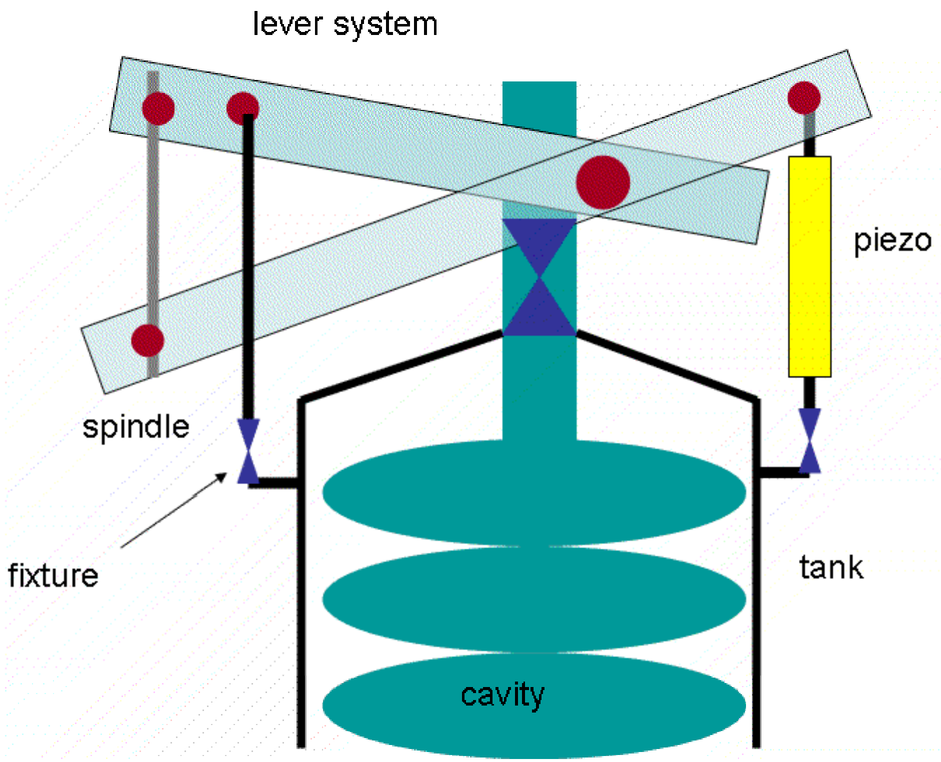

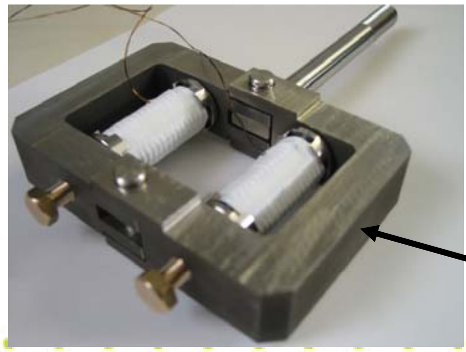

Modified piezo holder frame:
Higher wall thickness

Saclay II tuner

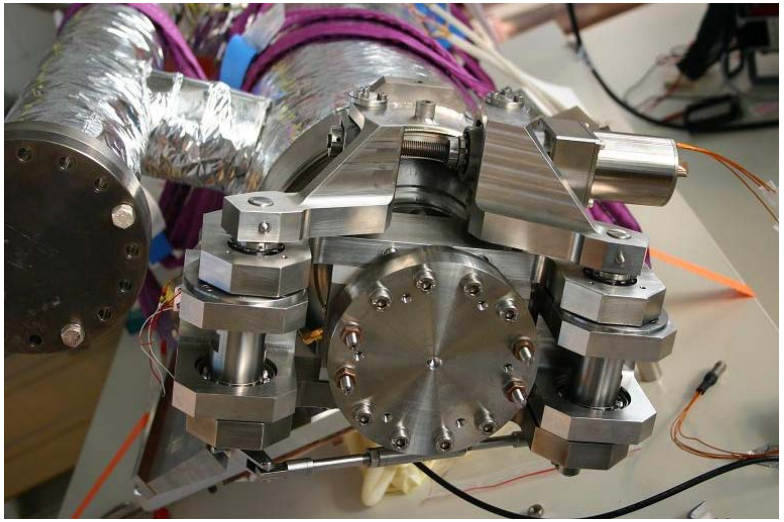

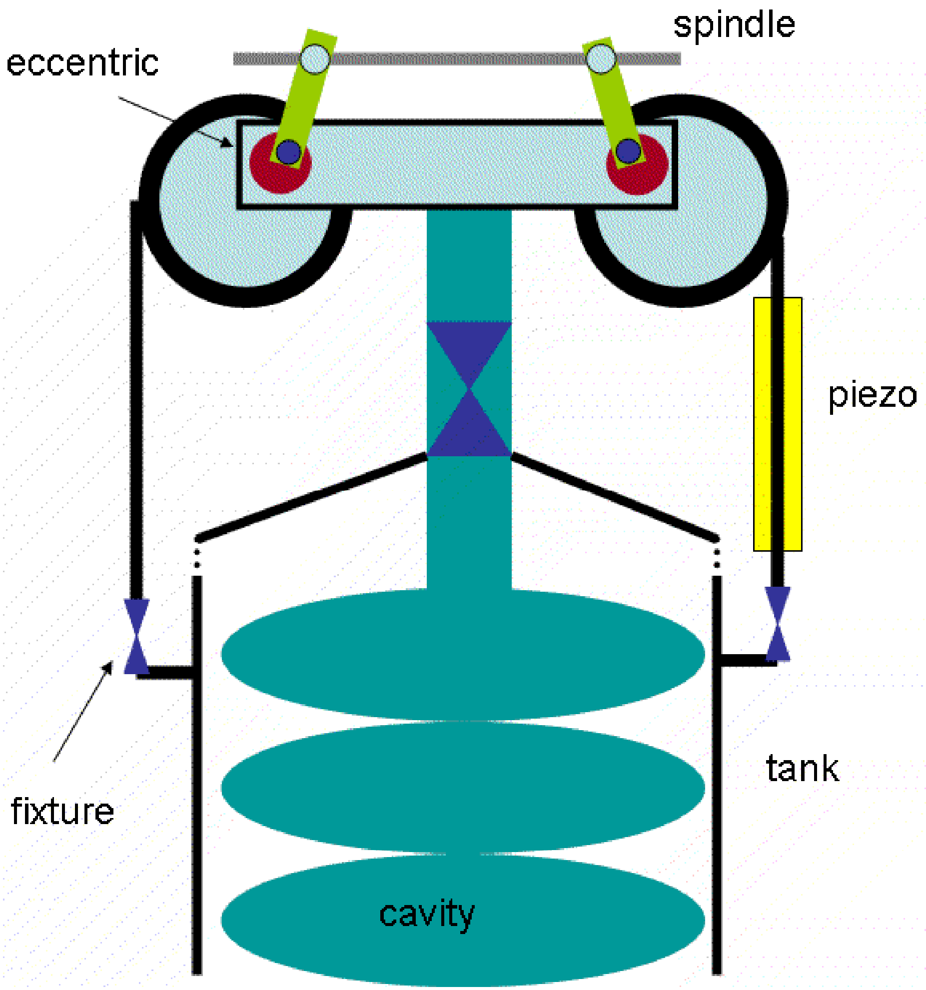

Saclay II tuner

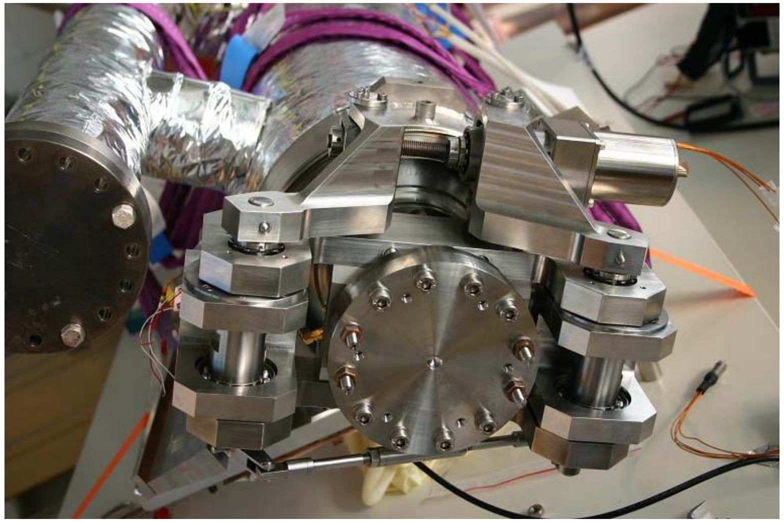

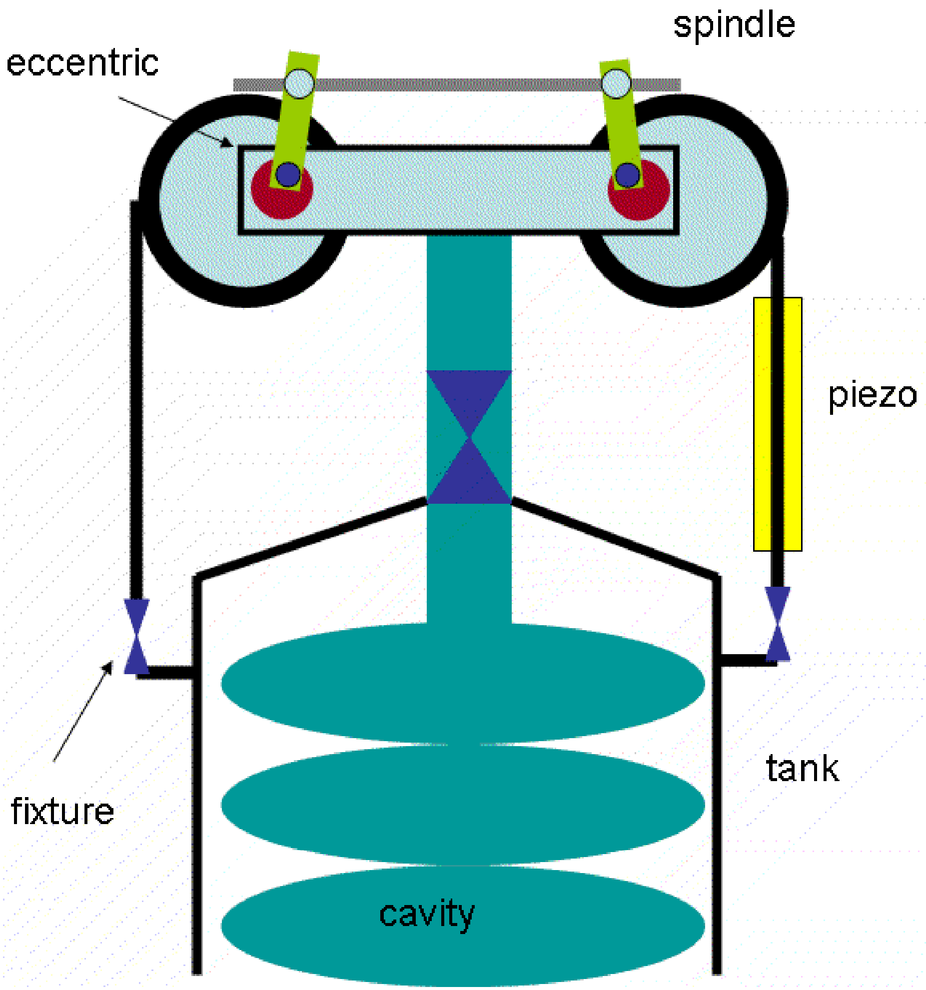

Overview of tuner properties

Design	Saclay I	Saclay II
Motor tuning range	750 kHz	500 kHz
Motor hysteresis	better	
Piezo tuning range	840 Hz	1420 Hz
Group delay	360 μs	150 μs
Stiffness	lower	higher

favored

Blade Tuner Design

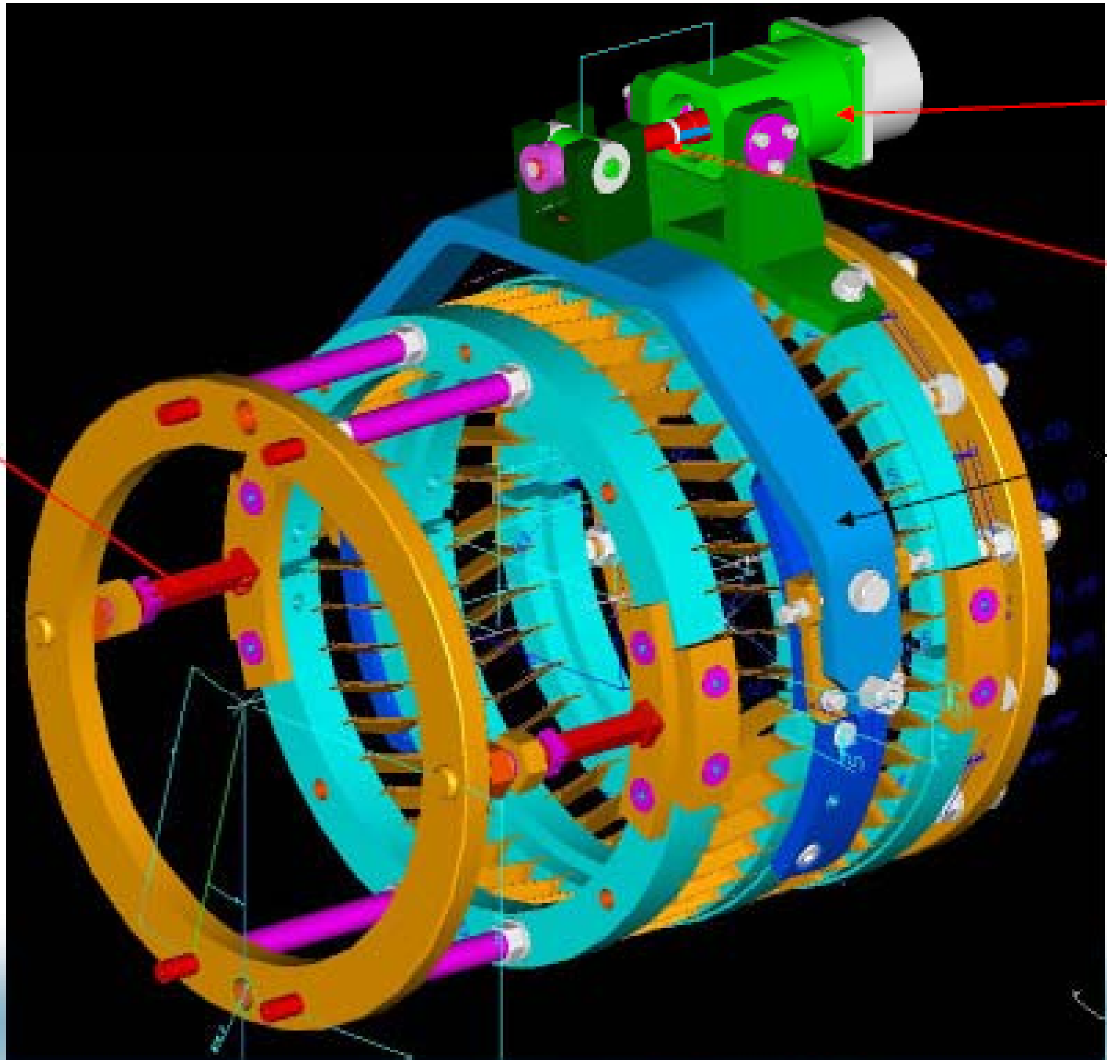

Shuichi Noguchi,SRF2007,10.7 16

Blade Tuner 25 N/μm

Not Stiff, Fatigue of Blade, K_S=13N/μm

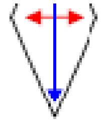

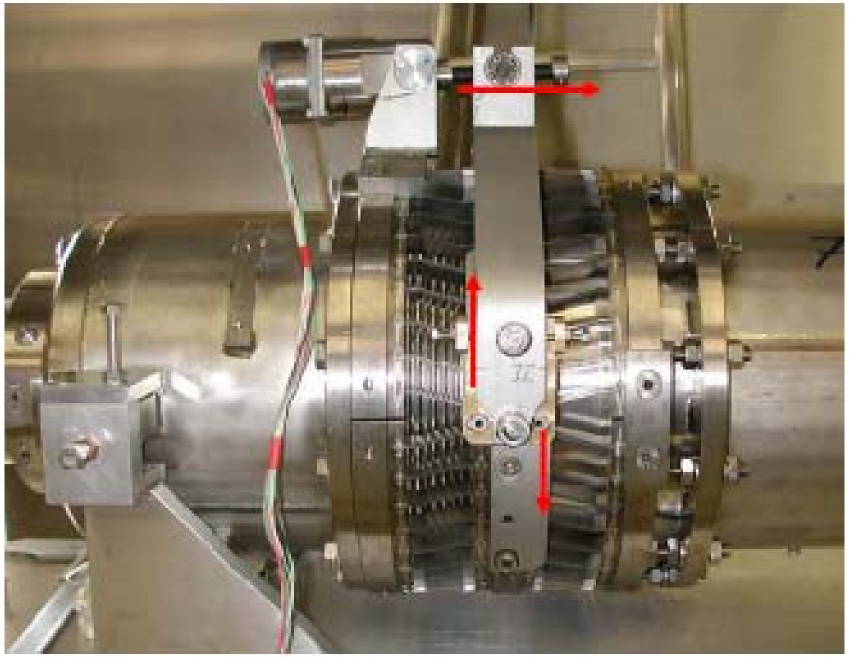

Original DESY | Revised INFN

Coaxial Ball Screw 500N/μm

Ball Screw : Large Ball Screw

Need Long Stroke Piezo

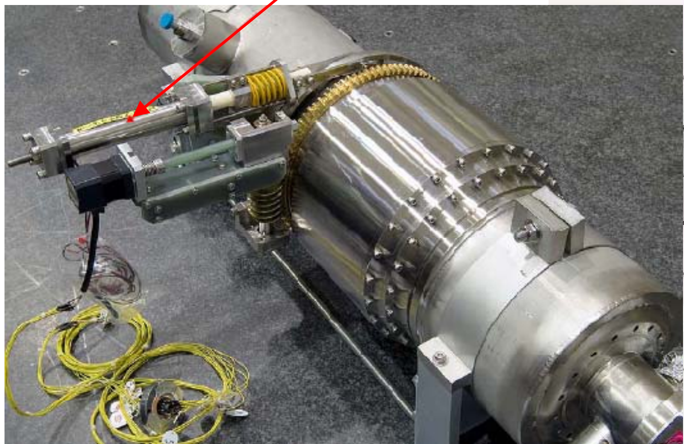

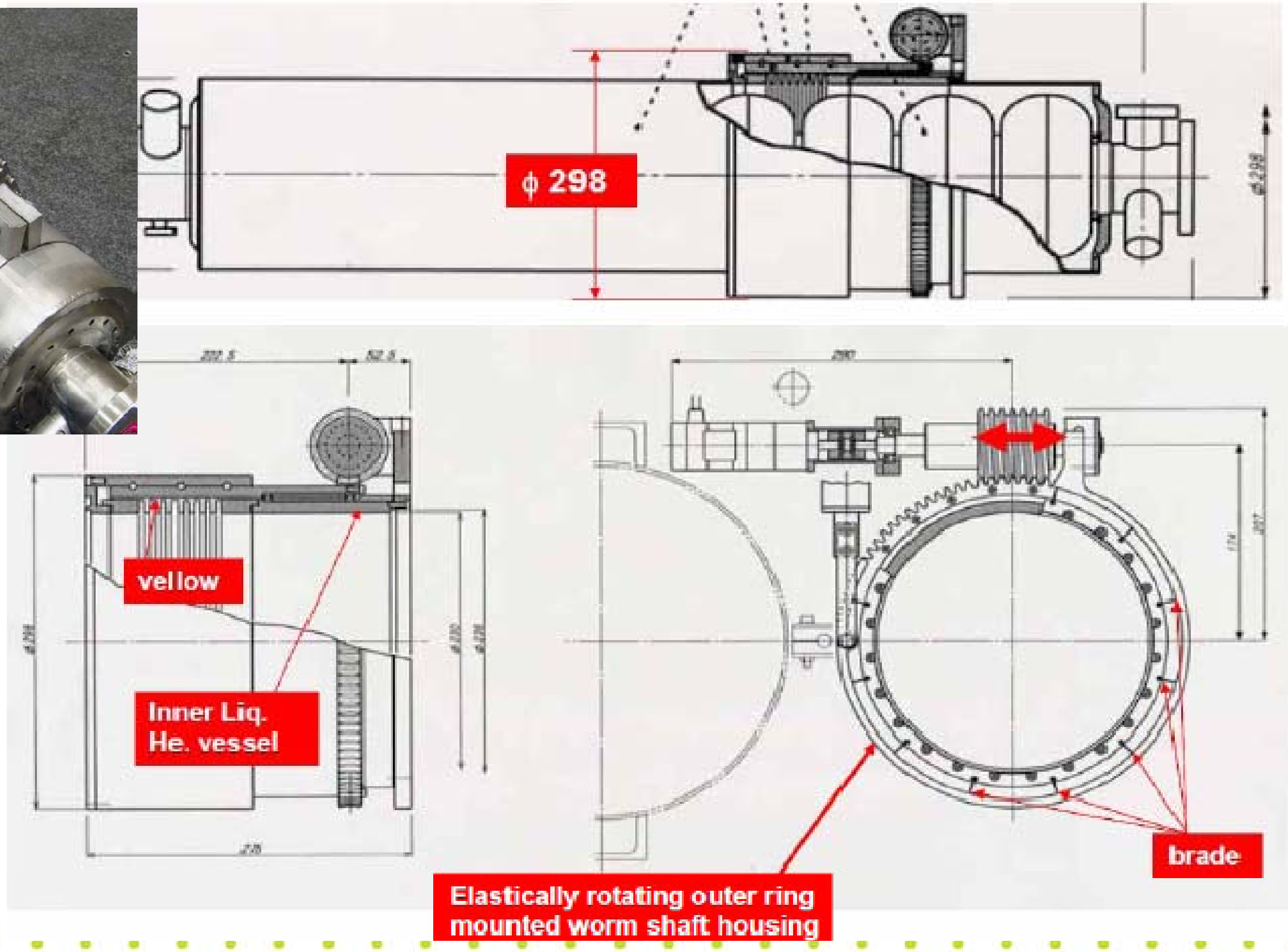

Side Jack Tuner (KEK)